Toward physics-based Earthquake Forecasting

Jean-Philippe Avouac
California Institute of Technology

Forecasting = assessing the probability of an earthquake with magnitude exceeding some chosen value, in a particular area, over a particular time window.

Physics-based = consistent with current knowledge of earthquake physics and phenomenology.

Toward physics-based Earthquake Forecasting

I. Introduction

II. EQ phenomenology-point source and Finite source models

III EQ phenomenology-Scaling properties

IV ‘Elastic Dislocation’ and ‘crack’ models

V Interseismic deformation

VI Postseismic deformation

VII Kinematic to Dynamic models of the seismic cycle

VIII The seismic cycle in the Himalaya

IX Earthquake forecasting

Earthquake Forecasting

"Earthquake forecasting and prediction involve statements about the location, time, and magnitude of future fault ruptures."

Earthquake Forecasting Model

"An earthquake forecasting model is a systematic method for calculating the probabilities of target events within future space-time domains."

International Commission on Earthquake Forecasting for Civil Protection (2011)

Seismotectonics-Basic notions

- Strain, Stress, Morh Circle
- Coulomb Failure criterion, ΔCFF
- Rate&State friction
- Anderson theory of faulting
- ‘Elastic Dislocation’
- Moment, Magnitude, STF, Moment tensor, stress drop
- Pulse and crack rupture
- Rupture velocity, slip velocity
- Gutenberg-Richter Law
- Mainshocks, aftershocks, Foreshocks, Swarms
- Omori Law, inverse Omori Law
- Creep, interseismic coupling (locking)
- GNSS, SAR,

Background reading

- Scholz, C. H. (2002), The Mechanics of Earthquakes and Faulting, *Cambridge Univ. Press.*, *2nd edition*.
- Segall, P. (2010), *Earthquake and Volcano Deformation*, Princeton University Press.
- Avouac, J.-P. (2015), From Geodetic Imaging of Seismic and Aseismic Fault Slip to Dynamic Modeling of the Seismic Cycle, *Annu. Rev. Earth Planet. Sci. 2015. 43:233–71*, *43*, 233-271.
- Avouac, J.-P. (2015), Mountain Building: From Earthquakes to Geological Deformation, in *Treatise on Geophysics*, edited by A. B. Watts, pp. 377-439, Elsevier.

US Seismic Hazard Map

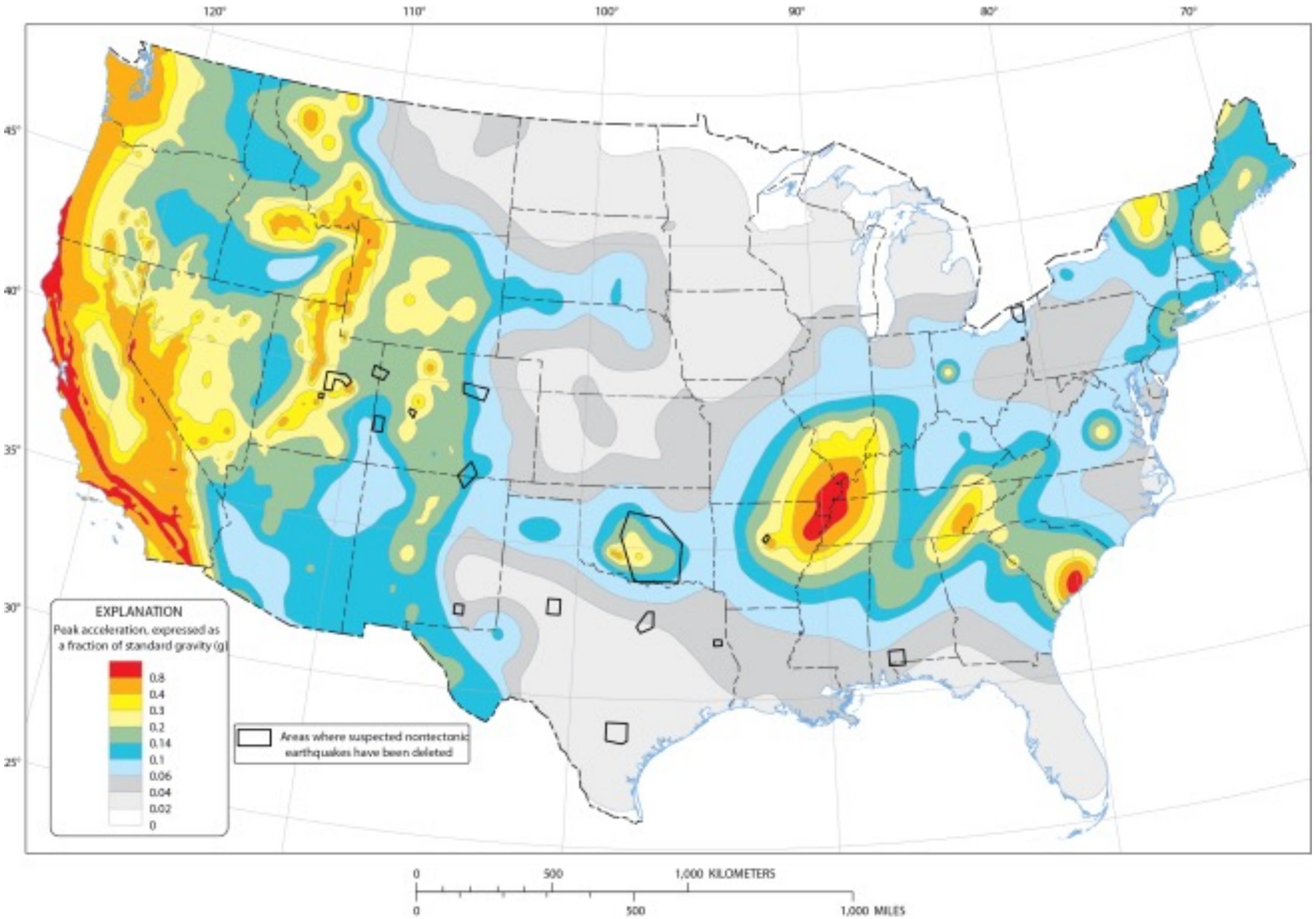

Two-percent probability of exceedance in 50 years map of peak ground acceleration

- Estimate of earthquake shaking hazard: Quantified as a probability of strength of shaking in a certain number of years
- Primary purpose is to set the seismic design provisions of building codes

What is hazard?
How does it differ from risk?

Hazard = Chance of an damaging ground motion

Risk = Chance of loss

Risk = Hazard x Exposure x Vulnerabiliy

Faulting, shaking
landsliding
liquifaction
innundation

Extent & density of
built environment

Structural fragility
Non-structural vulnerability

(Bill Ellsworth, USGS)

Probabilistic Seismic Hazard Analysis

1. Where will earthquakes occur in the future?

2. How often will they happen and how large can they get?

3. How hard will they shake the ground?

4. When answers are available for Steps 1-3: Add up all of the sources to find the probability of exceeding damaging shaking.

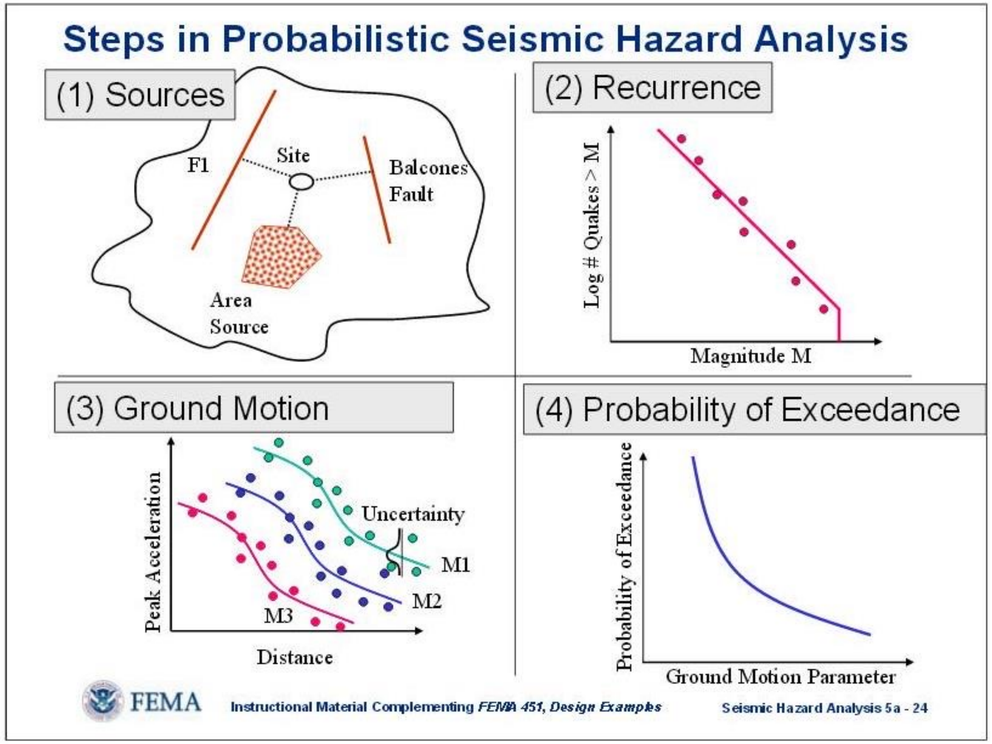

(Bill Ellsworth, USGS)

Contents lists available at ScienceDirect

Physics of the Earth and Planetary Interiors

journal homepage: www.elsevier.com/locate/pepi

Why is Probabilistic Seismic Hazard Analysis (PSHA) still used?

Francesco Mulargia[a], Philip B. Stark[b], Robert J. Geller[c,*]

[a] Dipartimento di Fisica e Astronomia, Settore di Geofisica, Università di Bologna, viale Berti Pichat 8, 40127 Bologna, Italy
[b] Department of Statistics, Code 3860, University of California, Berkeley, CA 94720-3860, USA
[c] Department of Earth and Planetary Science, School of Science, University of Tokyo, Hongo 7-3-1, Bunkyo-ku, Tokyo 113-0033, Japan

Earthquake catalogs show clustering in time and space

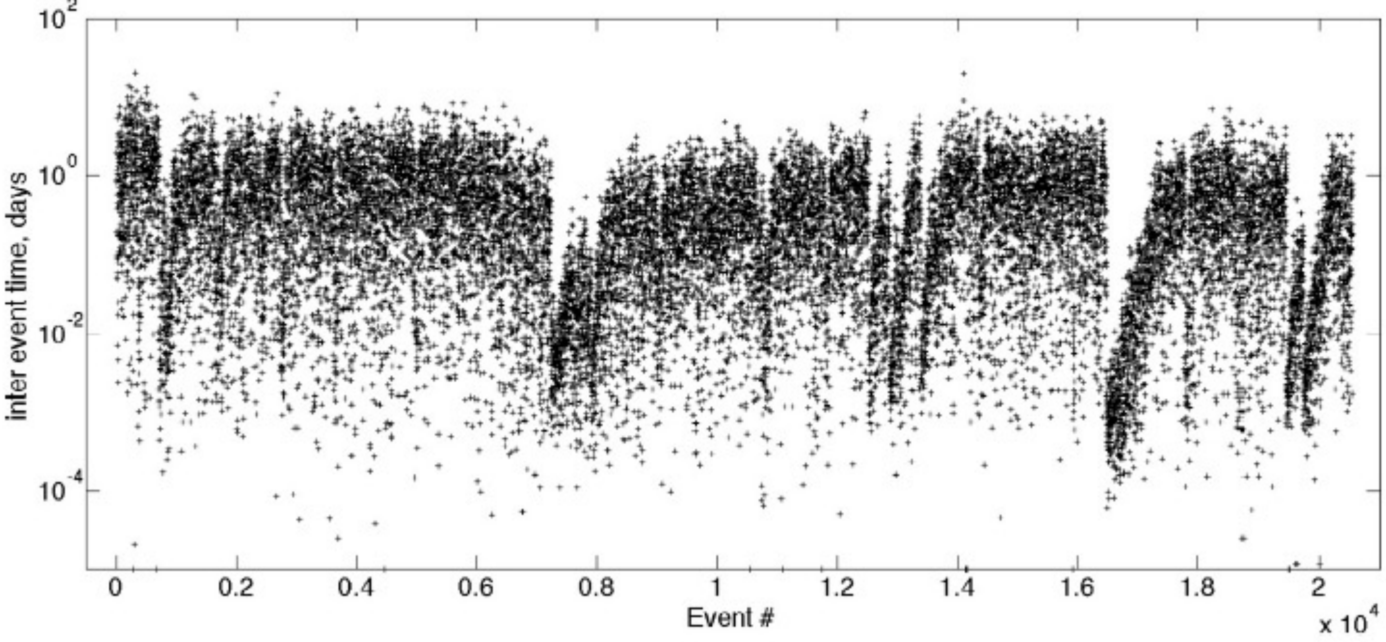

Seismicity of Italy

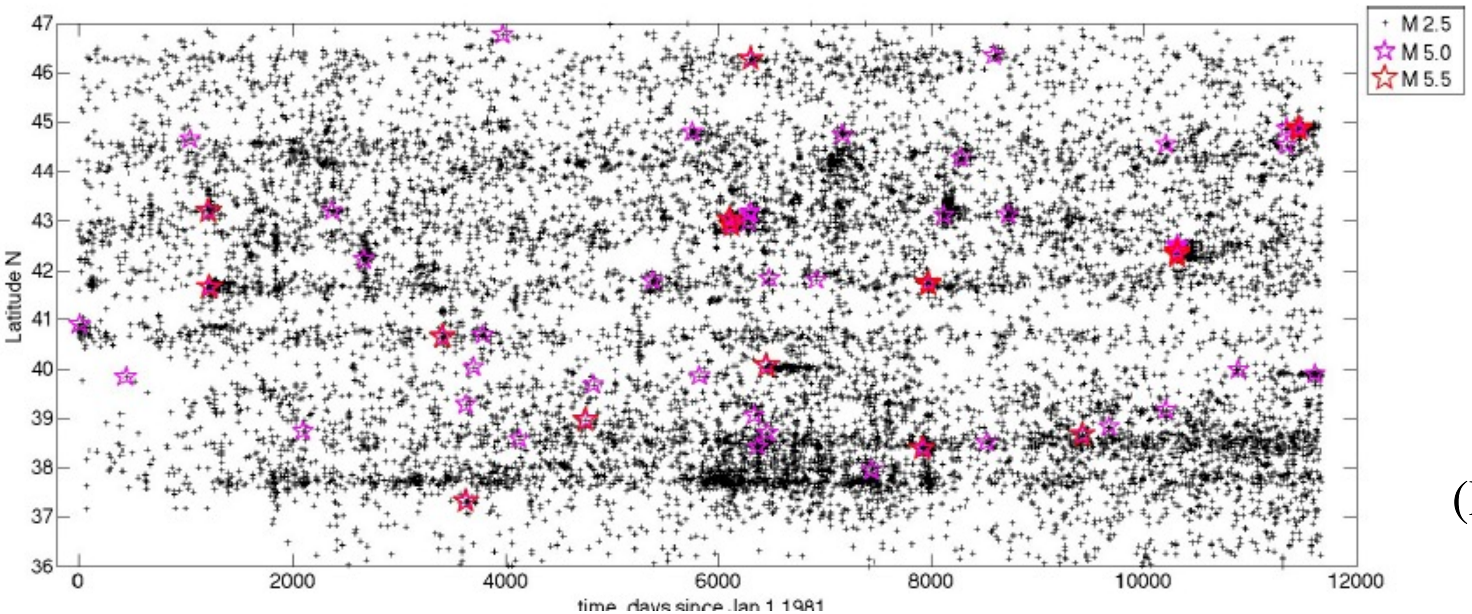

(Mulargia et al., 2017)

-> Earthquakes do exhibit "memory", earthquake probability is not uniform in space

Earthquake Renewal Process

Bulletin of the
Seismological Society of America

Vol. 64 October 1974 No. 5

IS THE SEQUENCE OF EARTHQUAKES IN SOUTHERN CALIFORNIA, WITH AFTERSHOCKS REMOVED, POISSONIAN?

BY J. K. GARDNER and L. KNOPOFF

ABSTRACT

Yes.

Poisson process: Assume earthquakes are independent events that happen randomly in time at the rate λ.

$$\mathrm{P}(t) = \lambda e^{-\lambda t} \qquad \mathrm{P}(t \le T) = 1 - e^{-\lambda t} \qquad \mathrm{P}(t > T) = e^{-\lambda t}$$

The Poisson process is memory less

-> Probabilities are independent of earthquake history,

Earthquake Renewal Process

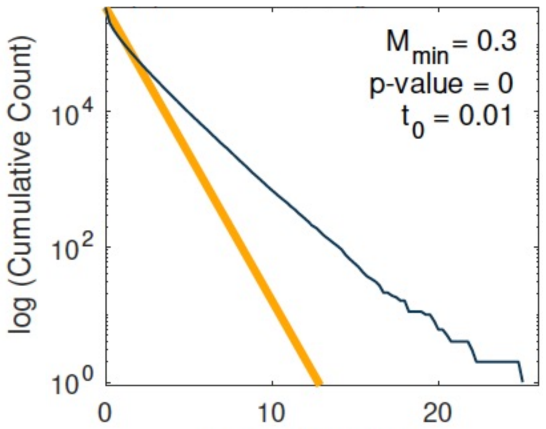

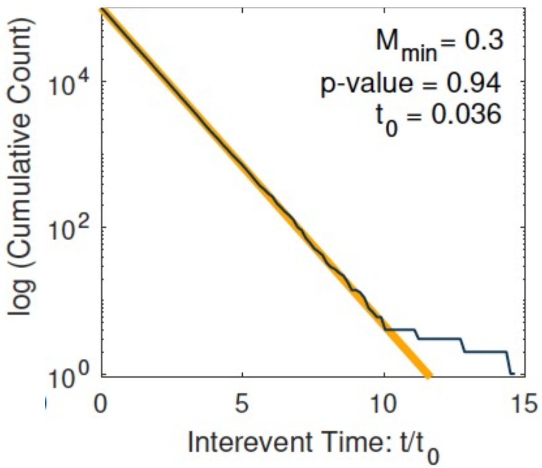

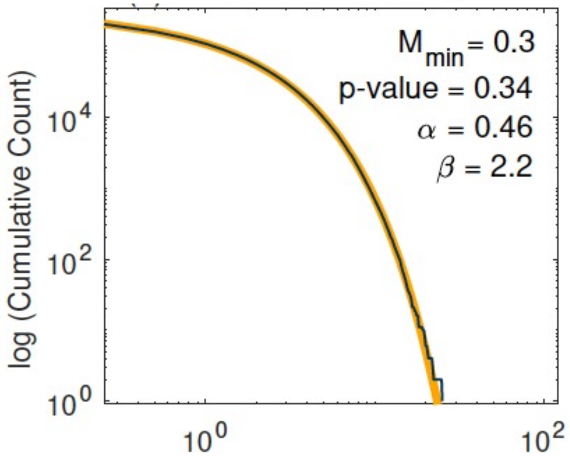

Interevent time distribution $\mathrm{P}(t > T)$

Catalog of California (Ross et al., 2019)
M>0.3 events

$$\mathrm{P}(t > T) = e^{-\lambda t}$$

Declustered Catalog is Poisson, consistent with Gardner and Knopoff (1974)

The effect of clustering is well represented by the gamma distribution (Corral, 2004; Hainzl, 2006) to using the QTM catalog of California (Ross et al., 2019)

$$P(\tau) = \frac{\beta^{-\gamma}\tau^{\gamma-1}e^{-\tau/\beta}}{\Gamma(\gamma)}$$

(Erin Hightower)

Is recurrence of large earthquakes ('system size') Poissonian or quasi-periodic?

The San Andreas Fault Example

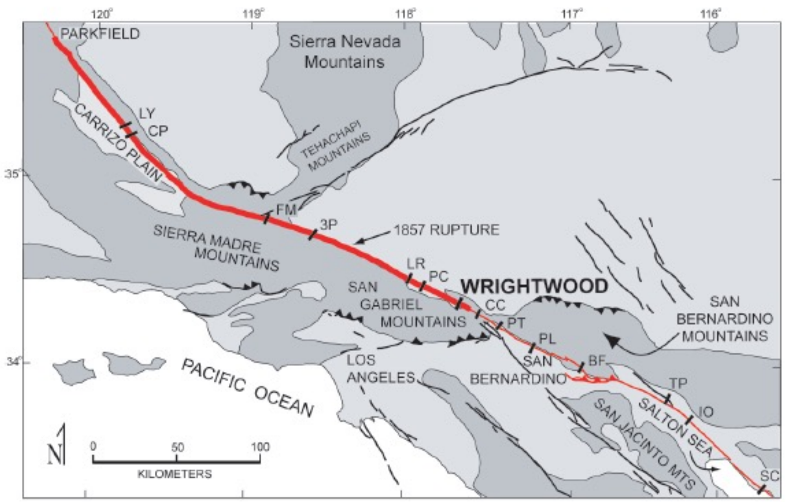

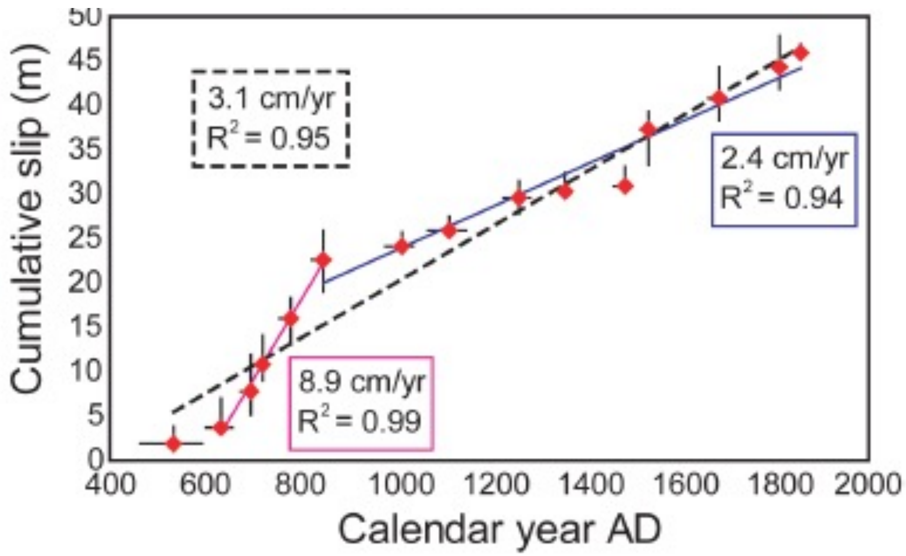

(Weldon et al. 2004)

Is recurrence of large earthquakes ('system size') Poissonian or quasi-periodic?

Geophysical Research Letters

RESEARCH LETTER
10.1029/2020GL089272

Periodicity and Clustering in the Long-Term Earthquake Record

Jonathan D. Griffin[1,2], Mark W. Stirling[1], and Ting Wang[3]

Key Points:
- We characterize the distribution of

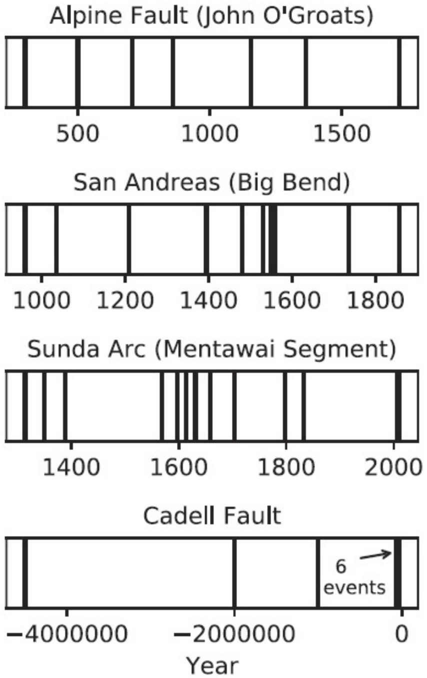

80 long terms records worldwide were collected

σ- STD of interevent time
μ- mean interevent time
τ- interevent time

(Griffin et al., 2020)

Is recurrence of large earthquakes ('system size') Poissonian or quasi-periodic?

τ- interevent time
μ- mean interevent time
σ- STD of interevent time

Coefficient **O**f **V**ariation = σ/μ

COV = 0-1 quasi periodic
COV ~ 1 random (poisson)
COV > 1 clustering

Burstiness= (σ-μ)/(σ+μ)

B = (-1) - (-0.33) strongly periodic
B = (-0.33) - 0 weakly periodic
B > 0 clustering (bursty)

Memory= $\frac{1}{N-1}\sum_{i=1}^{N-1}\frac{(\tau_i-\mu_2)(\tau_{i+1}-\mu_2)}{\sigma_1\sigma_2}$

M < 0 alternate occurrence (short-long-short)
M ~ 0 no memory effect
M > 0 successive correlation (short-short long-long)

μ_1 and σ_1 are the mean and standard deviation of the sequence of interevent times τ_i (i = 1, 2, …, N – 1)
μ_2 and σ_2 are the mean and standard deviation of the sequence of interevent times τ_i (i = 2, 3, …, N)

(Griffin et al., 2020)

Is recurrence of large earthquakes ('system size') Poissonian or quasi-periodic?

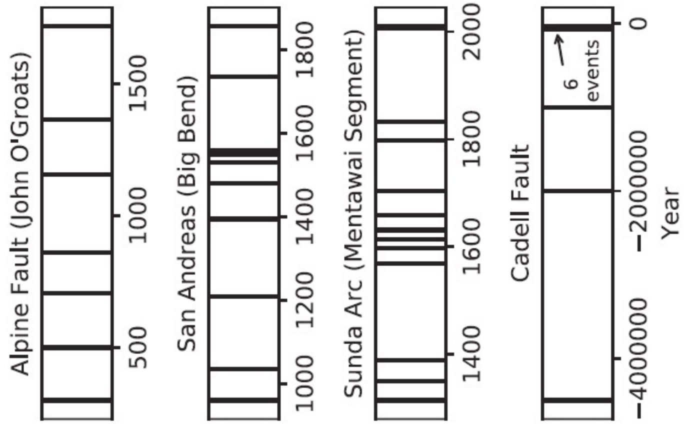

80 long terms records worldwide:

Burstiness= (σ-μ)/(σ+μ)

Memory= $\frac{1}{N-1}\sum_{i=1}^{N-1}\frac{(\tau_i-\mu_2)(\tau_{i+1}-\mu_2)}{\sigma_1\sigma_2}$

Majority of studied faults show weakly periodic and uncorrelated large earthquake recurrence

many low activity-rate (annual occurrence rates < 2 × 10^{-4}) faults show random or clustered earthquake recurrence

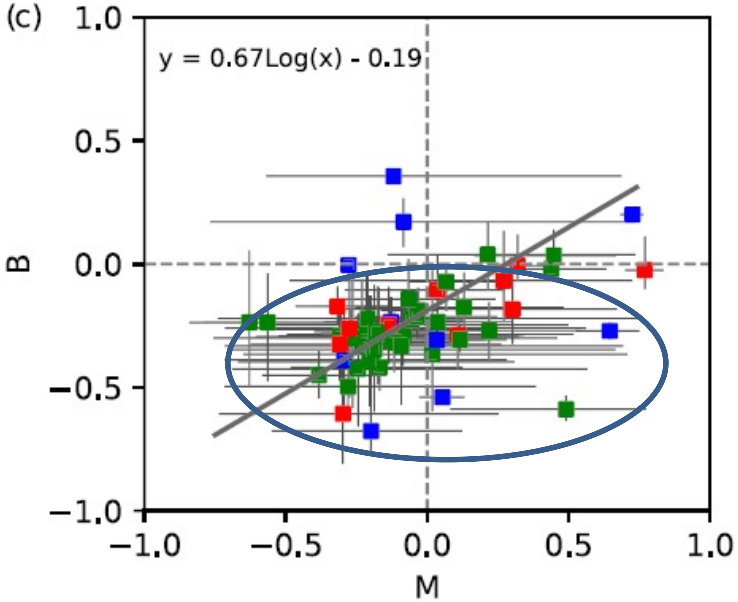

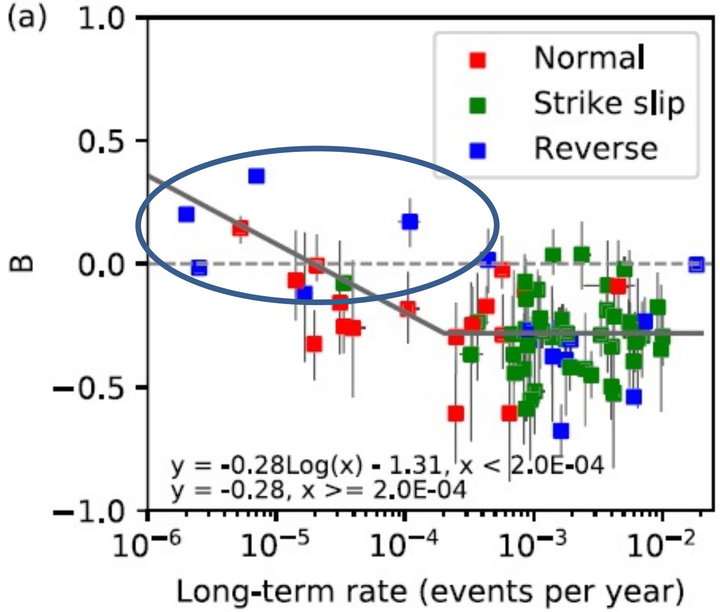

(Griffin et al., 2020)

Is recurrence of large earthquakes ('system size') Poissonian or quasi-periodic?

The North Anatolian Fault Example

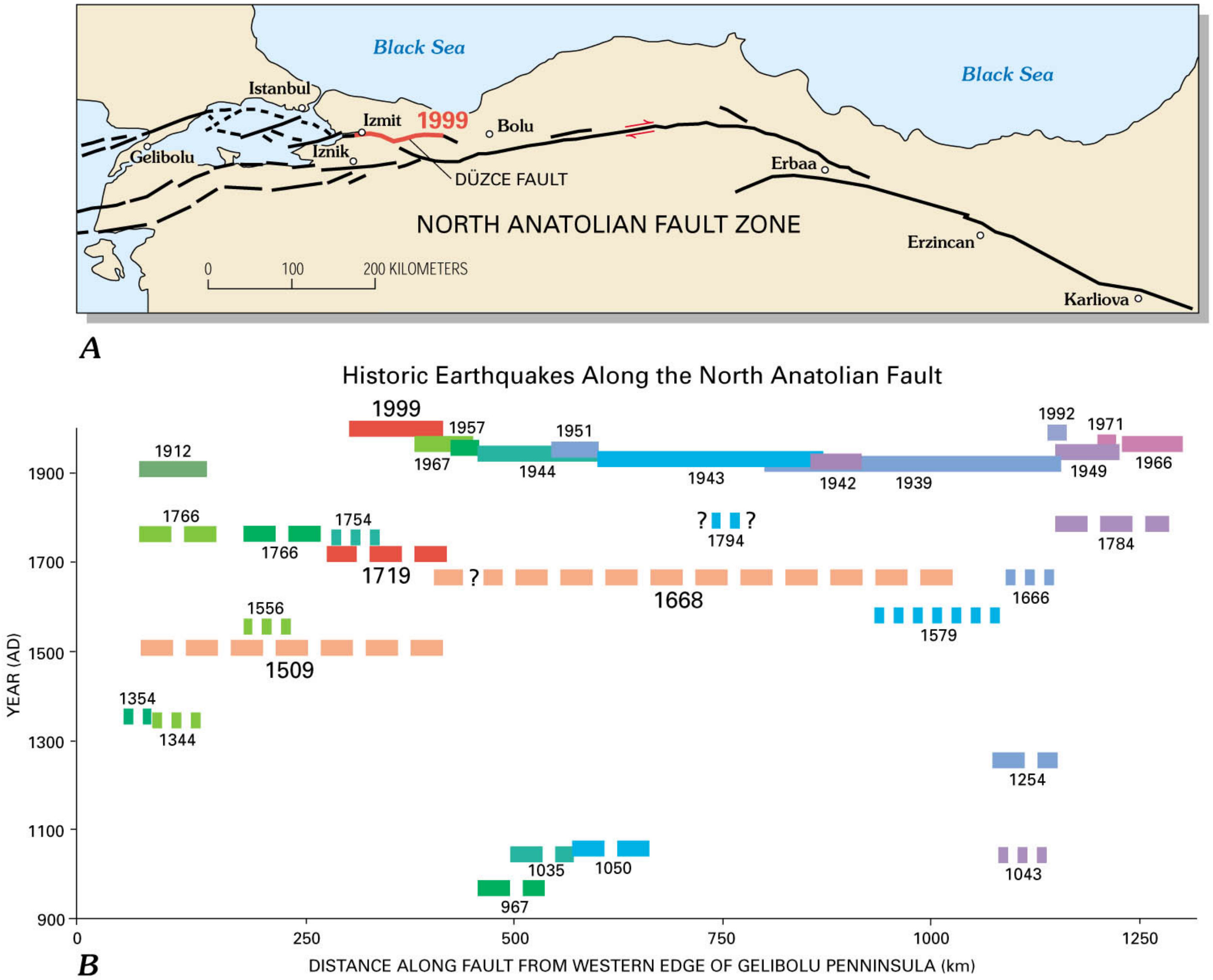

USGS report, 2000

Is recurrence of large earthquakes ('system size') Poissonian or quasi-periodic?

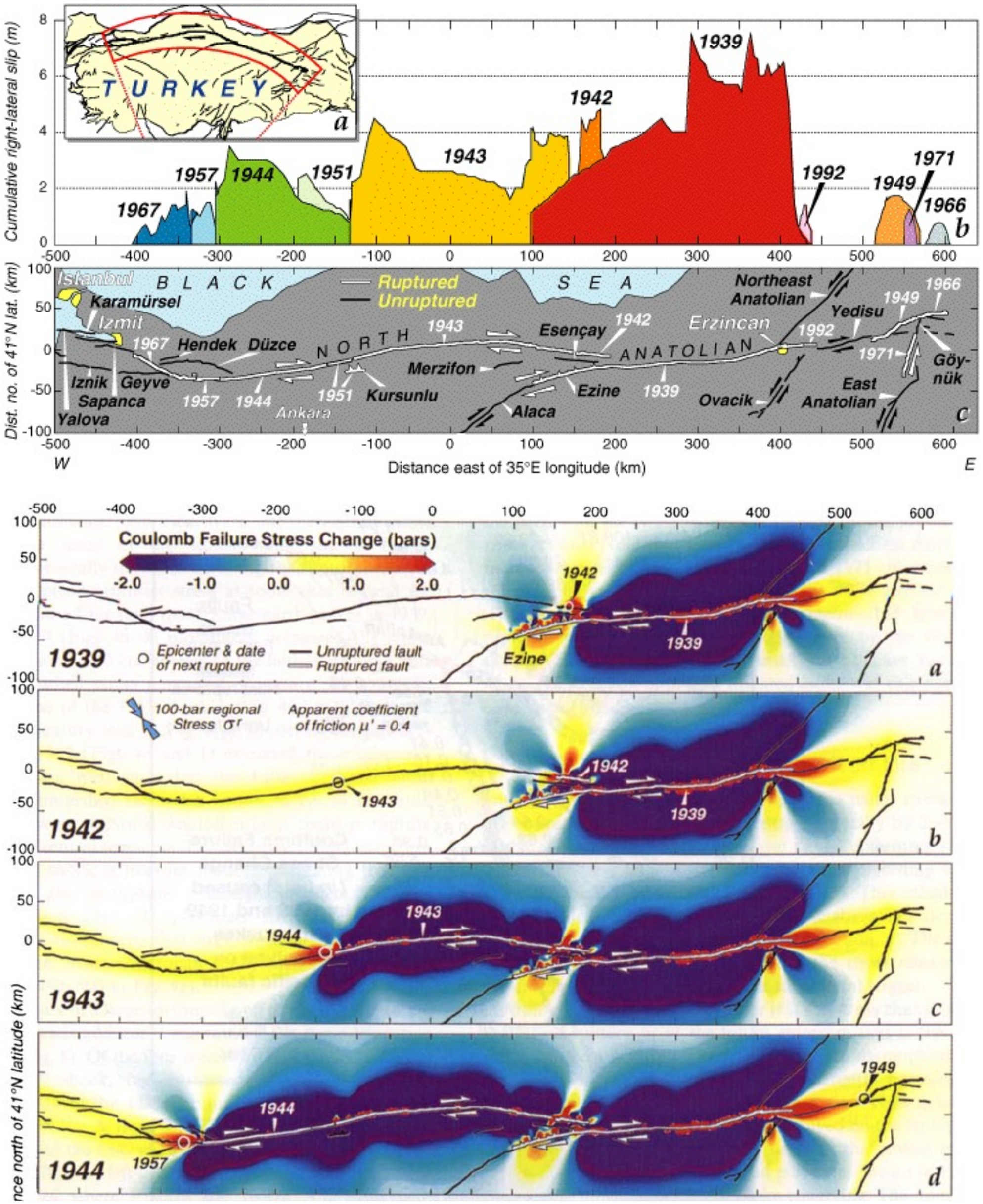

The North Anatolian Fault Example

- 8 Mw>7.0 events in ~60 years
- The return period of each single event should be ~100-200yr on average

1939, Mw 7.8

1942, Mw 7.0

1943, Mw7.2

1944, Mw 7.2

1957, Mw 7.1

1992, Mw 7.6

1999, Mw 7.6

1999, Mw 7.2

(Stein et al., 1997)

UCERF3-TI

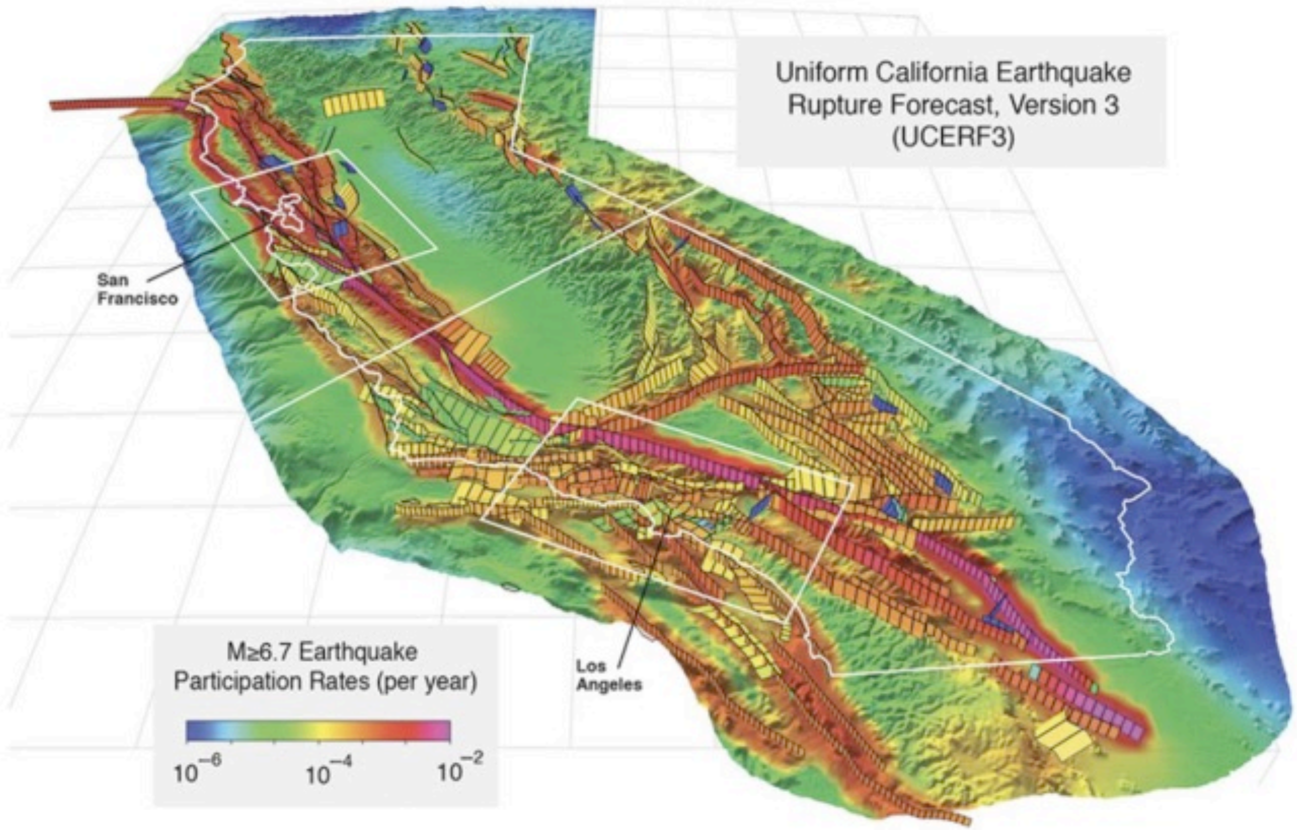

Field et al., (2014), Uniform California Earthquake Rupture Forecast, Version 3 (UCERF3) -The Time-Independent Model, *Bulletin of the Seismological Society of America*, *104*(3), 1122-1180.

UCERF3 – Time Dependent

By adding:

- Renewal models (elastic-rebound) using the timing of past seismicity
- Spatiotemporal clustering to model aftershocks and triggered events (ETAS)

Field et al. (2015)

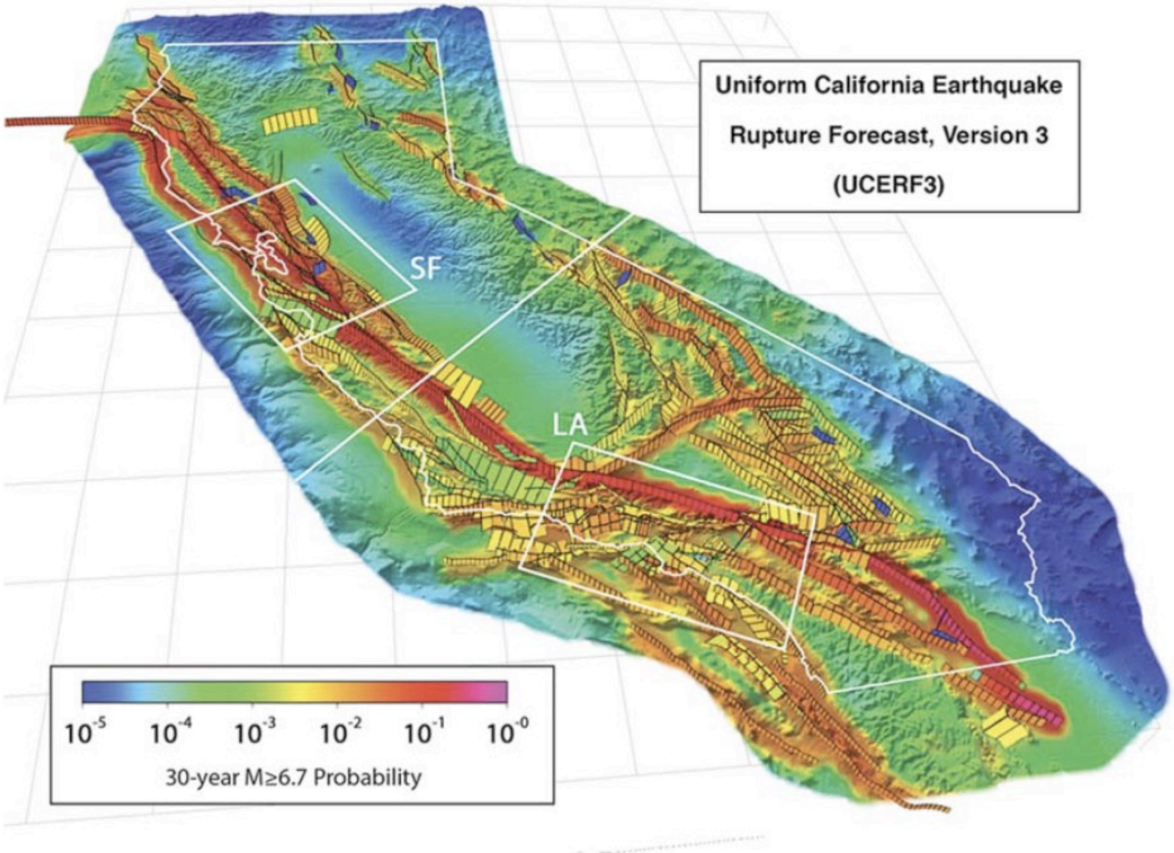

How to bring more physics into seismic hazard assessment methods?

- Seismicity responds to stress variations which can vary in space and time. Earthquake themselves are a source of stress variations (co and post). Can we account for these variations?
- Is the PSHA framework still adequate?
- Can we move to using numerical model the ‘seismic cycle’?

Dynamic Modeling the Parkfield EQs Sequence on the San AF

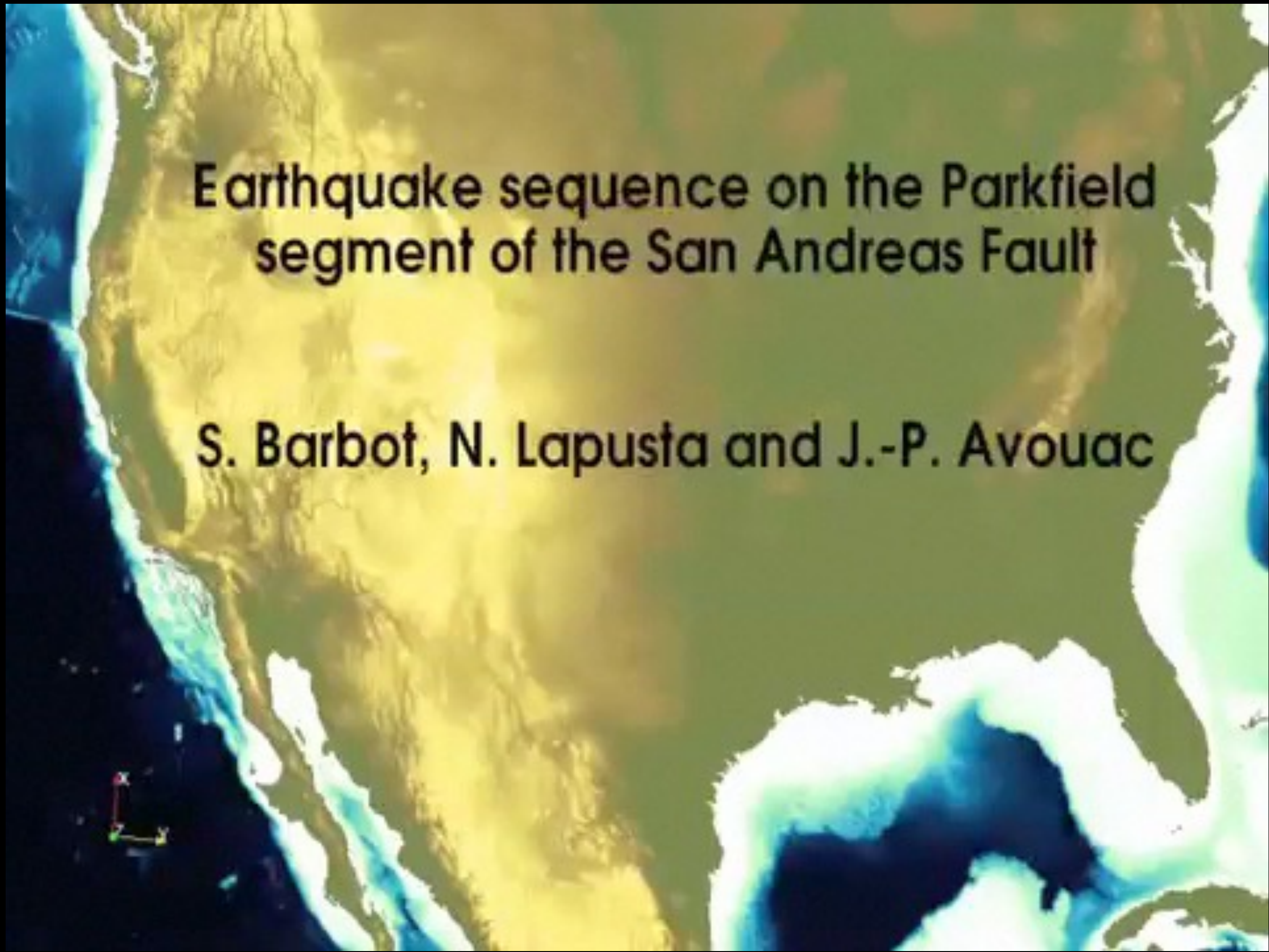

[Barbot et al, Science, 2012]

How to calibrate and validate such models?

References-Intro

Barbot, S., N. Lapusta, and J. P. Avouac (2012), Under the Hood of the Earthquake Machine: Toward Predictive Modeling of the Seismic Cycle, *Science*, *336*(6082), 707-710.

Corral, A. (2004), Long-term clustering, scaling, and universality in the temporal occurrence of earthquakes, *Physical Review Letters*, *92*(10).

Field et al., (2014), Uniform California Earthquake Rupture Forecast, Version 3 (UCERF3) -The Time-Independent Model, *Bulletin of the Seismological Society of America*, *104*(3), 1122-1180.

Field et al., (2015), Long-Term Time-Dependent Probabilities for the Third Uniform California Earthquake Rupture Forecast (UCERF3), *Bulletin of the Seismological Society of America*, *105*(2A), 511-543.

Gardner, J. and Knopoff , L. (1974). Is The Sequence of Earthquakes in Southern California, with Aftershocks Removed, Poissonian?, Bull. Seismol. Soc. Am. 64(5): 1363{1367.

Gerstenberger, M. C., W. Marzocchi, T. Allen, M. Pagani, J. Adams, L. Danciu, E. H. Field, H. Fujiwara, N. Luco, K. F. Ma, C. Meletti, and M. D. Petersen (2020), Probabilistic Seismic Hazard Analysis at Regional and National Scales: State of the Art and Future Challenges, *Reviews of Geophysics*, *58*(2).

Griffin, J. D., M. W. Stirling, and T. Wang (2020), Periodicity and Clustering in the Long-Term Earthquake Record, *Geophysical Research Letters*, *47*(22).

Mulargia, F., Stark, P.B. & Geller, R.J., 2017. Why is Probabilistic Seismic Hazard Analysis (PSHA) still used?, *Physics of the Earth and Planetary Interiors,* 264, 63-75.

Stein, R., A. Barka, and J. Dieterich (1997), Progressive failure on the North Anatolian fault since 1939 by earthquake stress triggering, *Geophys.J.Inter.*, *128*, 594-604.

Weldon, R., T. Fumal, and G. Biasi (2004), Wrightwood and the earthquake cycle: What a long recurrence record tells us about how faults works, *GSA Today*, *14*(9), 4-10.

Toward physics-based Earthquake Forecasting

I. Introduction

II. EQ phenomenology-point source and Finite source models

III EQ phenomenology-Scaling properties

IV ‘Elastic Dislocation’ and ‘crack’ models

V Interseismic deformation

VI Postseismic deformation

VII Kinematic to Dynamic models of the seismic cycle

VIII The seismic cycle in the Himalaya

IX Earthquake forecasting

Quantification of EQs sources

Point source approximation in seismology

- Hypocenter (epicentral location, depth) and origin time
- Moment (function of time) $M_0 = \mu A s$
- Moment tensor

$$\underline{\underline{M_0(t)}} = \mu A\left(\underline{s}\cdot{}^t\underline{n}+\underline{n}\cdot{}^t\underline{s}\right) = M_0(t)\left(\underline{u}\cdot{}^t\underline{n}+\underline{n}\cdot{}^t\underline{u}\right)$$

μ: shear modulus
A: fault area
$\underline{u}$; unit vector // slip
$\underline{n}$: unit vector ⊥ fault

- Total cumulated moment release and duration
- Source spectrum ->Fault area, Stress drop

Moment- Magnitude

$$\mathrm{M_w} = \frac{2}{3}\log M_0 - 6$$

where M_0 is expressed in N.m

(Hanks and Kanamori, BSSA, 1979)

Double-Couple

- Earthquake sources in the point source approximation can generally be represented by a double-couple (~shear dislocation)

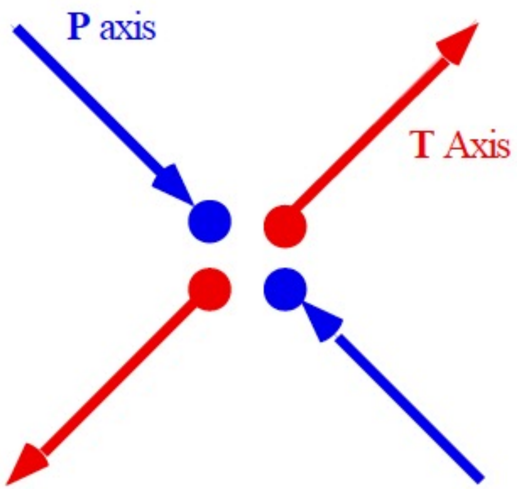

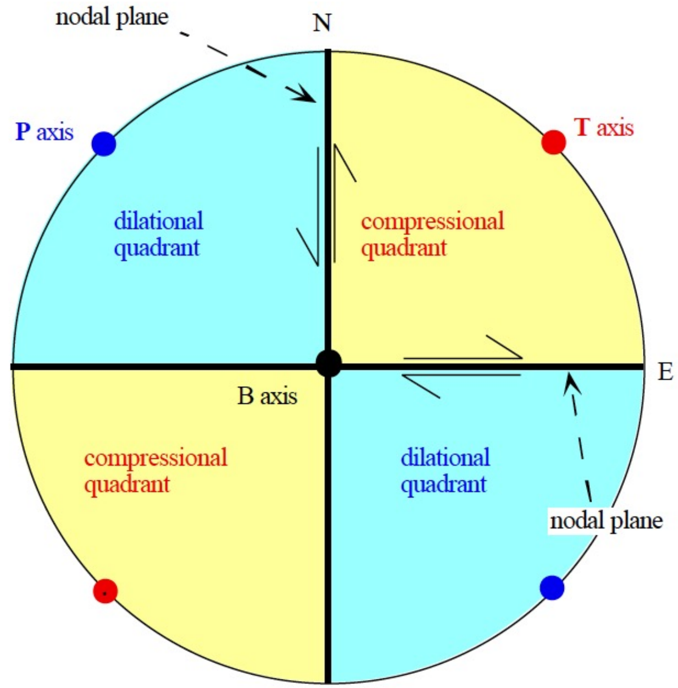

Nuclei of pure shear with (P, T, B) being the principal directions of the deviatoric stress tensor (P: compressional, T: tensional, B intermediary)

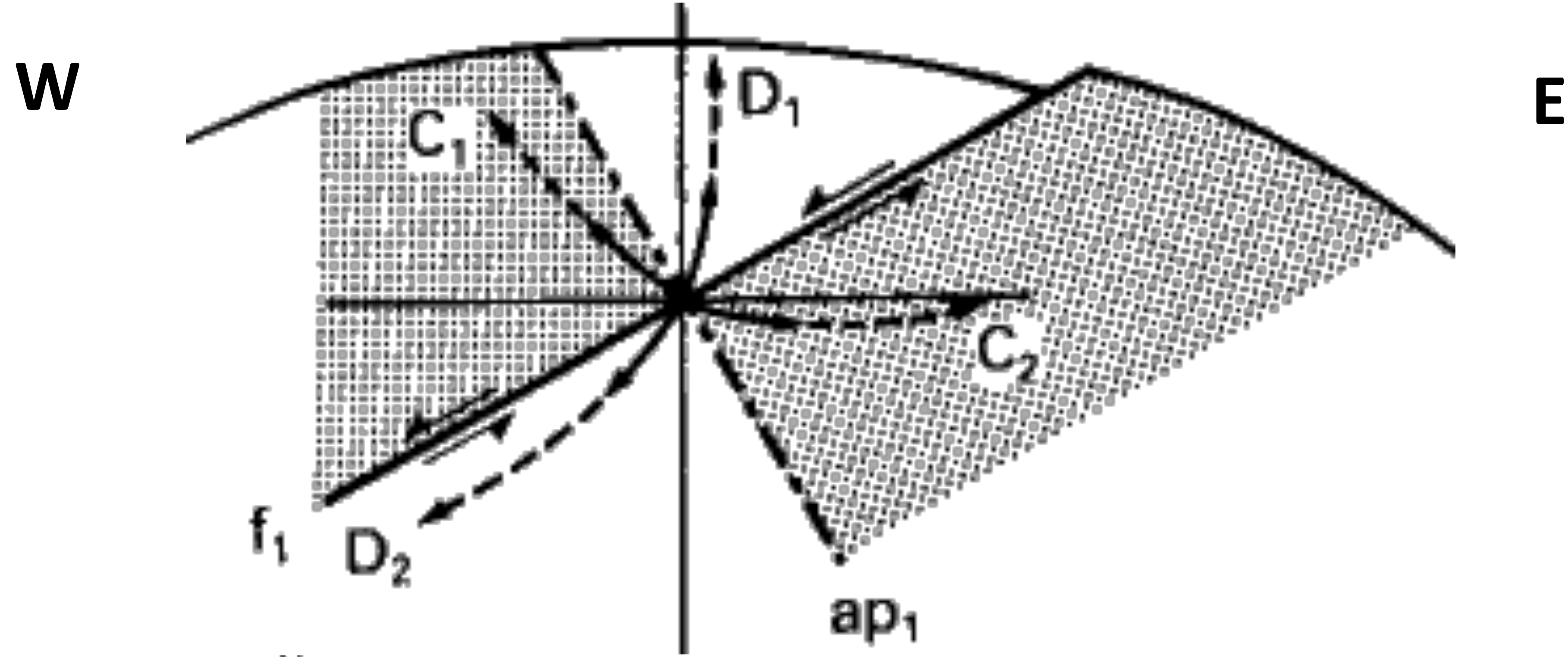

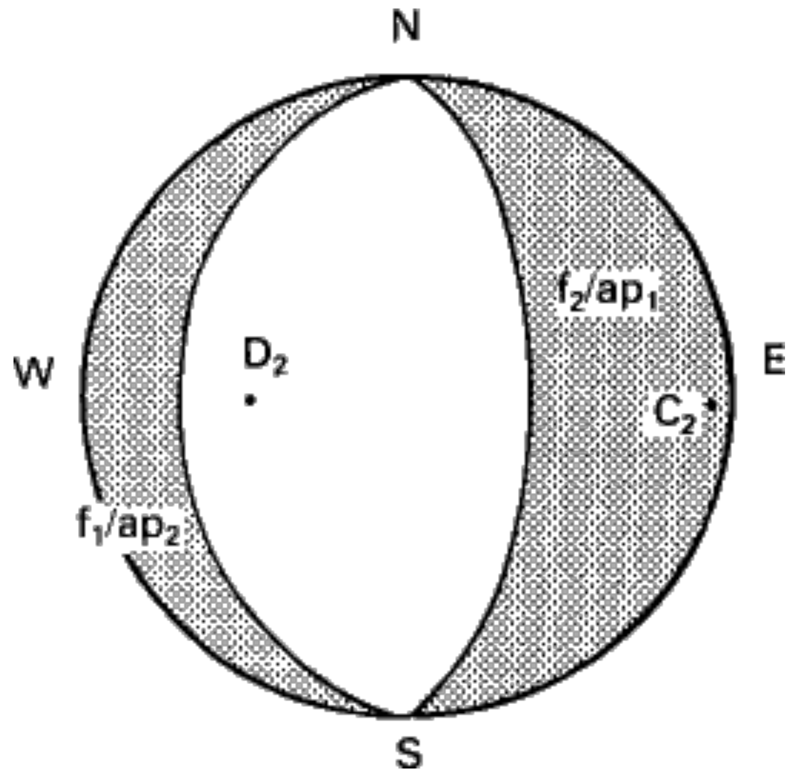

‘Beach ball’ representation of earthquake focal mechanisms

(= fault plane solutions)

Earthquake Focal Mechanisms

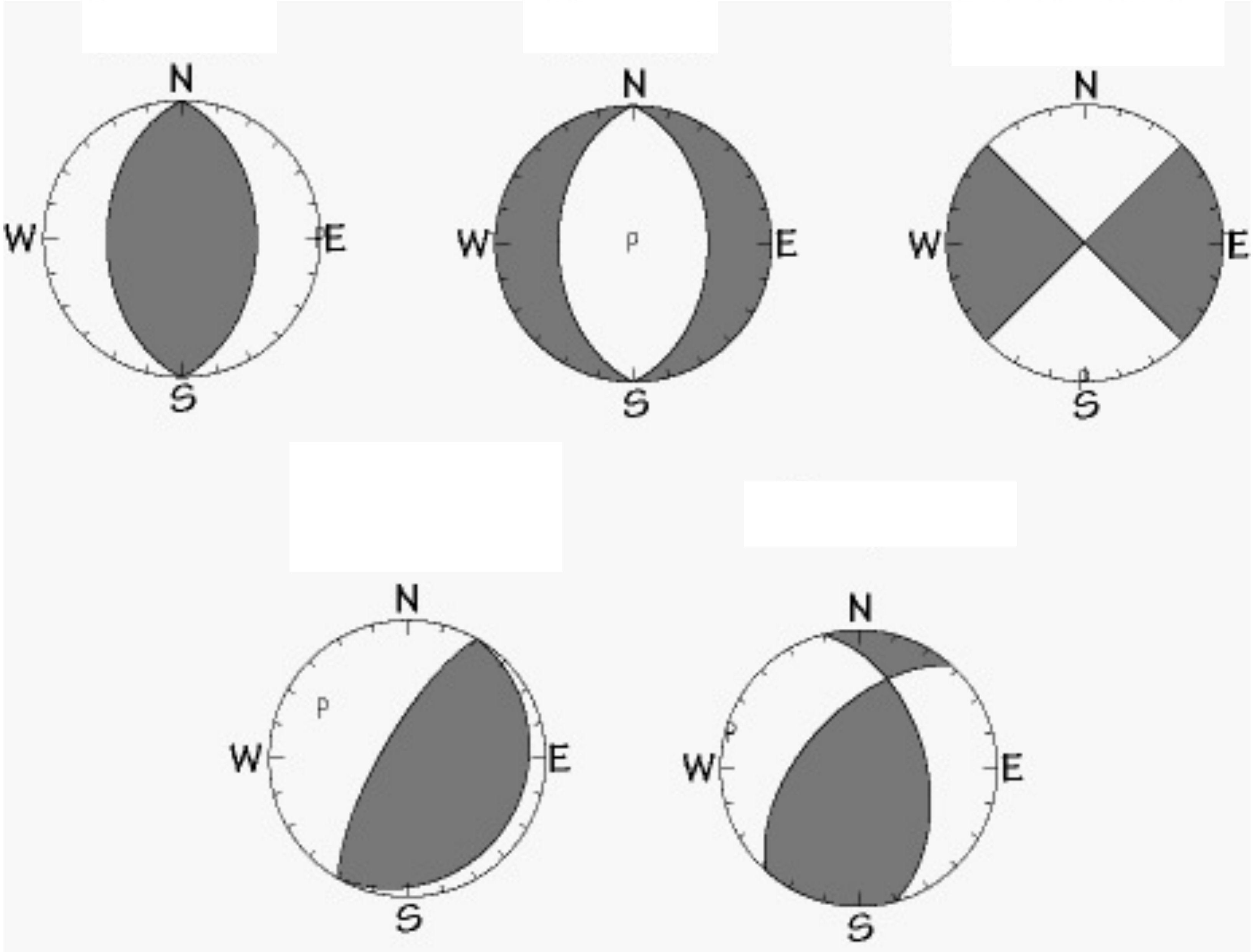

Earthquake Focal Mechanisms

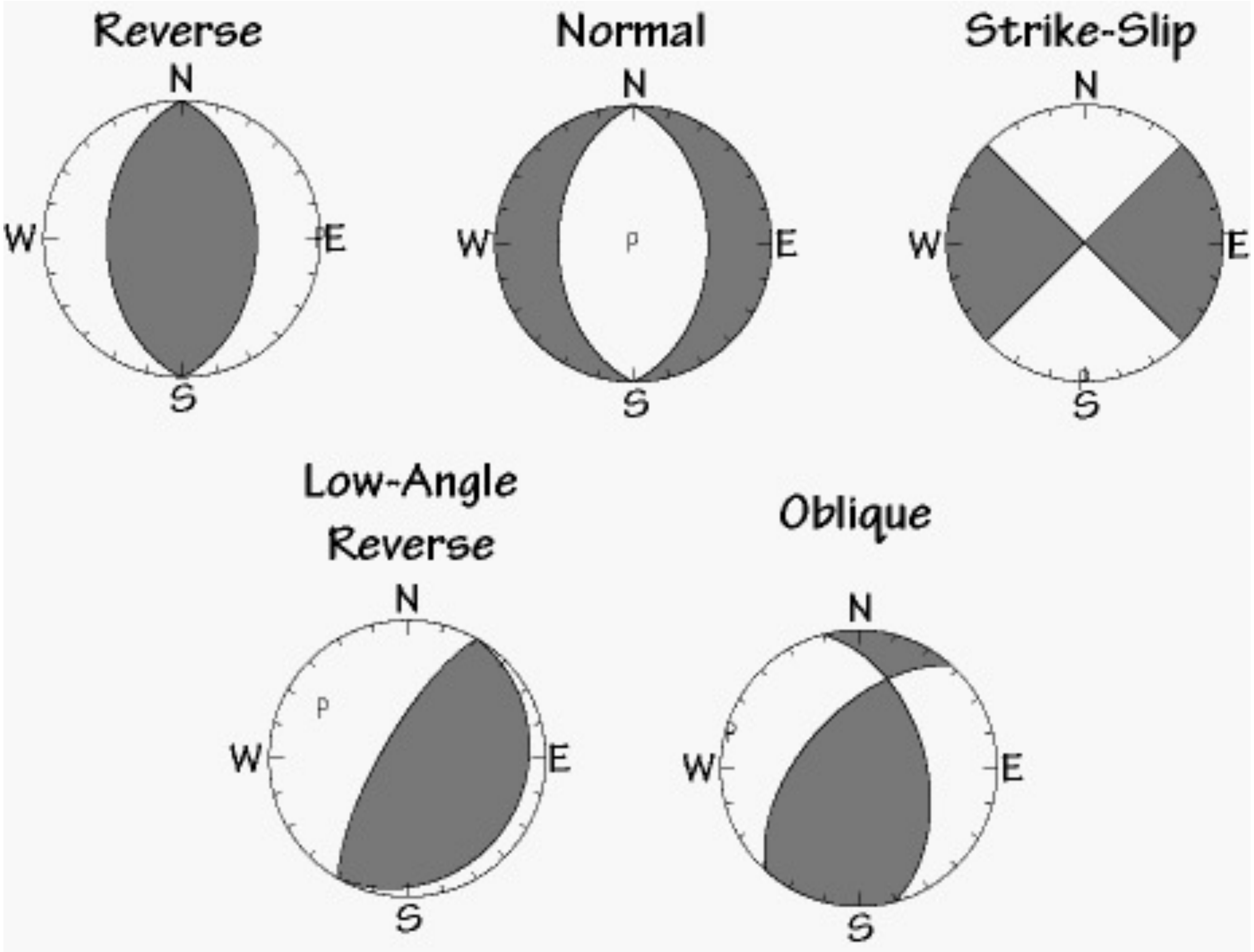

Quantification of EQs sources

Finite fault source model

Static quantities

- Fault geometry and Rupture area (A)
- Slip distribution.
- Moment: M_0 $\underline{\underline{M_0(t)}}$

Kinematic quantities

- Moment rate function
- Source Duration: T
- Rupture velocity, Slip Time function

Quantification of EQs sources

Seismic Moment tensor
(N.m)

$$\underline{\underline{M_0}} = \iint_{Fault\_area} \mu(\underline{s} \cdot {}^t\underline{n} + \underline{n} \cdot {}^t\underline{s})\, dx\, dy$$

where s is slip, $\underline{n}$ is unit vetor nomal to fault
And μ is elastic shear modulus (30 to 50 GPa)

Scalar seismic Moment
(N.m)

$$M_0 = \mu S_{mean} A = \mu \iint_{Fault\_area} S(x,y)\, dx\, dy$$

where S_{mean} is average slip, A is surface area
and 'μυ' is elastic shear modulus (30 to 50 GPa)

Slip Potency (in m^3):

$$P = SA = \iint_{Fault\_area} s(x,y)\, dx\, dy$$

Moment Magnitude:

(where M_0 in N.m)

$$\mathrm{M_w} = \frac{2}{3} \log M_0 - 6$$

Earthquake Phenomenology

- The 2013 Balochistan EQ
- The 2015, Gorkha EQ
- The 1992, Landers EQ

Reference: Avouac, J. P., F. Ayoub, S. J. Wei, J. P. Ampuero, L. S. Meng, S. Leprince, R. Jolivet, Z. Duputel, and D. Helmberger (2014), The 2013, Mw 7.7 Balochistan earthquake, energetic strike-slip reactivation of a thrust fault, *Earth and Planetary Science Letters*, *391*, 128-134.

The Sept, 24, 2013, Mw7.7 Balochistan Earthquake

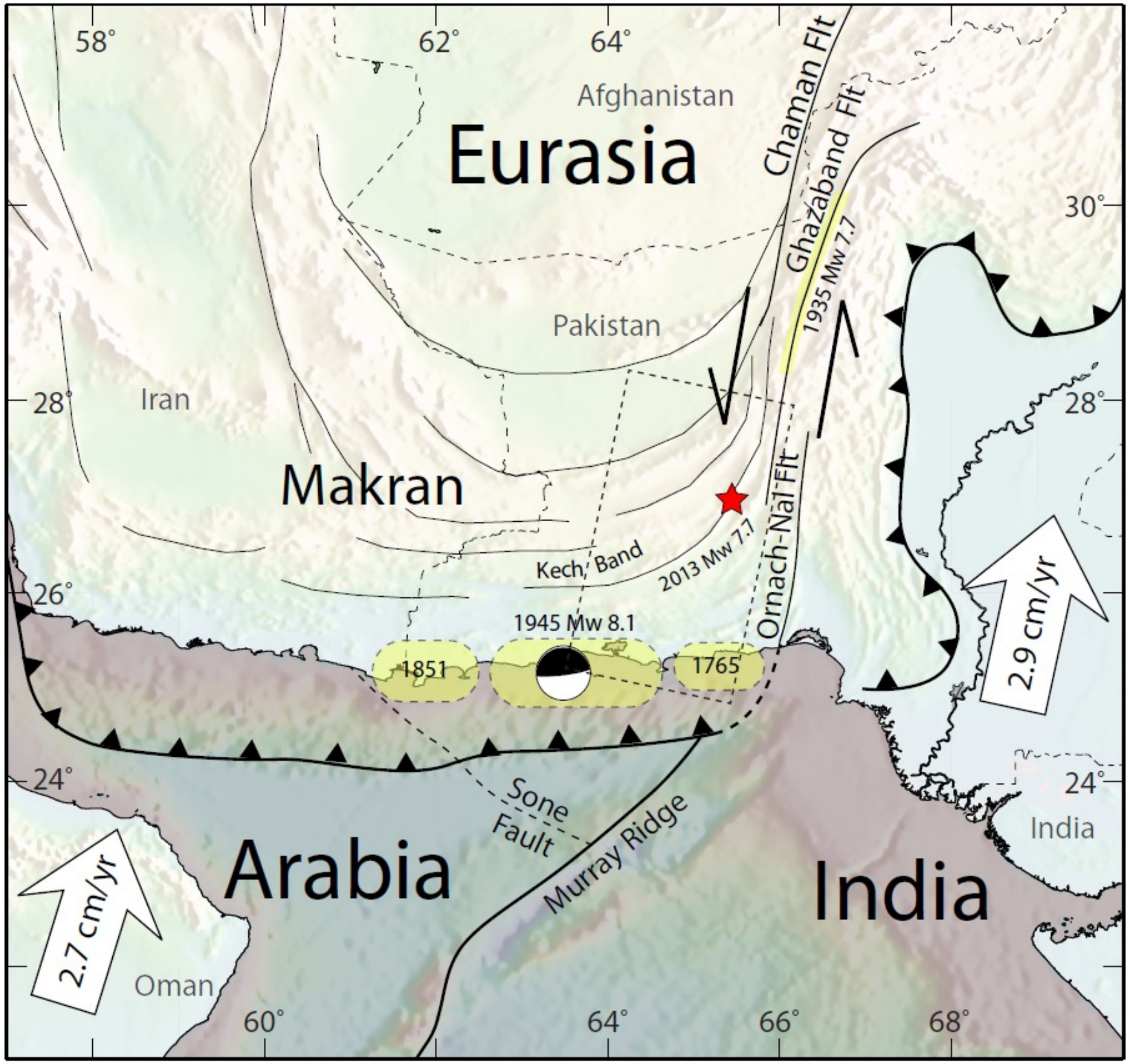

Mww moment tensor

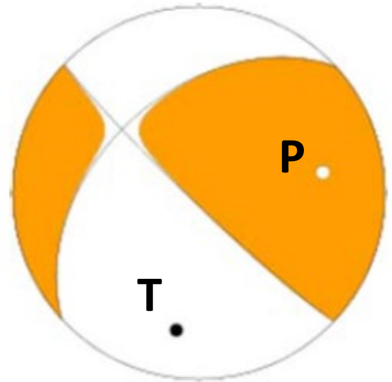

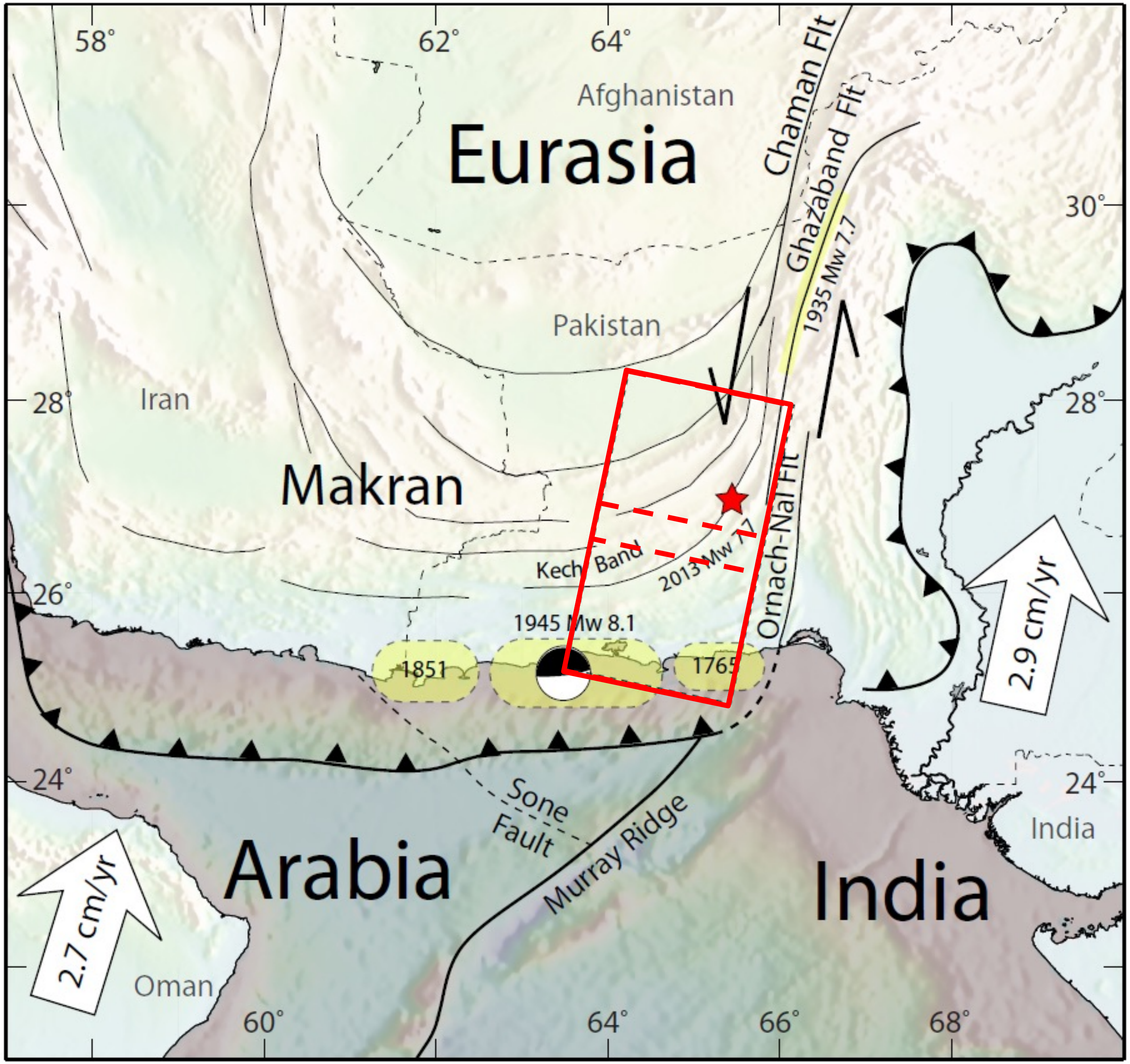

Landsat-8 images:

- USGS website
- GSD: 15 meters
- Pre-earthquake images September, 10, 2013 (14 days before)
- Post-earthquake images September, 26, 2013 (2 days after)

Image Processing (COSI-Corr)

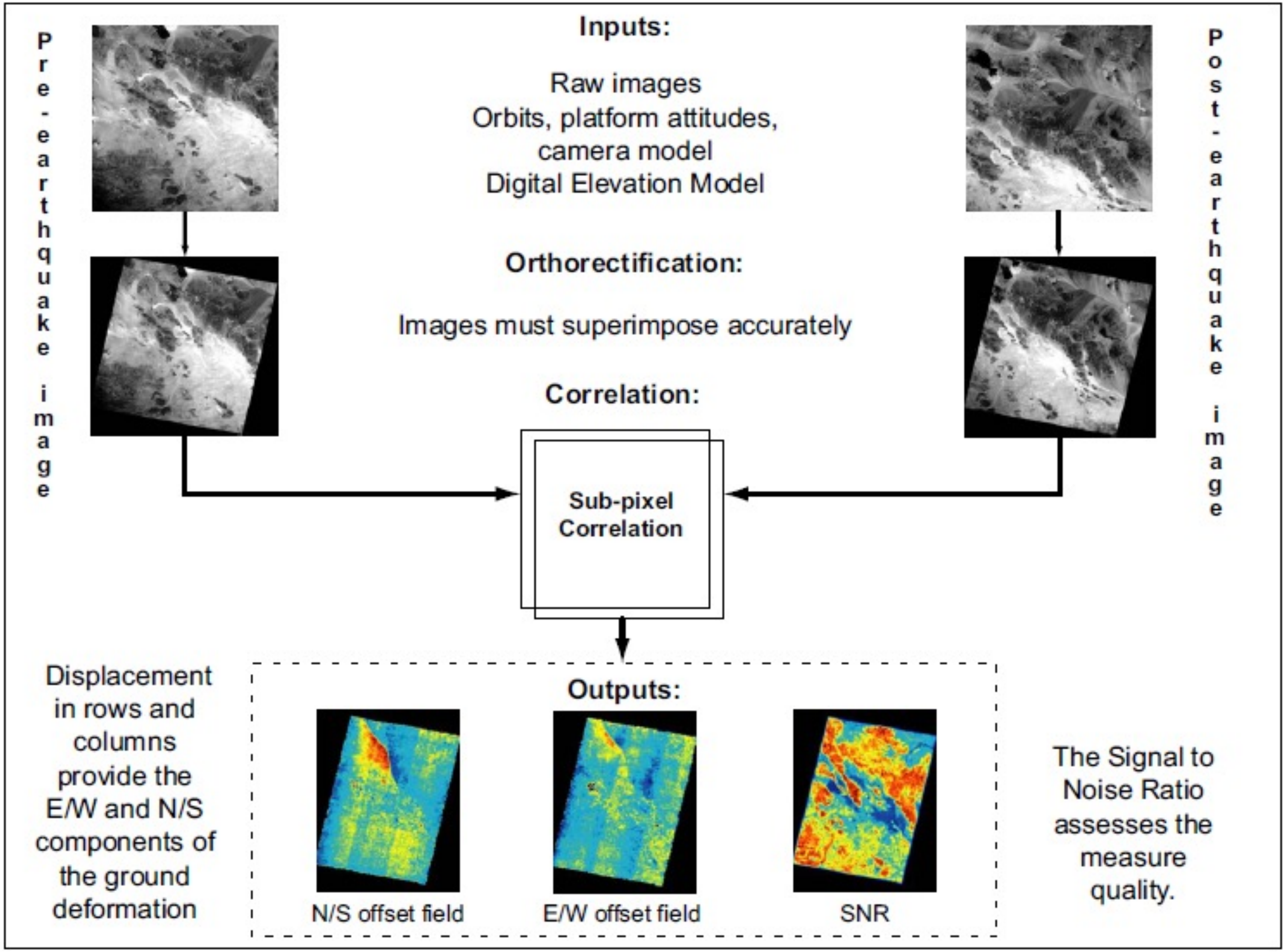

(Leprince et al, 2007)

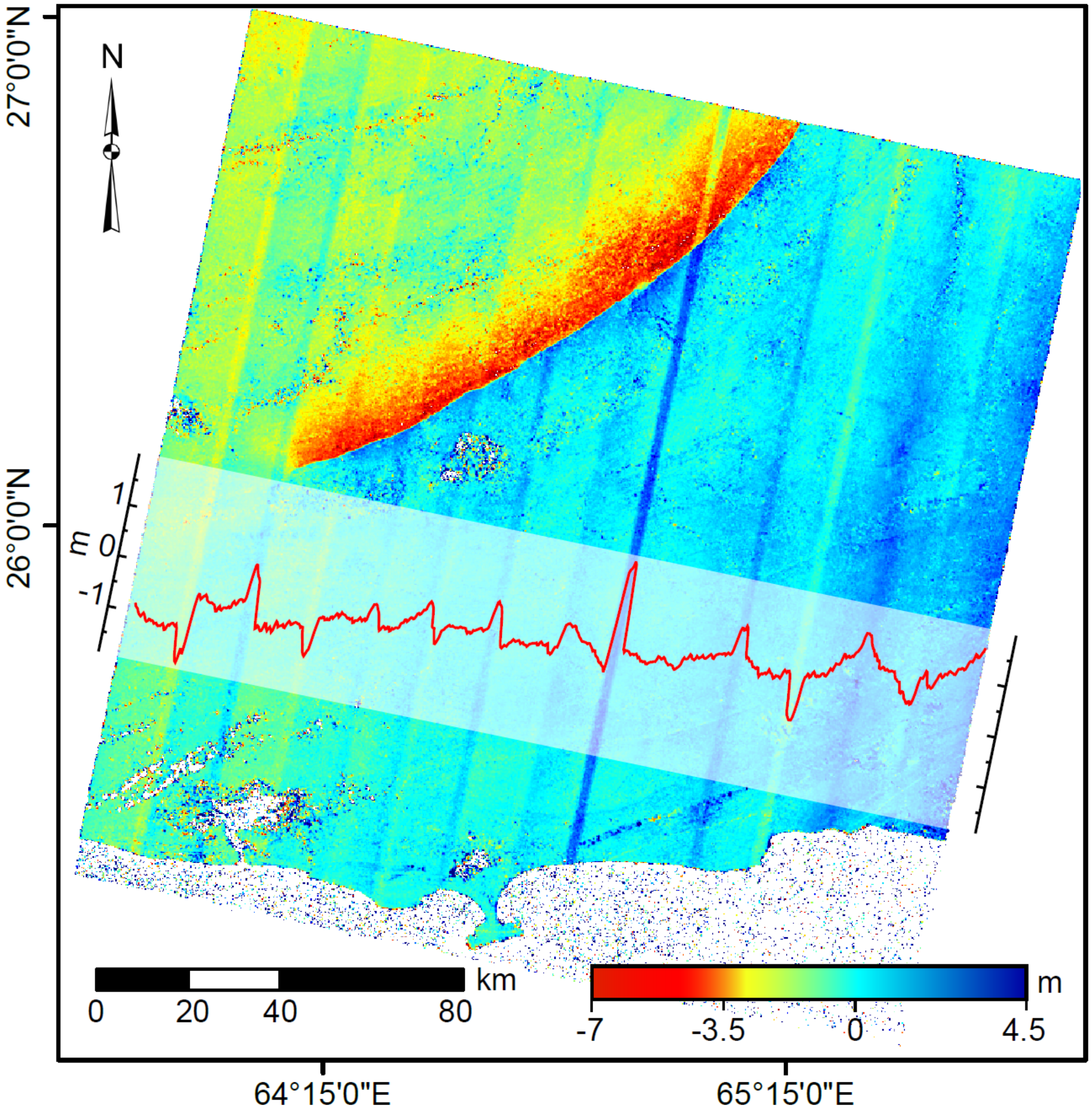

27°0'0"N
26°0'0"N
N
m
1
0
-1
km
0
20
40
80
m
-7
-3.5
0
4.5
64°15'0"E
65°15'0"E

Measured Surface Displacement Field

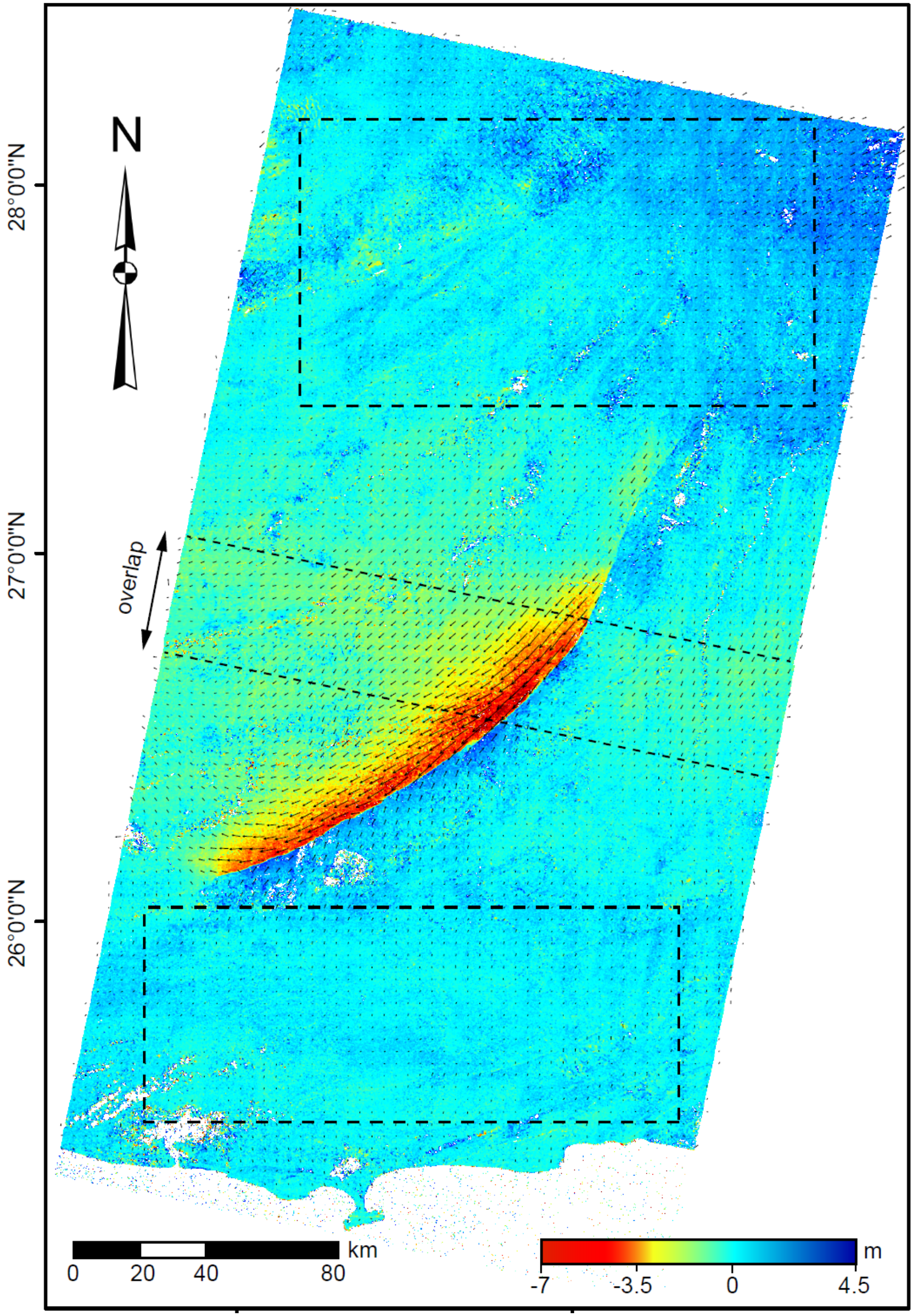

- Window size : 64x64 pixels (960x960 m)
- Step (GSD of displacement maps): 16 pixels (**240 m**)
- 1-σιγμα uncertainly: **30 cm**

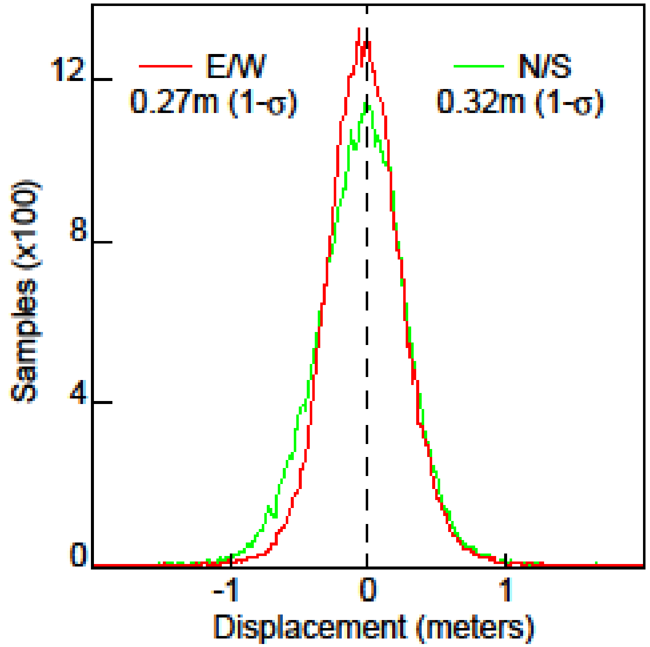

- Amplitude of NS component
- Horizontal displacement vector field

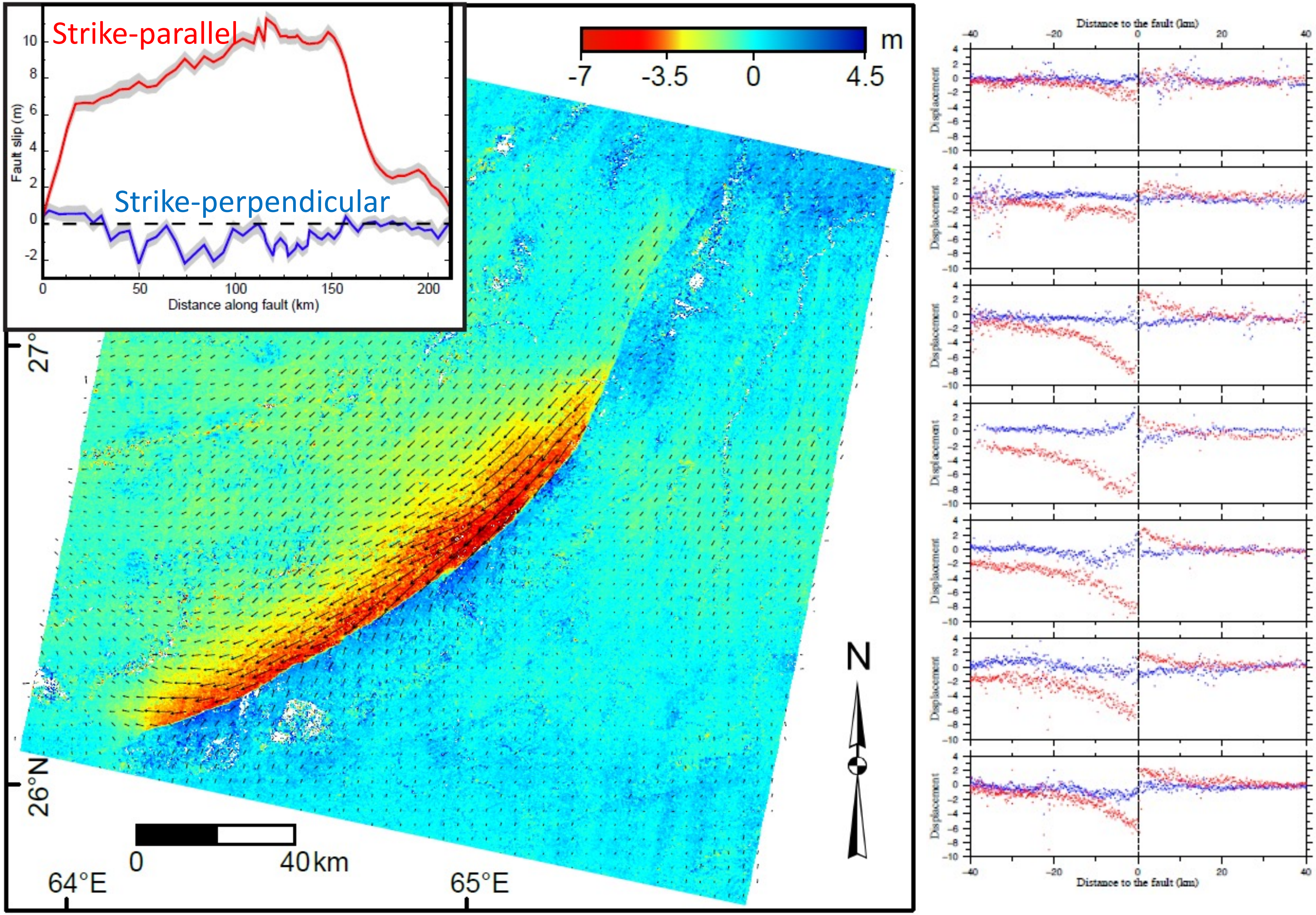

Strike-parallel
Strike-perpendicular
Fault slip (m)
Distance along fault (km)
-7
-3.5
0
4.5
m
27°
26°N
0
40km
64°E
65°E
N
Distance to the fault (km)
Displacement

The Sept, 24, 2013, Mw7.7 Balochistan Earthquake

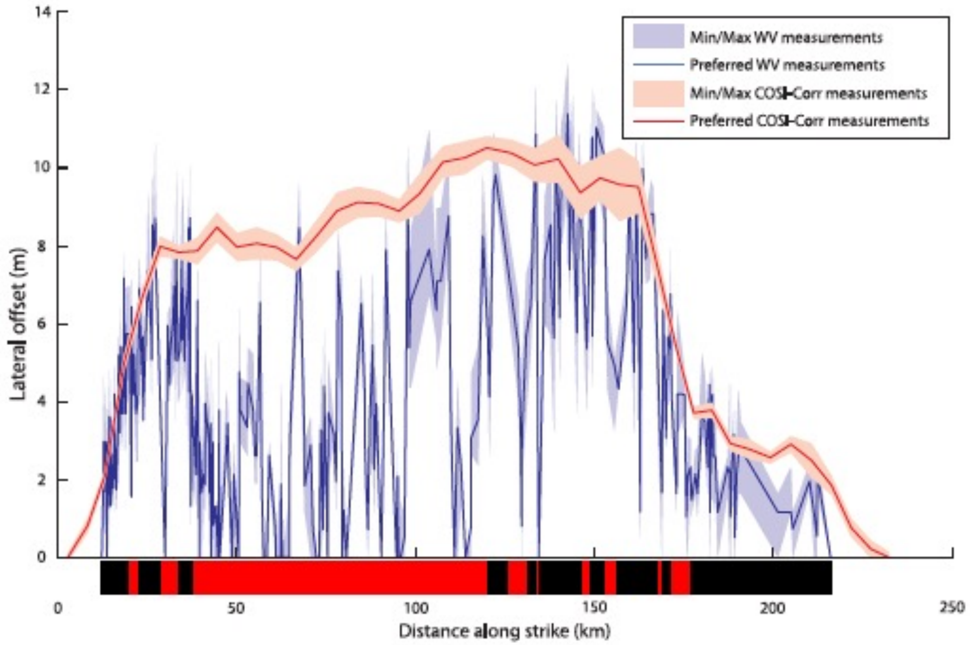

Figure 6. Comparison of offset measurements as a function of distance along the rupture. Red line represents offset measurements from COSI-Corr analysis of Landsat-8 data. Blue line shows offset of geomorphic features measured along the main trace of the rupture as determined by visual analysis of WorldView <0.6 m resolution satellite images. Shaded fields represent the maximum and minimum reasonable slip values. The colors along the bottom of the figure represent structurally simple (black) and structurally complex (red) sections of the fault.

(Zinke, Hollingsworth and Dolan, 2015)

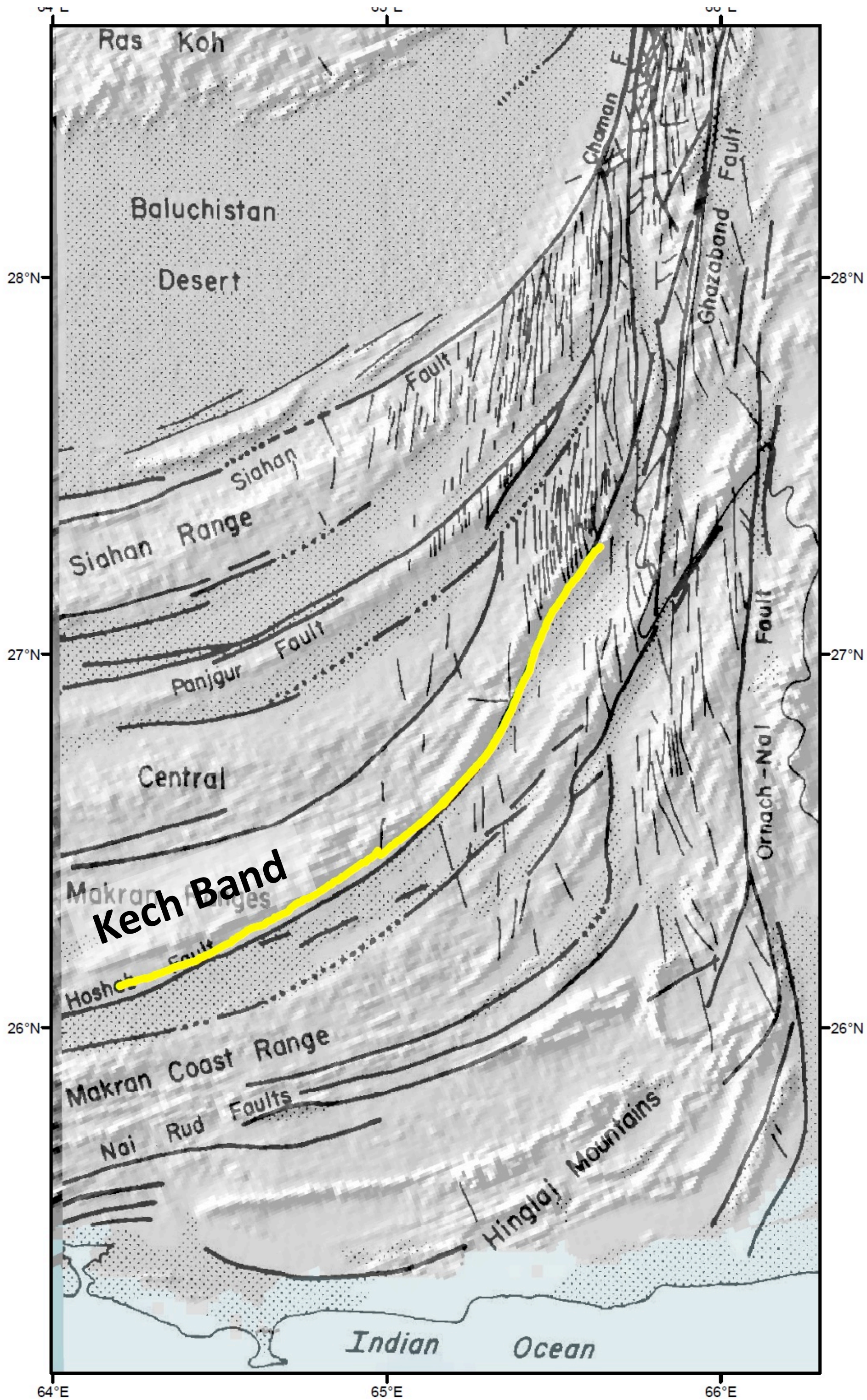

The rupture falls on the **Hosbah fault** along the front of the **Kech Band**, a preexisting thrust fault within the Makran accretionnary prism

(Lawrence, Kahn,Dejong, Farah and Yeats, 1981)

Rupture kinematics from backprojection of Teleseismic waveforms

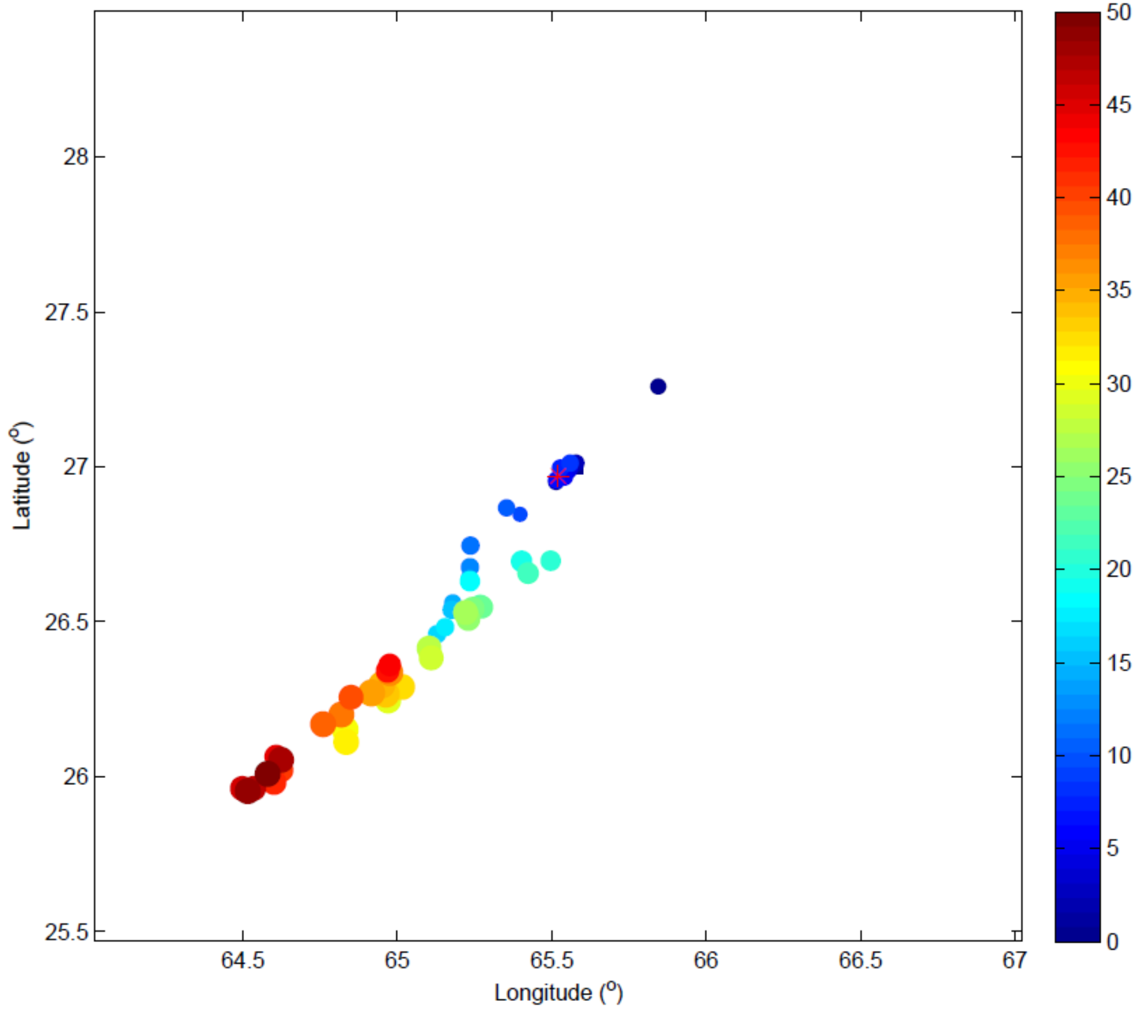

- Data: **Japanese Hi-net** seismic network
- **Multitaper-MUSIC array** processing technique (Meng et al, 2011)
- Frequency band: **0.5-2Hz**
- HF source duration: **50s**

Rupture kinematics from backprojection of Teleseismic waveforms

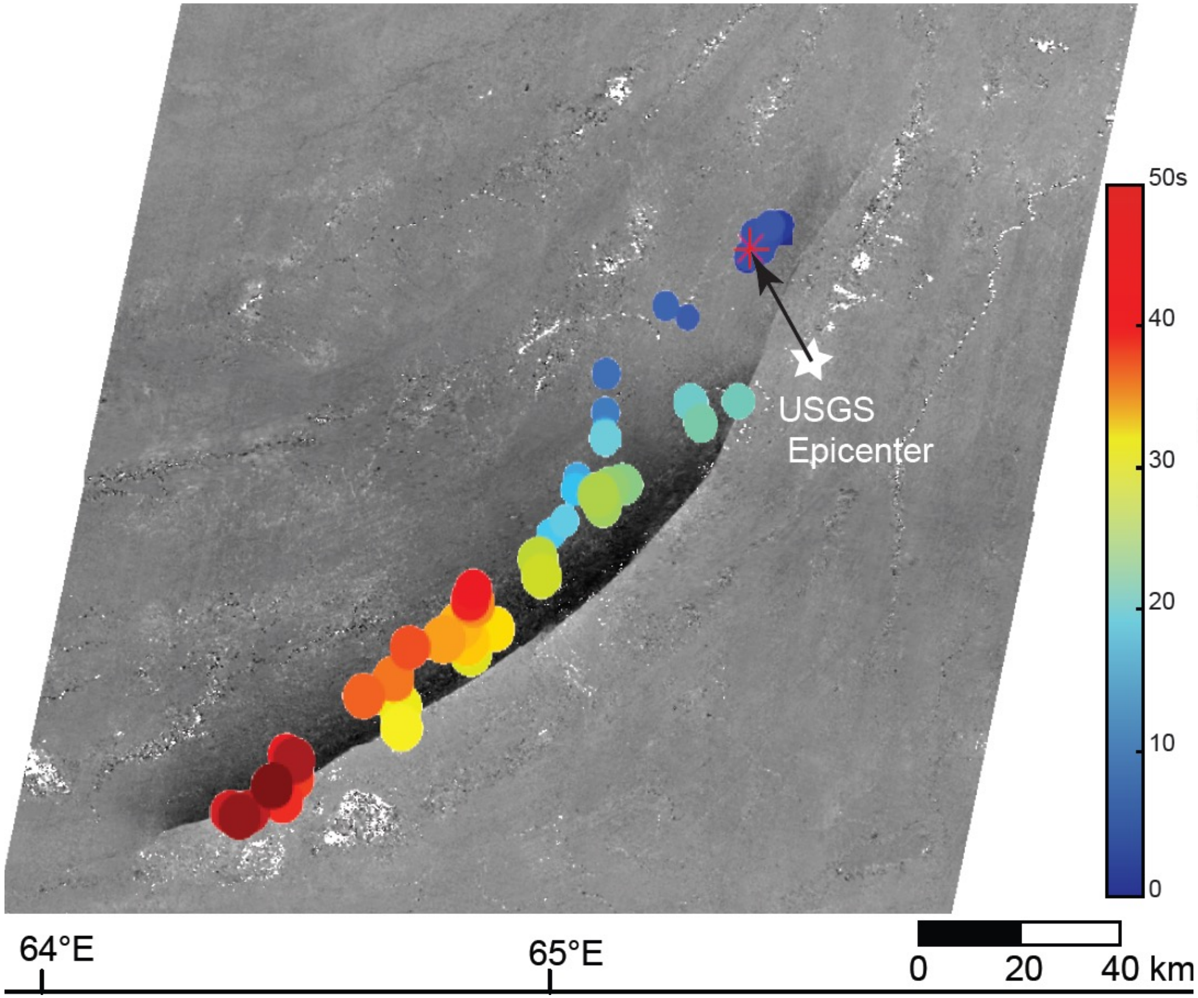

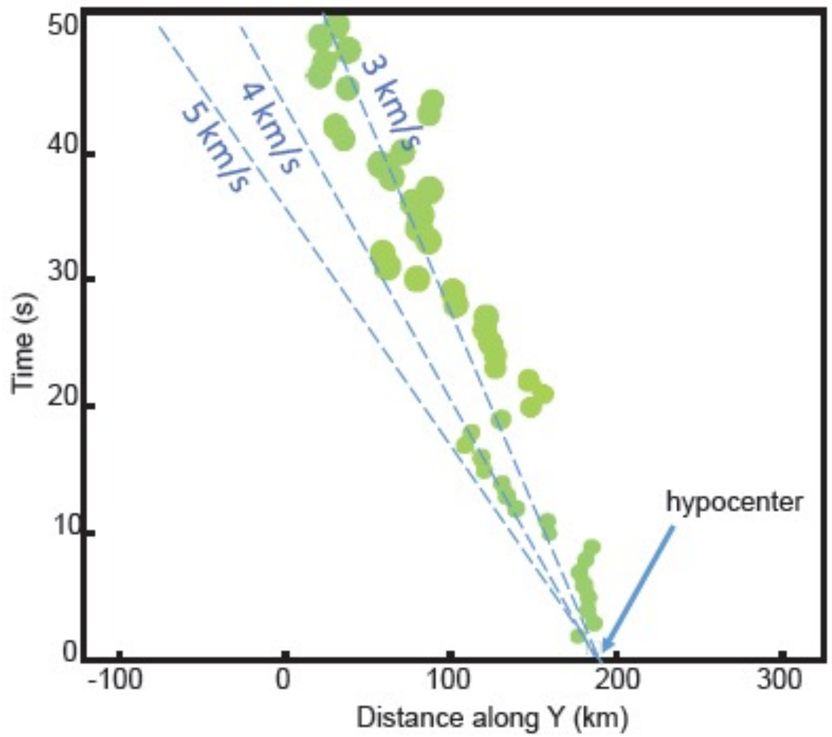

Backprojection of teleseismic waveforms (Hi-NET), 0.5-2Hz

Finite Source Model

Forward modeling of ground velocity: (assuming a pulse-like source)

$$u(t) = \sum_{j=1}^{n}\sum_{k=1}^{m} D_{jk}[\cos(\lambda_{jk})Y_{jk}^{1}(v_{jk},t) + \sin(\lambda_{jk})Y_{jk}^{2}(v_{jk},t)]\dot{S}_{jk}(t)$$

Y_{jk}^{1} : *Green's Functions along strike*

Y_{jk}^{2} : *Green's Functions along dip*

λ_{jk} : *Rake*

$S_{jk}(t)$: *Source time function*

D_{jk} : *Final slip at* (j,k)

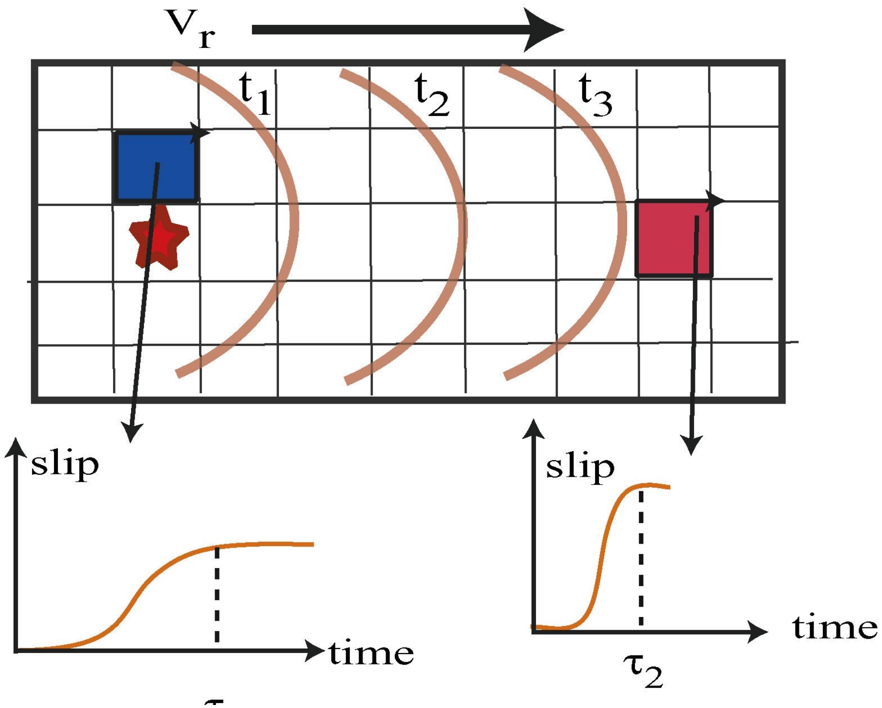

$$\dot{S}(t) = \frac{1 - \cos(2\pi\ t/r)}{r}, \quad 0 < t < r.$$

NB: Green's functions are calculated with a crustal layered structure in the source region, then use ray theory to propagate to the receiver

Inversion:

A simulated annealing algorithm is used to simultaneously invert for the slip, rise time and rupture velocity

(Ji, C., D. J. Wald and D. V. Helmberger, 2002a.b, *BSSA)*

Finite Source Model

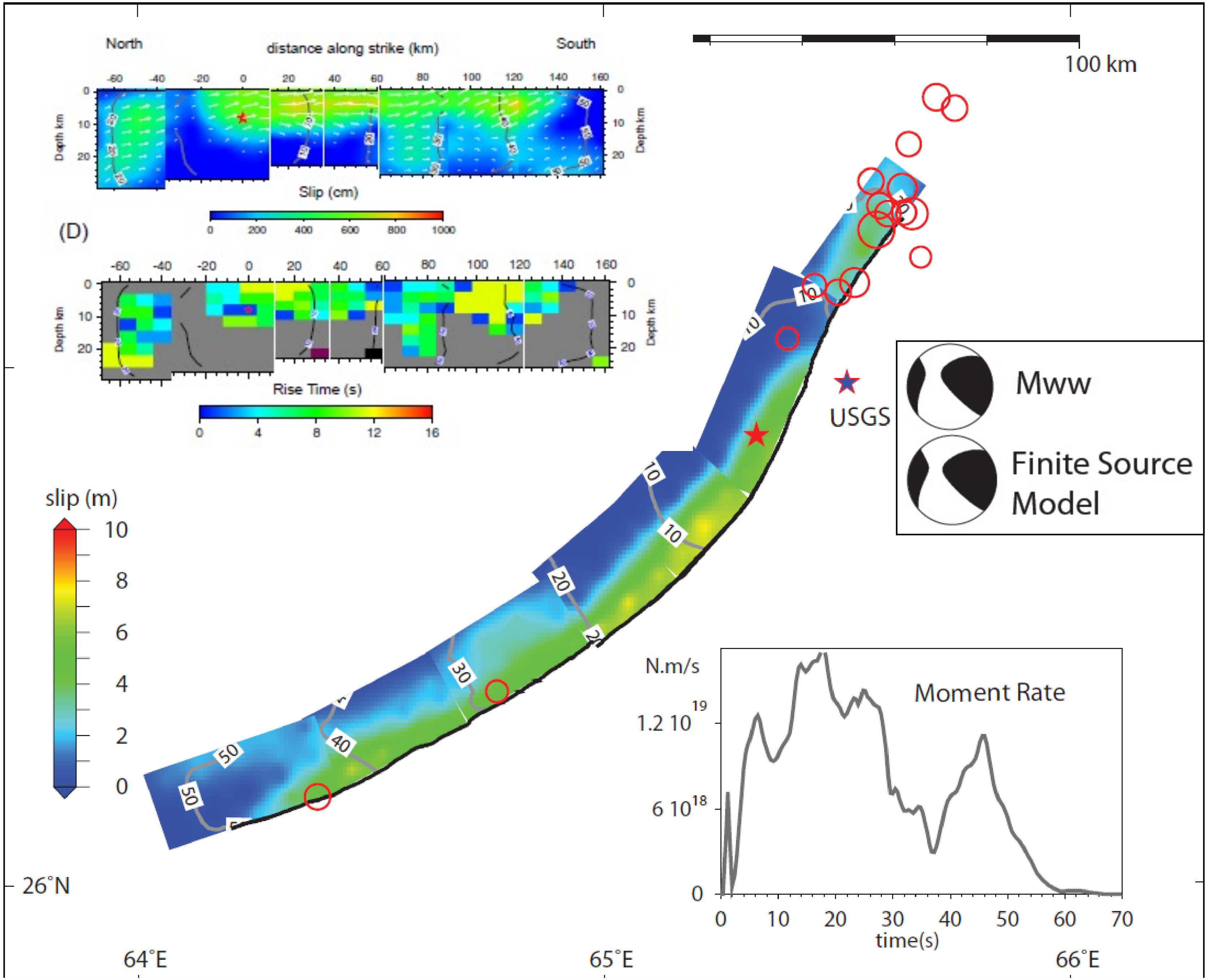

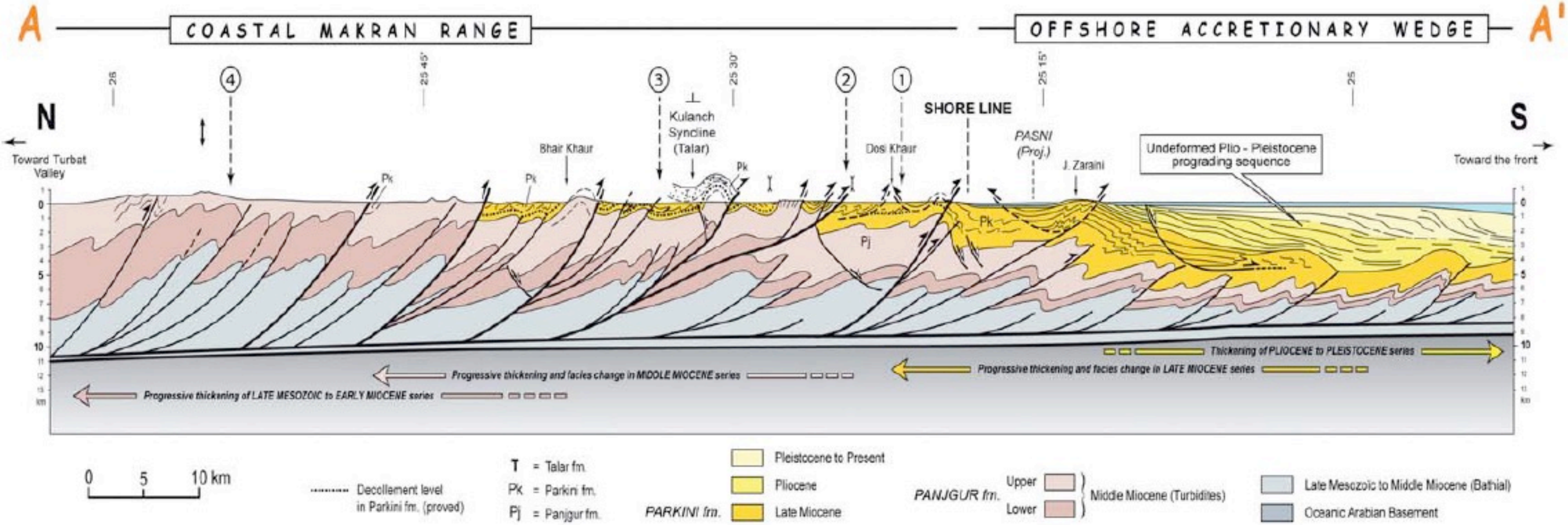

Fig. 8. North-South cross-section from Turbat to Pasni: the age of the basal detachment is unknown, but probably located in Paleogene or older bathial series; note (1) the tectonic progression of the prism while sedimentary wedges are prograding over the already deformed Miocene series; (2) the strong disharmony at the base of Parkini slope fm, level locally used as a secondary décollement.; (3) normal faults which are progressively younger to the south

(Ellouz-Zimmermann et al, 2007)

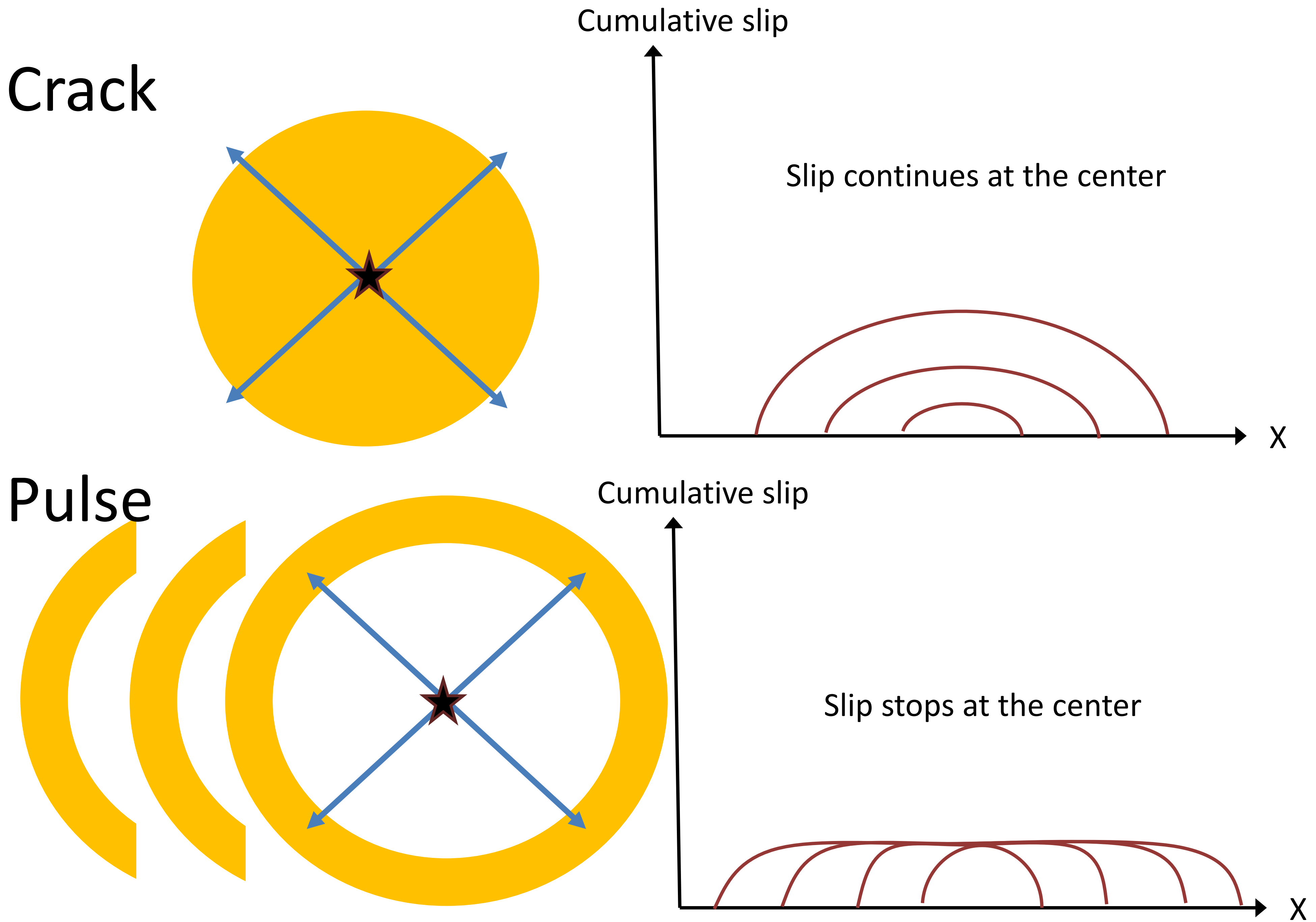
Crack
Cumulative slip
Slip continues at the center
X
Pulse
Cumulative slip
Slip stops at the center
X

Phenomenology of earthquake ruptures

- Seismic ruptures "pulse like" (e.g, Heaton, 1990) for large earthquakes (Mw>7) with rise times of the order of 3-10s typically
- the rupture velocity is variable during the rupture but generally 0.7 to 0.9 the shear wave velocity. (2.5-3.5 kms). It is occasionnally 'supershear' (>3.5-4km/s).
- Seismic sliding rate is generally of the order of 1m/s
- Large earthquakes typically ruptures faults down to 15km within continent and down to 30-40km along subduction Zones.
- Seismic ruptures are affected by fault geometries. They often stop at geometric complexities but can jump across significant stepovers
- Slip variability measured at the small scale is probably due to off-fault anelastic defomation

References-EQ phenomenology

Avouac, J. P., F. Ayoub, S. J. Wei, J. P. Ampuero, L. S. Meng, S. Leprince, R. Jolivet, Z. Duputel, and D. Helmberger (2014), The 2013, Mw 7.7 Balochistan earthquake, energetic strike-slip reactivation of a thrust fault, *Earth and Planetary Science Letters*, *391*, 128-134.

Barbot, S., N. Lapusta, and J. P. Avouac (2012), Under the Hood of the Earthquake Machine: Toward Predictive Modeling of the Seismic Cycle, *Science*, *336*(6082), 707-710.

Heaton, T. H. (1990), Evidence for and implications of self-healing pulses of slip in earthquake rupture, *Physics of the Earth and Planetary Interiors*, *64*, 1-20.

Ji, C., D. Wald, and D. V. Helmberger (2002), Source Description of the 1999 Hector Mine, California Earthquake, Part I: Wavelet Domain Inversion Theory and Resolution Analysis, *Bulletin of the Seismological Society of America*, *92*(4), 1192-1207.

Kanamori, H., and E. E. Brodsky (2004), The physics of earthquakes, *Reports on Progress in Physics, 67(8), 1429-1496.*

Meng, L. S., J. P. Ampuero, Y. D. Luo, W. B. Wu, and S. D. Ni (2012), Mitigating artifacts in back-projection source imaging with implications for frequency-dependent properties of the Tohoku-Oki earthquake, *Earth Planets and Space*, *64*(12), 1101-1109

Toward physics-based Earthquake Forecasting

I. Introduction

II. EQ phenomenology-point source and Finite source models

III EQ phenomenology-Scaling properties

IV ‘Elastic Dislocation’ and ‘crack’ models

V Interseismic deformation

VI Postseismic deformation

VII Kinematic to Dynamic models of the seismic cycle

VII The seismic cycle in the Himalaya

VIII Earthquake forecasting

The Mw7.8 Gorkha earthquake

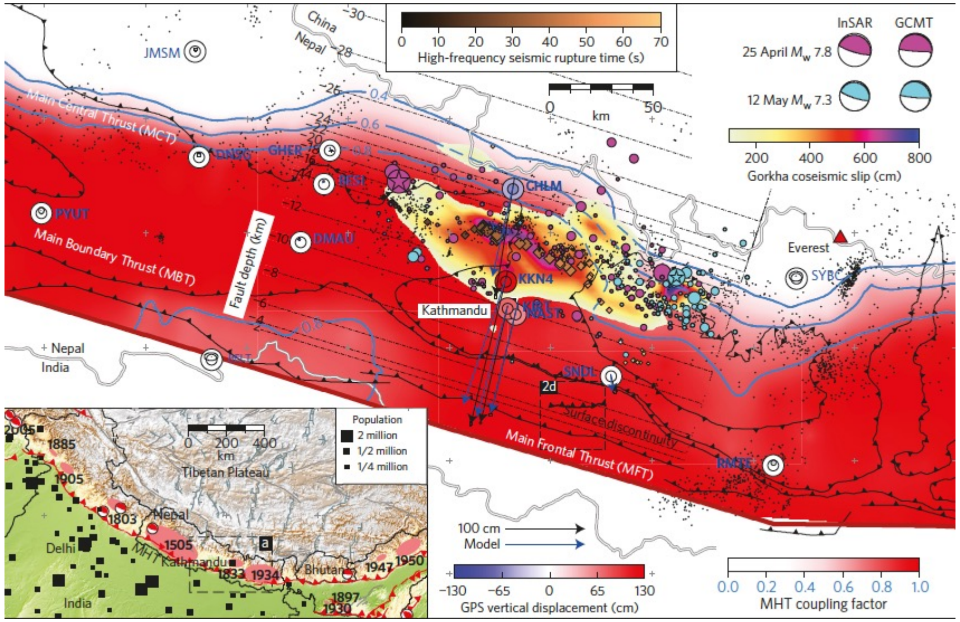

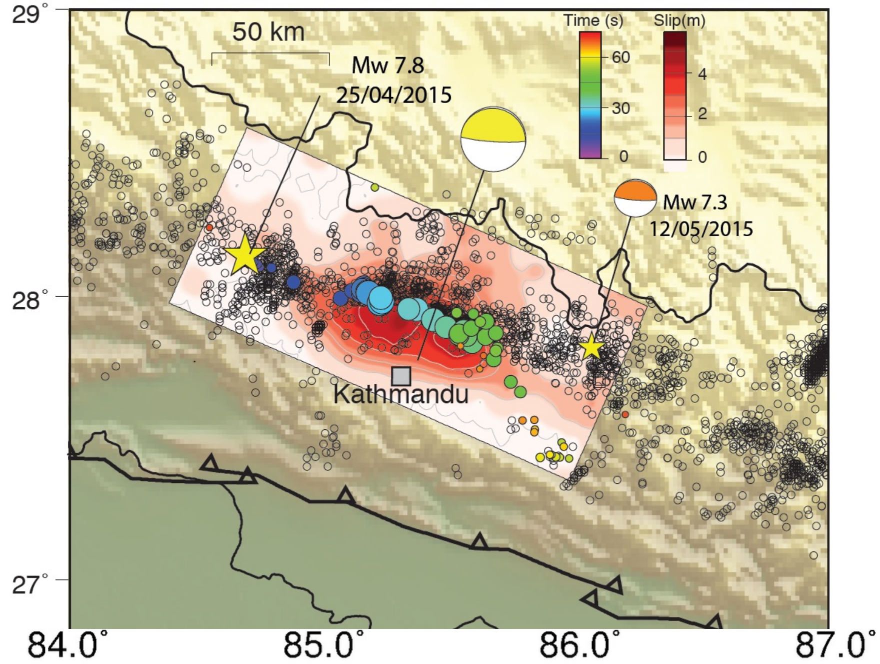

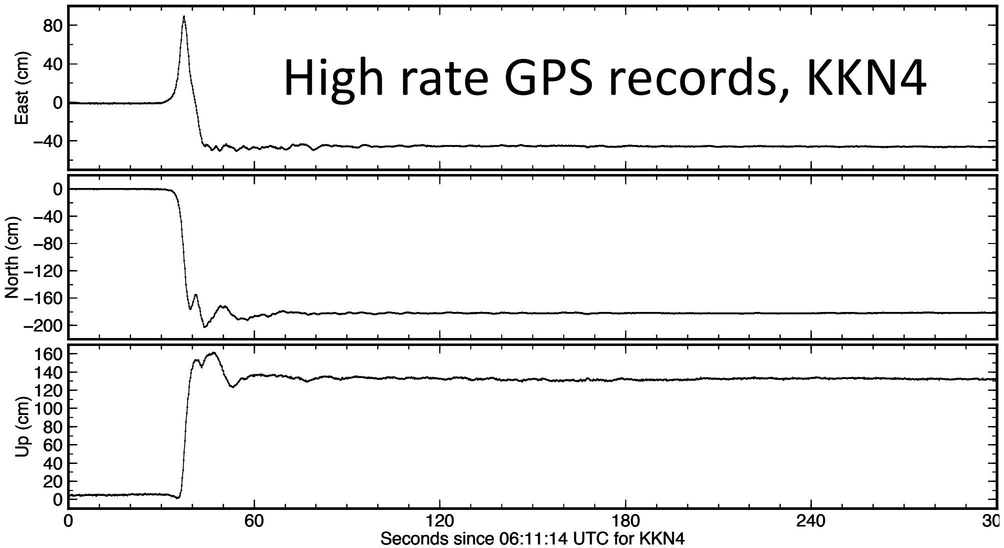

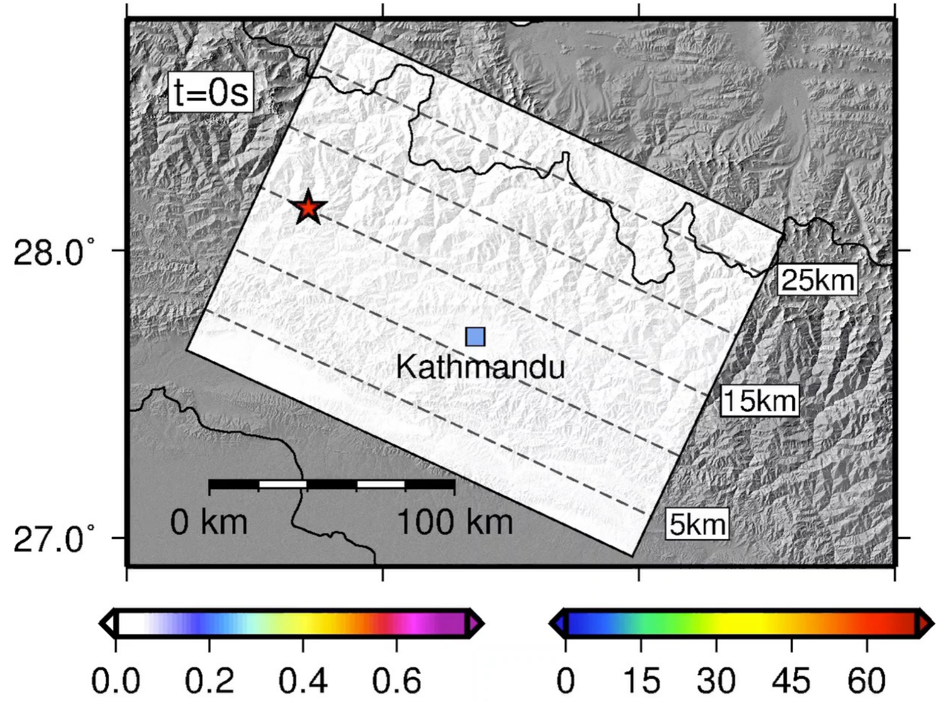

(Avouac et al., 2015; Galetzka et al., 2015)

The Gutenberg-Richter law

Let N (≥ M) be number of EQs per year with magnitude ≥ M

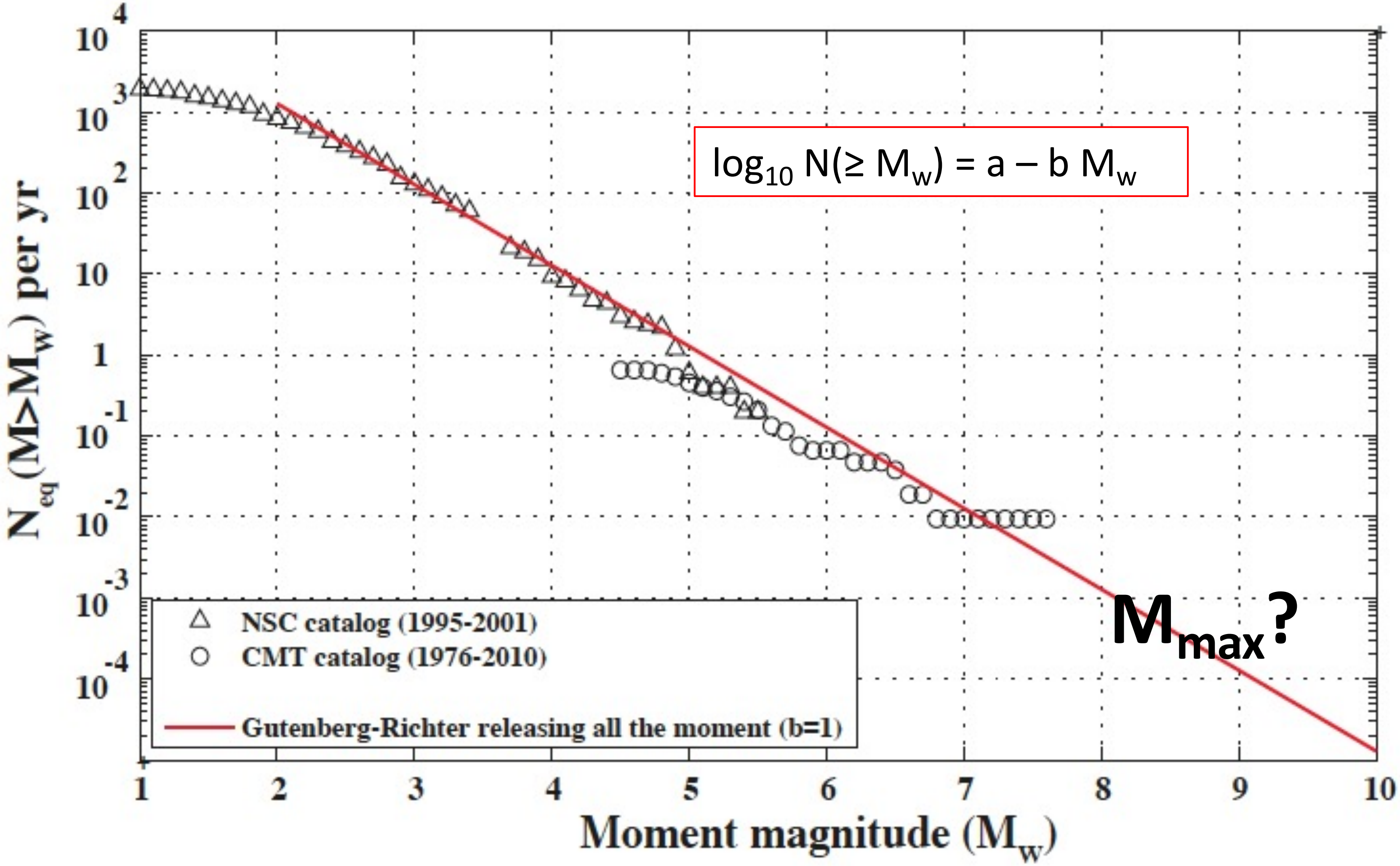

Expected Maximum Magnitude over 1 year: ~5

P(M>7, 1yr) ~ 10^{-2}

Earthquakes clustering in time and space

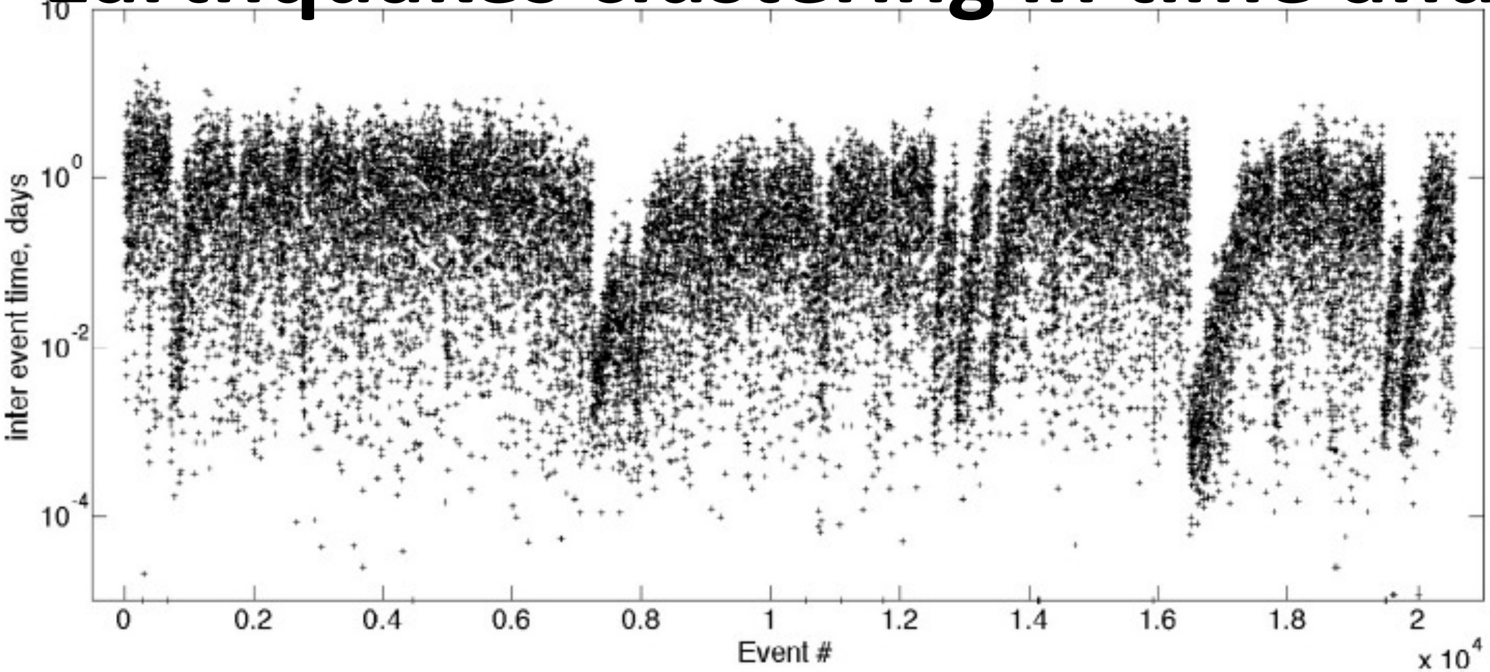

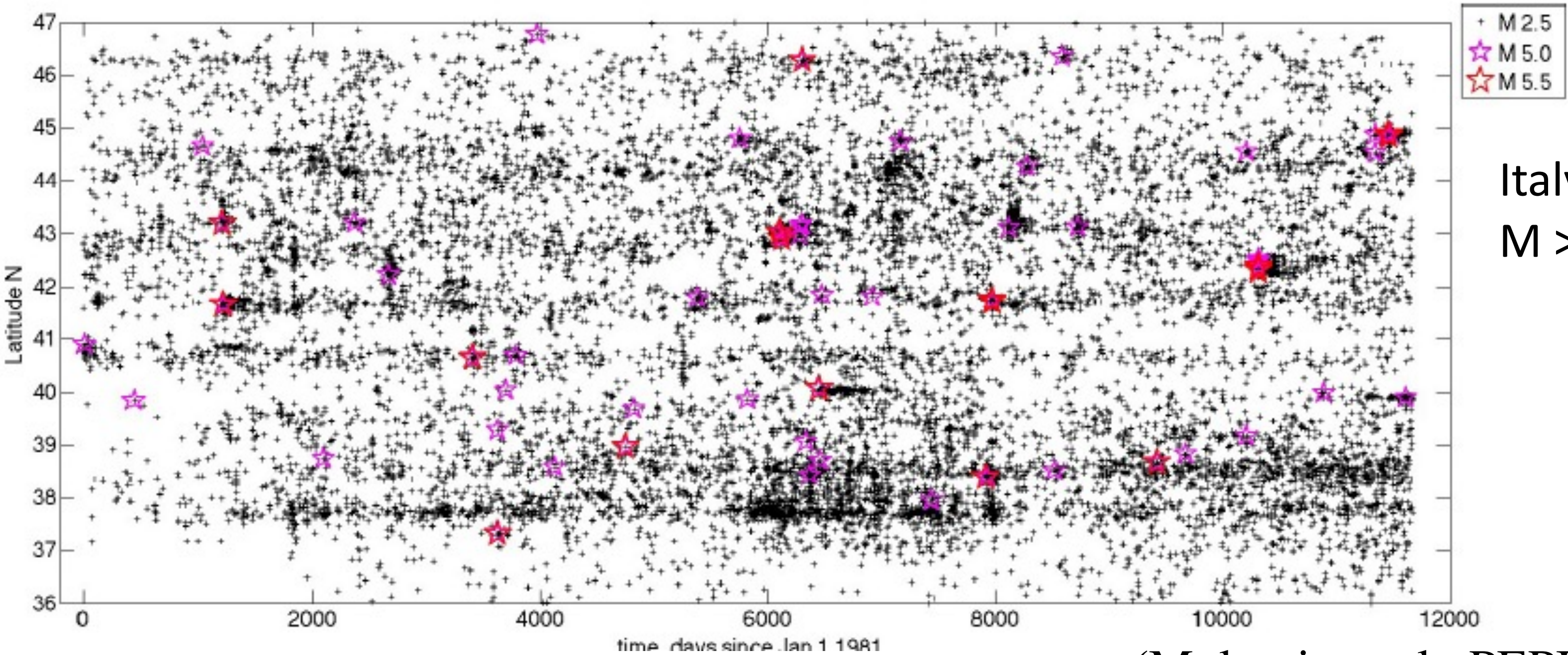

Italy, 1981-2015
M >2.5 events

(Mulargia et al., PEPI, 2017)

Earthquakes clustering in time and space

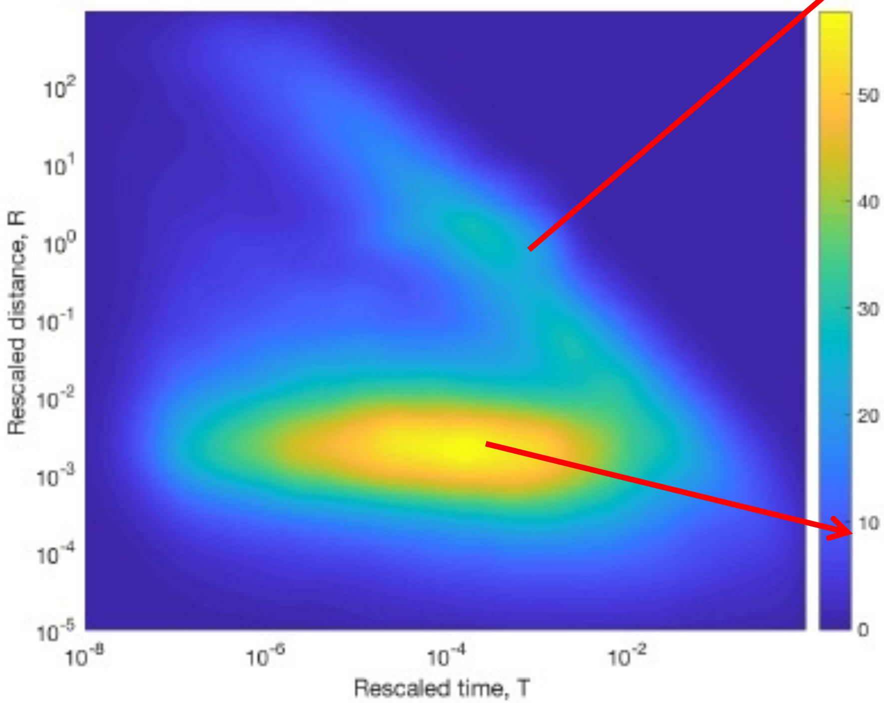

Background
Poisson process

Aftershocks,
Omori Law

$$n(t) = \frac{n(0)}{(1+t/\tau)^p}$$

where p ~ 1

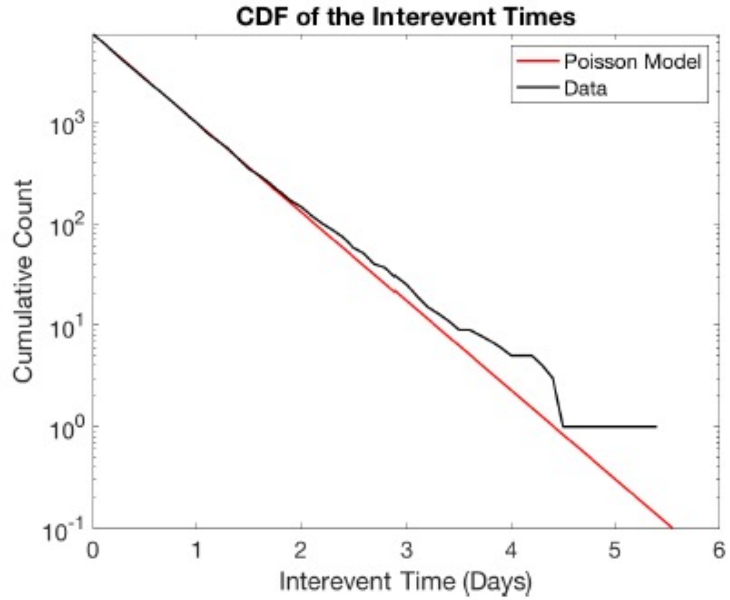

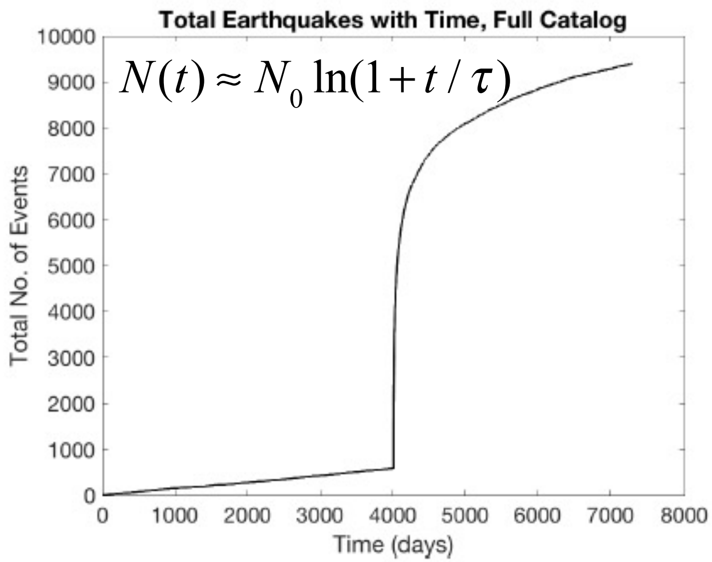

Spatio-temporal Interevent distribution (Zaliapin and Ben-Zion, 2013) Southern California (Ross et al., 2019).

The Omori law (aftershocks)

The decay of aftershock activity follows a **power law**.
Many different mechanisms have been proposed to explain such decay: post-seismic creep, fluid diffusion, rate- and state-dependent friction, stress corrosion, etc… but in fact, we don't know…

$$n(t) = \frac{n(0)}{(1 + t/\tau)^p} \qquad \textbf{where p} \sim \textbf{1}$$

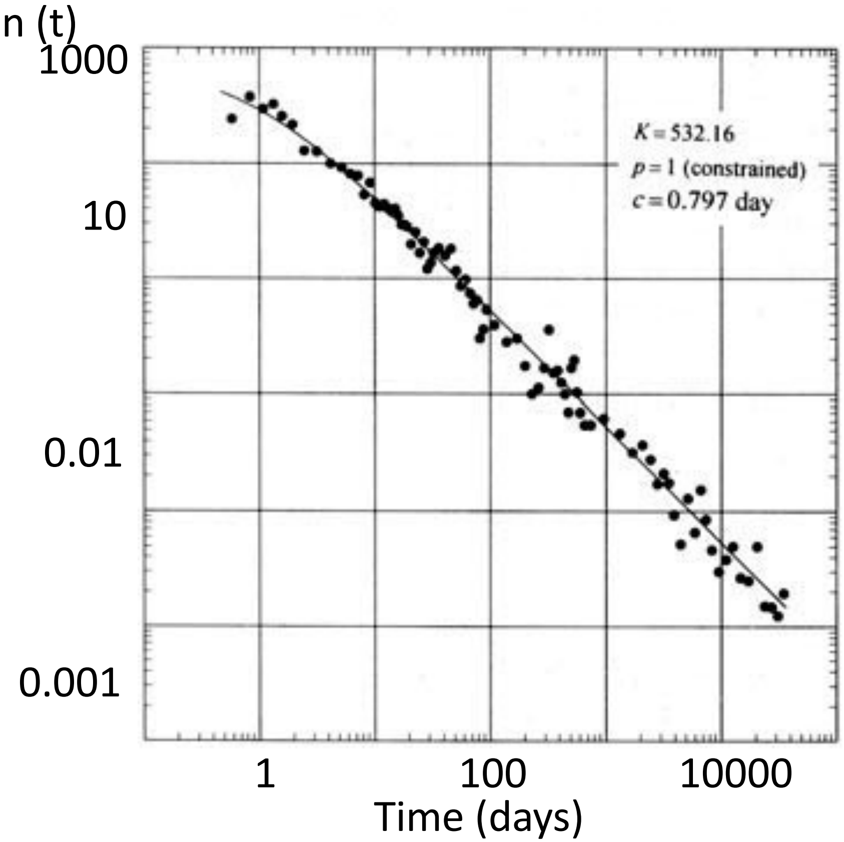

Aftershock decay since the 1891, M=8 Nobi EQ: the Omori law holds over a very long time!

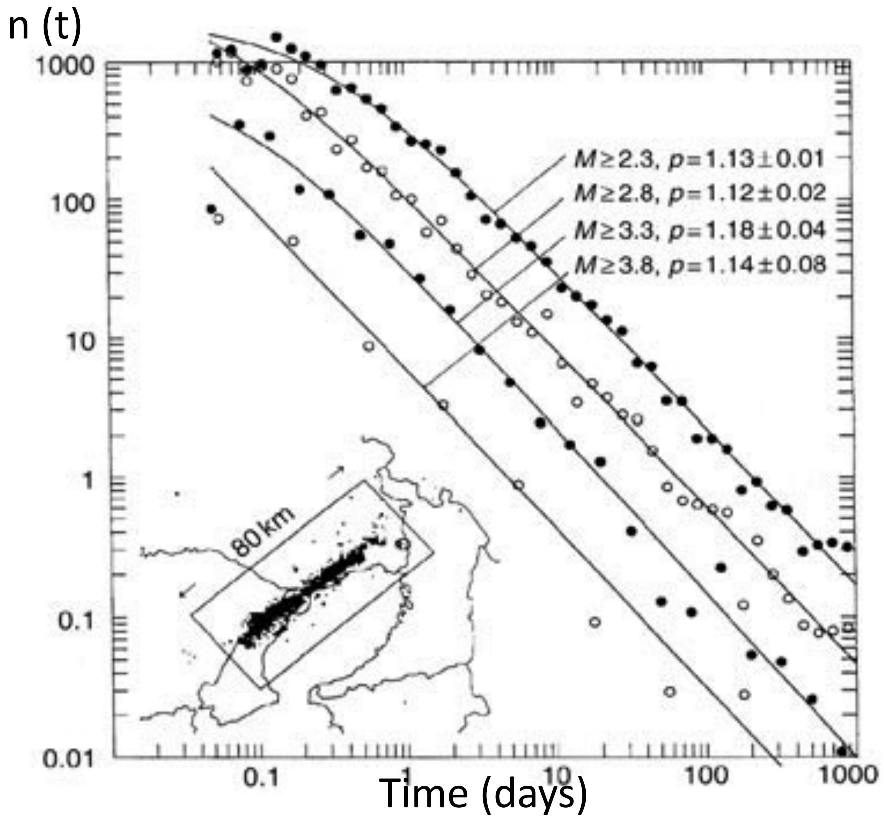

Same for 1995 Kobe EQ

Aftershocks

'Utsu' (1970) Productivity

$$\boxed{K(M) = K_0 \exp[\alpha (M - m_0)]}$$

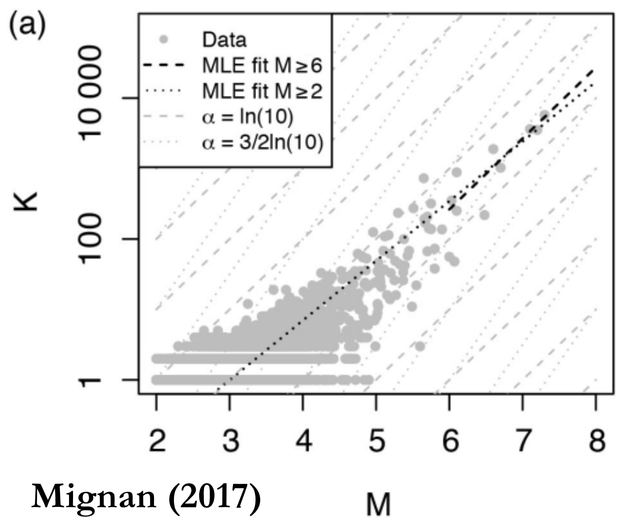

Mignan (2017)

'Omori' (1895) decay

$$\boxed{n(t) = \frac{n(0)}{(1 + t/\tau)^p}} \qquad p \sim 1$$

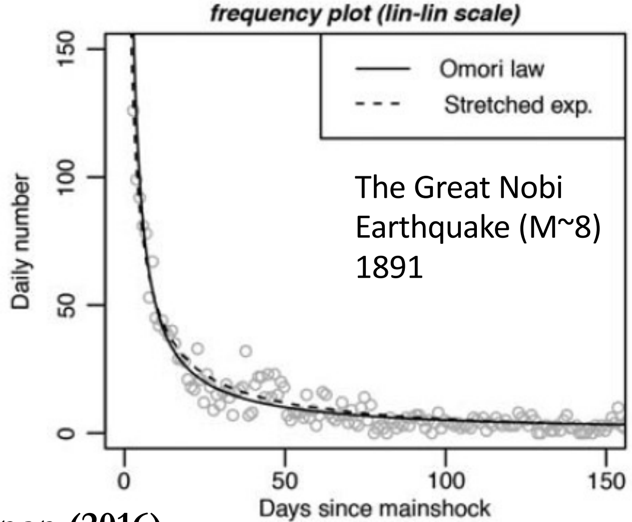

Mignan (2016)

$$\boxed{n(t) = \sum_{t_i < t} \frac{K(m_i)}{(t - t_i + c)^p},}$$

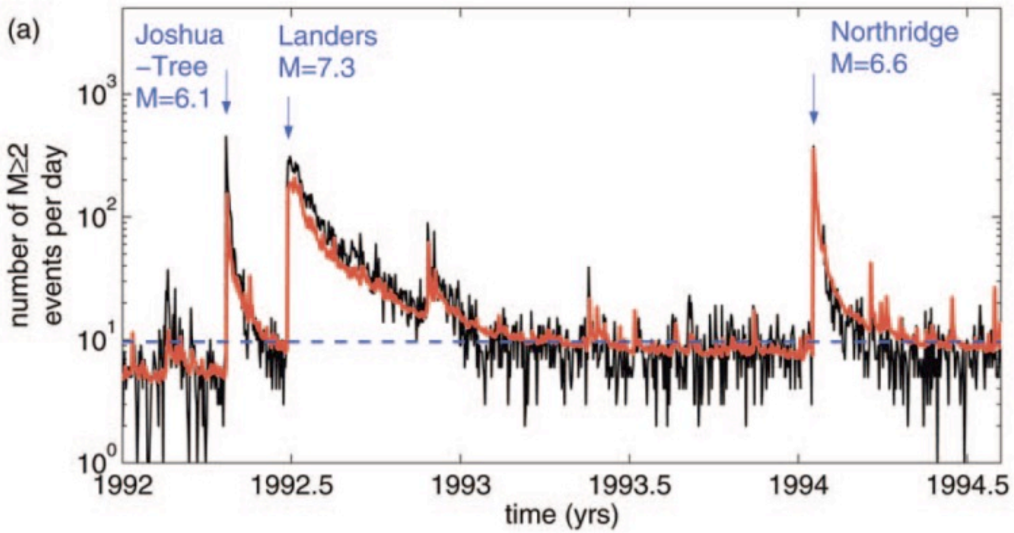

ETAS (*e.g.*, Kagan and Knopff, 1981; Ogata, 1988)

(Helmstetter et al., 2006)

Is recurrence of large earthquakes ('system size') Poissonian or quasi-periodic?

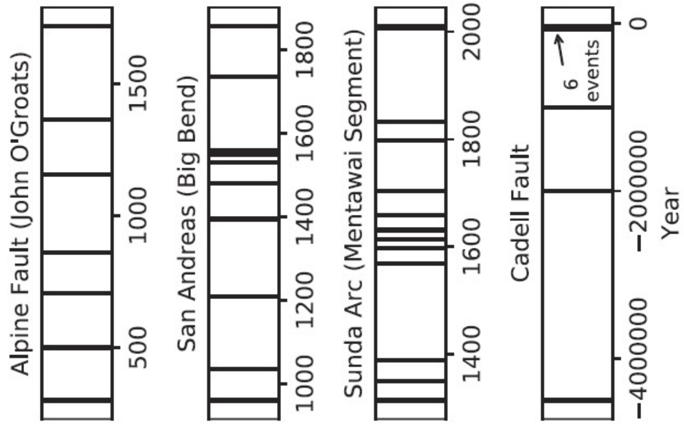

80 long terms records worldwide:

Burstiness= (σ-μ)/(σ+μ)

Memory= $\frac{1}{N-1}\sum_{i=1}^{N-1}\frac{(\tau_i-\mu_2)(\tau_{i+1}-\mu_2)}{\sigma_1\sigma_2}$

Majority of studied faults show weakly periodic and uncorrelated large earthquake recurrence

many low activity-rate (annual occurrence rates < 2 × 10^{-4}) faults show random or clustered earthquake recurrence

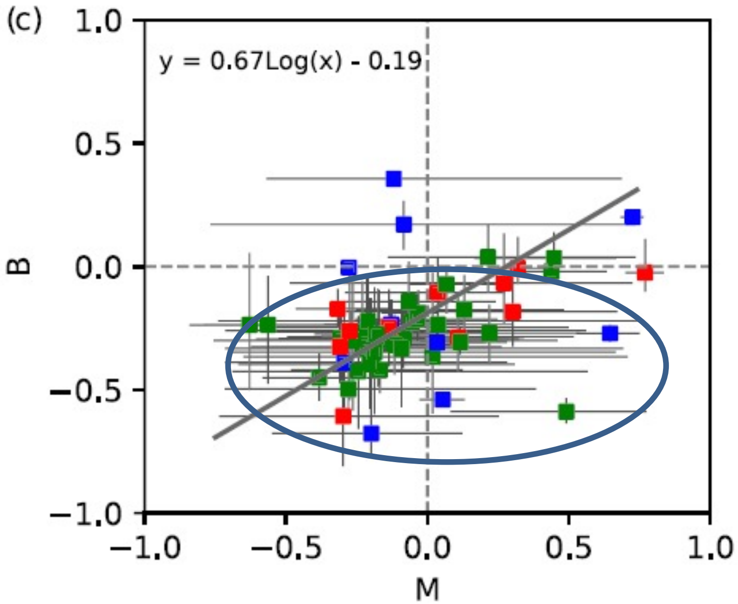

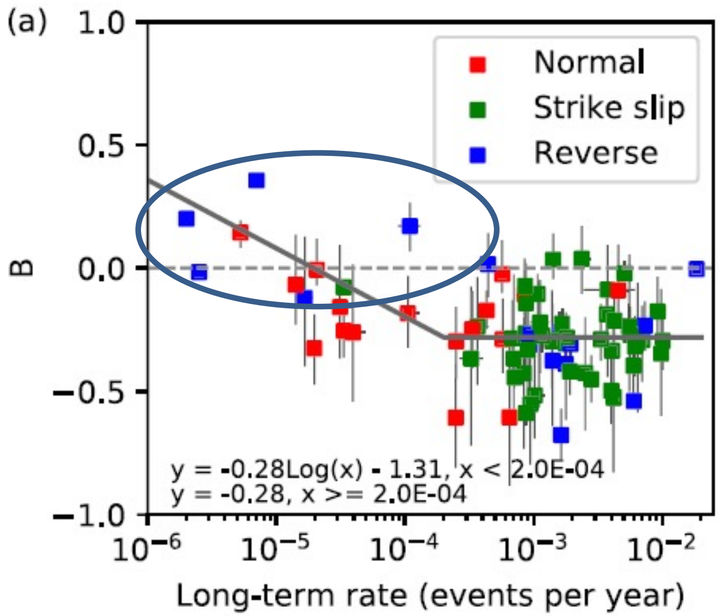

(Griffin et al., 2020)

Moment-Area and Moment-Duration Scaling

M_0: Moment
A: Rupture area
T: Earthquake Duration

$$M_0 = G \underbrace{\iint_{fault\ area} s(x,y)\, dxdy}_{\text{Potency}}$$

G : Shear modulus
s(x,y): slip at point (x,y)

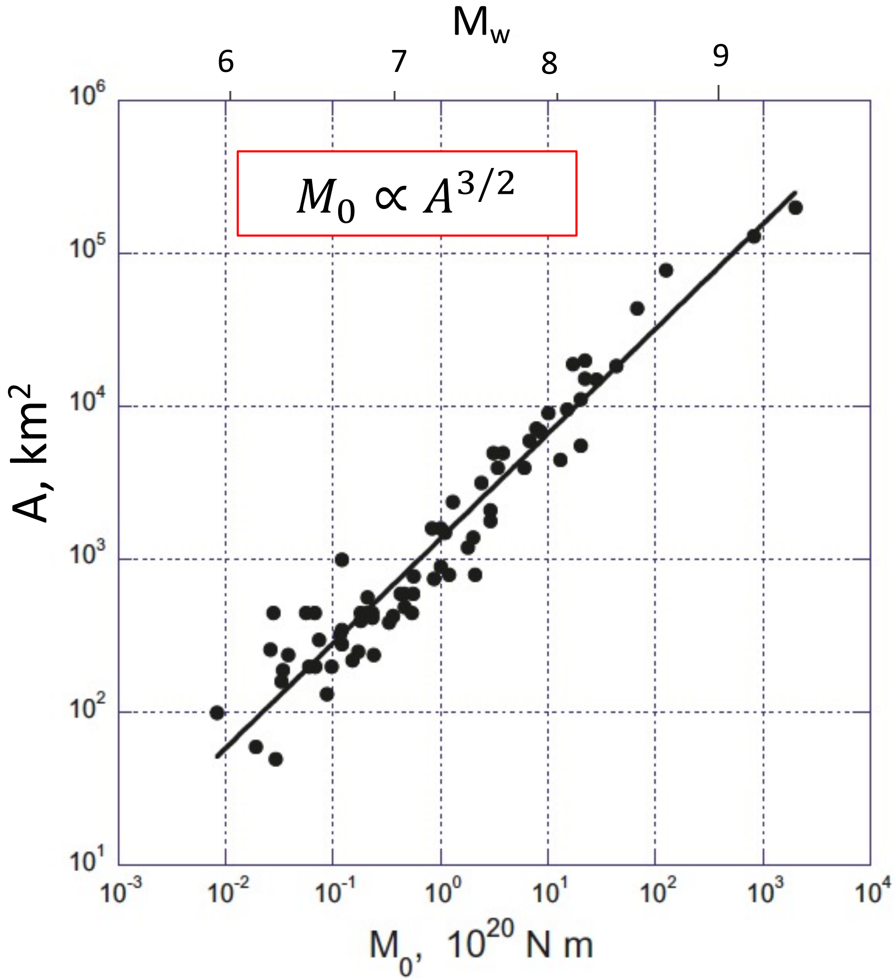

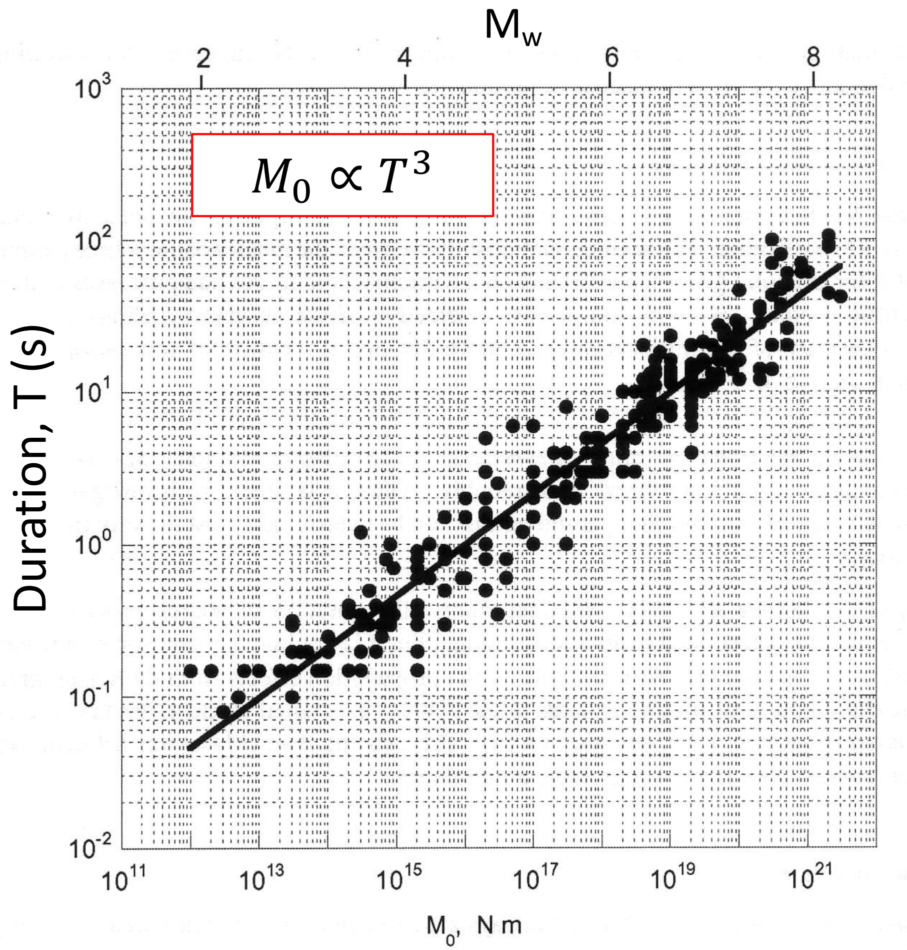

Modified from Kanamori & Brodsky (2004)

The Static Circular Crack Model

Circular crack of radius a with uniform stress drop, $\Delta\sigma$, in a perfectly elastic body (Eshelby, 1957)

$$\boxed{s = \frac{4}{\pi}\frac{(1-\nu)}{(2-\nu)}\frac{\Delta\sigma}{G}\sqrt{a^2 - x^2}}$$

-->

$$S_{mean} = \frac{8}{3\pi}\frac{(1-\nu)}{(2-\nu)}\frac{\Delta\sigma}{G}a$$

G: Shear modulus

ν : Poisson coefficient

Slip

Stress

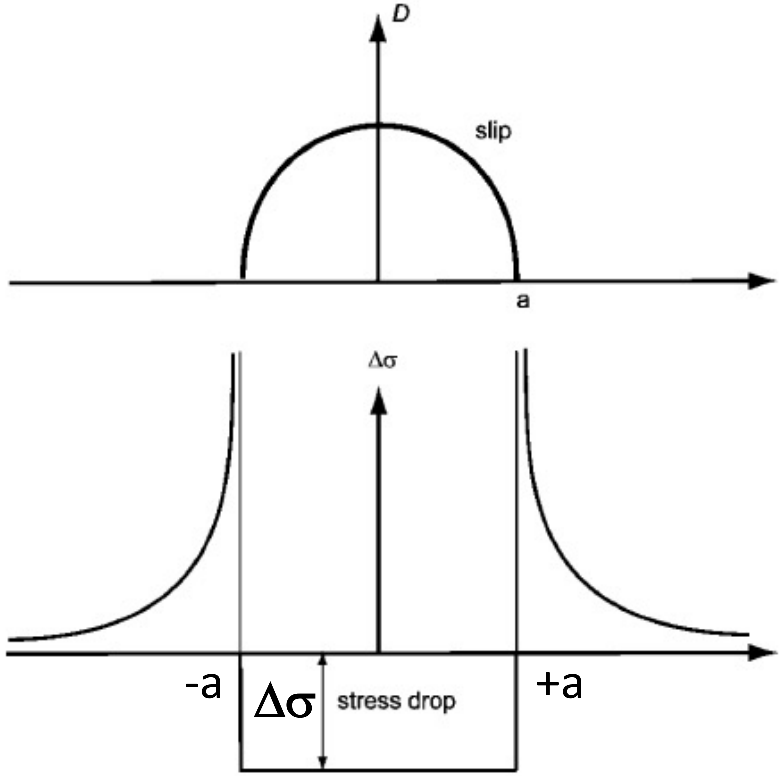

-->

$$\boxed{\Delta\sigma \simeq \frac{7\pi}{8} G \frac{S_{mean}}{\sqrt{A}}}$$

$$M_0 = S_{mean} \cdot A$$

$$\Delta\sigma \approx C \cdot M_0 \cdot A^{-3/2}$$

(e.g., Scholz, 1990)

Moment-Area Scaling

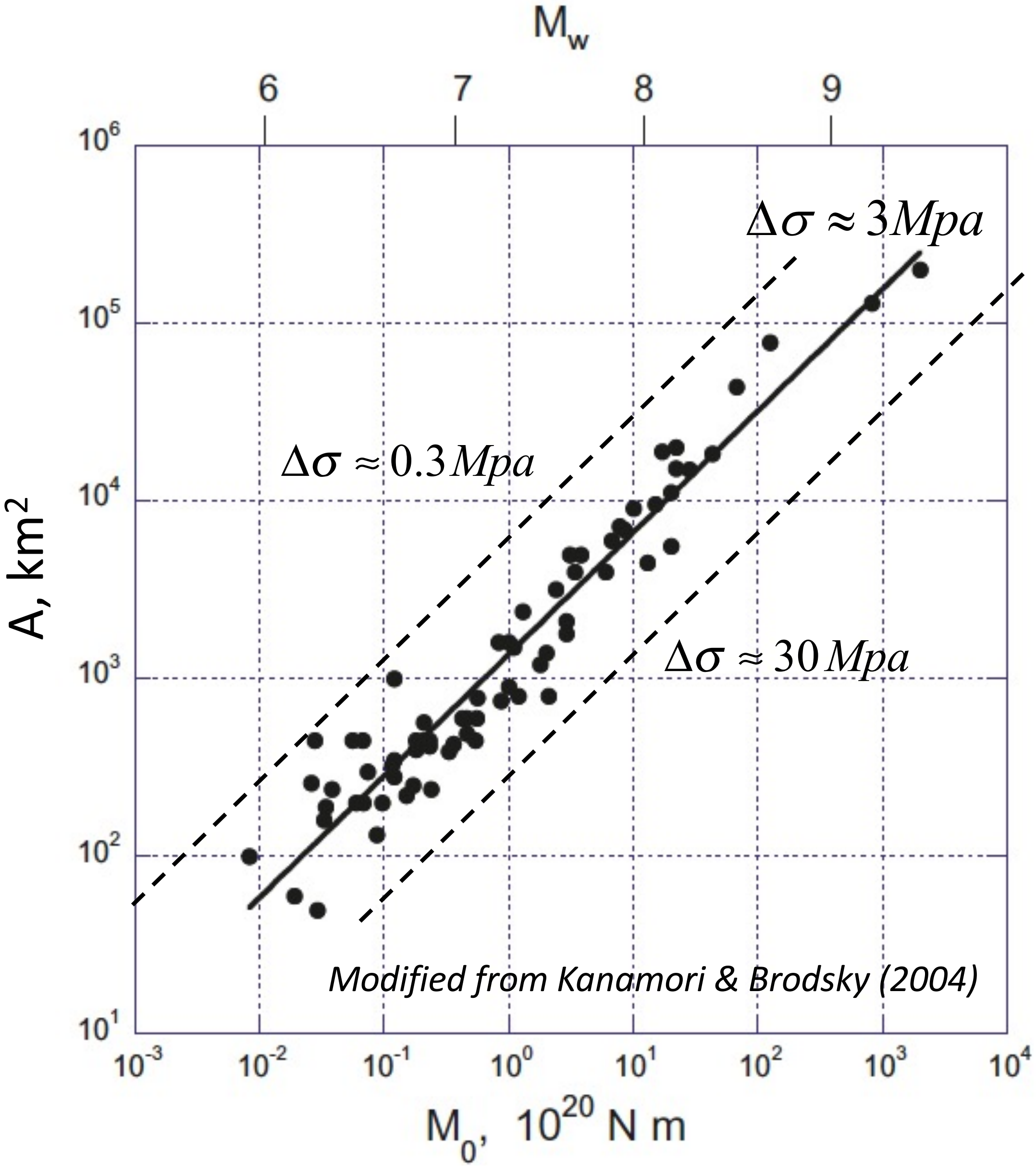

Modified from Kanamori & Brodsky (2004)

$$M_0 = G \iint_{fault\ area} s(x, y)\, dxdy$$

G: Shear modulus

S(x,y): slip at point (x,y) on fault

A: Rupture area

Linear Fracture Mechanics:

$$\Delta\sigma \approx C \cdot M_0 \cdot A^{-3/2}$$

$$\frac{2}{3}\log A \approx -\log\Delta\sigma + \log M_0 + \log C$$

- Seismic stress drop $\Delta\sigma$ looks relatively uniform, typically between 0.1MPa and 10MPa

Moment-Duration Scaling

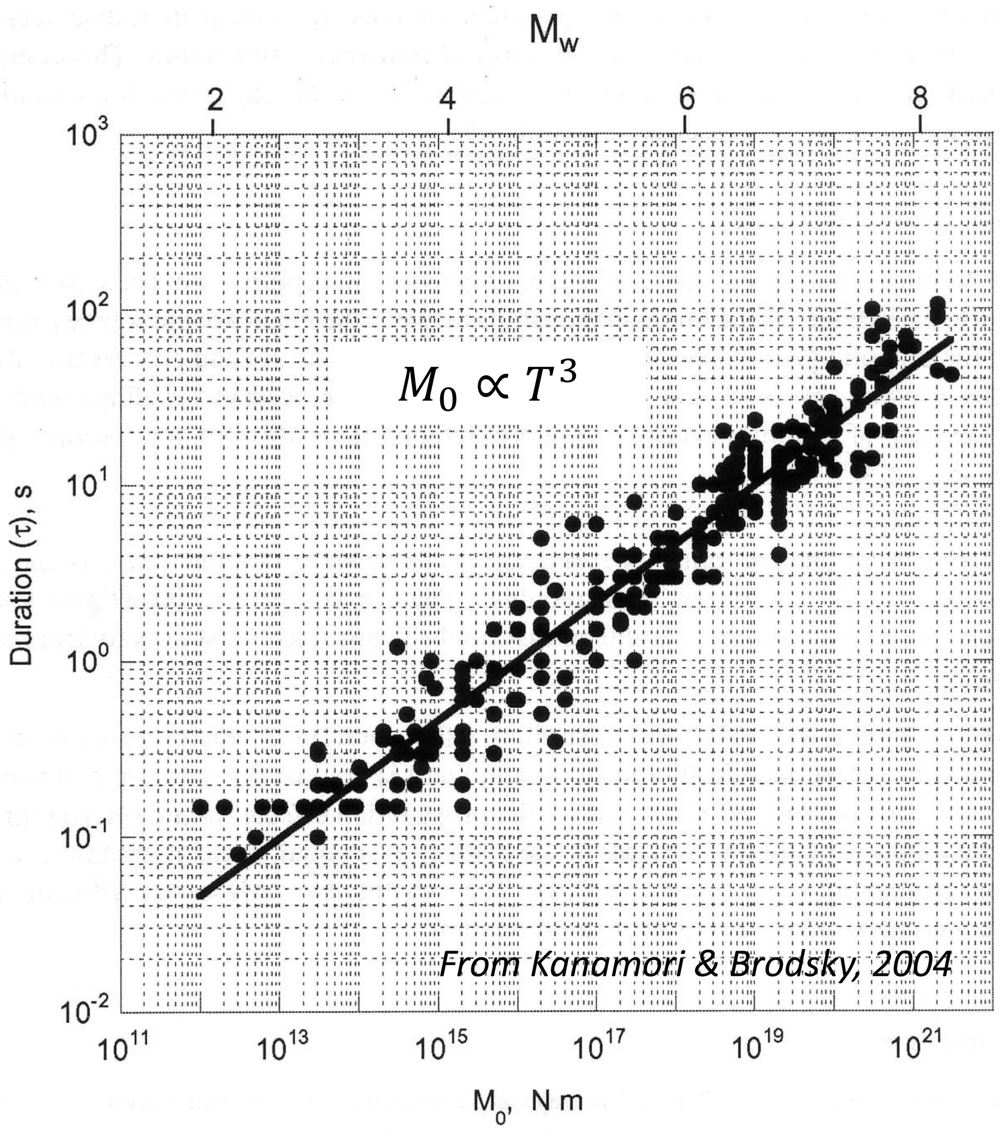

Rupture velocity, V_r ,during seismic ruptures doesn't vary much. Consistent with circular crack dynamics (*Madariaga, 1977*):

$$V_r = \alpha V_s \text{ , with } \alpha \sim 50 - 70\%$$

$$a = v_r T \Rightarrow A \propto T^2 , S \propto T$$

$$\Rightarrow M_0 = GSA \propto T^3$$

$$\left.\begin{matrix} A \propto T^2 \\ S \propto T^1 \end{matrix}\right\} M \propto T^3$$

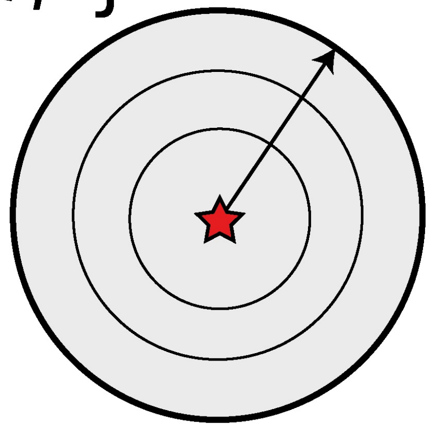

Moment-Duration Scaling

A circular crack rupture should follow a cubic moment-duration scaling relation

The scaling should switch to linear when slip events saturate the width of the seismogenic zone

Circular crack rupture

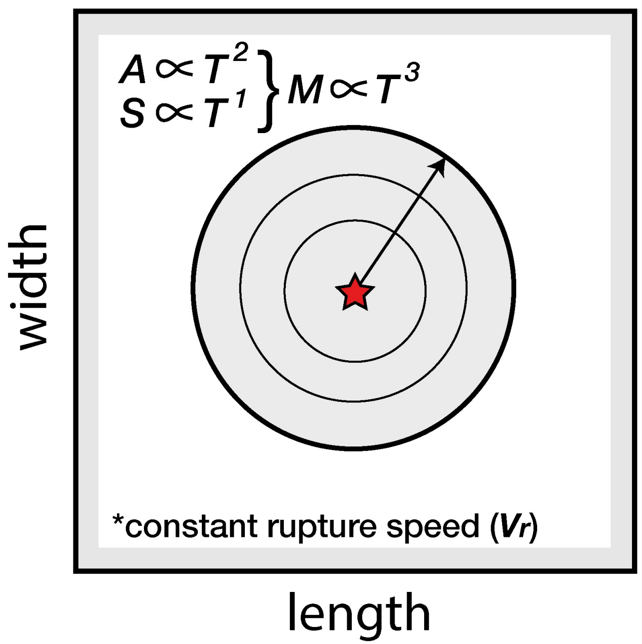

Bounded pulse-like rupture

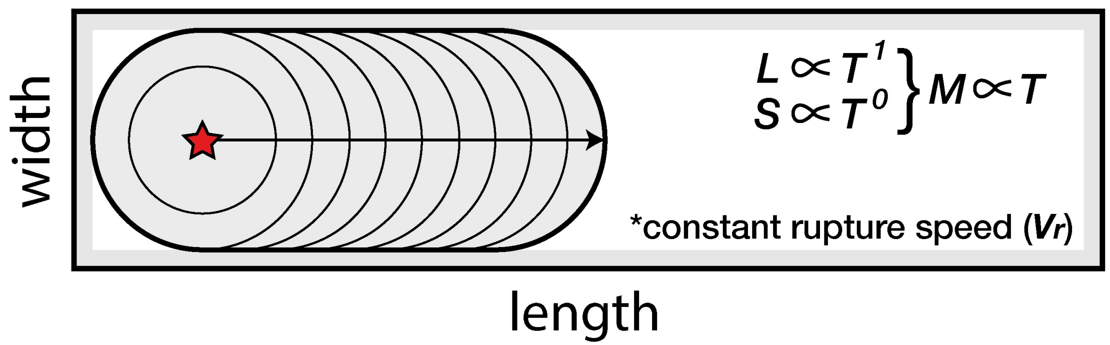

Kanamori and Anderson, 1975

Romanowicz and Rundle, 1993

References-Clustering and scaling Properties

Corral, A. (2004), Long-term clustering, scaling, and universality in the temporal occurrence of earthquakes, *Physical Review Letters*, *92*(10).

Hanks, T. C., and H. Kanamori (1979), A moment magnitude scale, *Journal of Geophysical Research*, *84*(B5), 2348-2350.

Kanamori, H., and E. E. Brodsky (2004), The physics of earthquakes, *Reports on Progress in Physics, 67(8), 1429-1496.*

Madariaga, R. (2009), Earthquake scaling laws, in *Encyclopedia of Complexity and System Science*, edited by M. R., pp. 2581–2600, Springer, New York.

Manighetti, I., M. Campillo, S. Bouley, and F. Cotton (2007), Earthquake scaling, fault segmentation, and structural maturity, *Earth and Planetary Science Letters, 253(3-4), 429-438.*

Marsan, D., and O. Lengline (2008), Extending earthquakes' reach through cascading, *Science*, *319*(5866), 1076-1079.

Mignan, A. (2012), Functional shape of the earthquake frequency-magnitude distribution and completeness magnitude, *Journal of Geophysical Research-Solid Earth*, *117*.

Mignan, A. (2016), Revisiting the 1894 Omori Aftershock Dataset with the Stretched Exponential Function, *Seismological Research Letters*, *87*(3), 685-689.

Ogata, Y. (1998), Space-time point-process models for earthquake occurrences, *Annals of the Institute of Statistical Mathematics*, *50*(2), 379-402.

Romanowicz, B., and J. B. Rundle (1993), On Scaling Relations for Large Earthquakes, *Bulletin of the Seismological Society of America*, *83*(4), 1294-1297.

Utsu, T., Y. Ogata, and R. S. Matsuura (1995), The Centenary of the Omori Formula for a Decay Law of Aftershock Activity, *Journal of Physics of the Earth*, *43*(1), 1-33.

Wells, D. L., and K. J. Coppersmith (1994), New Empirical Relationships Among Magnitude, Rupture Length, Rupture Width, Rupture Area, and Surface Displacement, *Bulletin of the Seismological Society of America*, *84*(4), 974-1002.

Wesnousky, S. G. (2008), Displacement and geometrical characteristics of earthquake surface ruptures: Issues and implications for seismic-hazard analysis and the process of earthquake rupture, *Bulletin of the Seismological Society of America, 98(4), 1609-1632.*

Zaliapin, I., and Y. Ben-Zion (2013), Earthquake clusters in southern California I: Identification and stability, *Journal of Geophysical Research-Solid Earth*, *118*(6), 2847-2864.

Toward physics-based Earthquake Forecasting

I. Introduction

II. EQ phenomenology-point source and Finite source models

III EQ phenomenology-Scaling properties

IV 'Elastic Dislocation' and 'crack' models

V Interseismic deformation

VI Postseismic deformation

VII Kinematic to Dynamic models of the seismic cycle

VII The seismic cycle in the Himalaya

VIII Earthquake forecasting

‘Elastic Dislocation’ and ‘crack’ models

- Theory
- Relation to crack models
- Application to relate slip on faults to deformation
- Inversion

Some elasticity solutions of use in tectonics

- **'Elastic dislocations'** in an elastic half-space (Steketee 1958; Cohen, Advances of geophysics, 1999)
  - The infinitely long strike-slip fault (Segall, 2010)
  - The infinitely long dip-slip fault (Manshina and Smylie, 1971, Rani and Singh, 1992; Singh and Rani, 1993, Cohen, 1996).
  - Rectangular (Okada, 1985; 1992) and triangular (Meade, 2007) fault patch in 3-D
- **Elastic dislocation in an spherical PREM Earth** model (Sun et al., 2009)
- **Point source of pressure** (the 'Mogi source')
- **Uniaxial poroelastic compaction** (Geertsma, 1973)
- The **Boussinesq pb** (normal point load at the surface of an elastic half-space); (Jaeger, Rock mechanics and Enegineering)
- The **Cerruti pb** (shear point load at the surface of an elastic half-space); (Jaeger, Rock mechanics and Enegineering)
- ….

‘Elastic Dislocation’

- Refers to the theory describing strain induced by slip on a surface embedded in an elastic medium.
- The theory allows to determine deformation of an elastic medium due to slip localized on a fault.
- The theory is widely used to model geodetic strain due to co-seismic or interseismic deformation.

In crack mechanics, 3 modes are distinguished

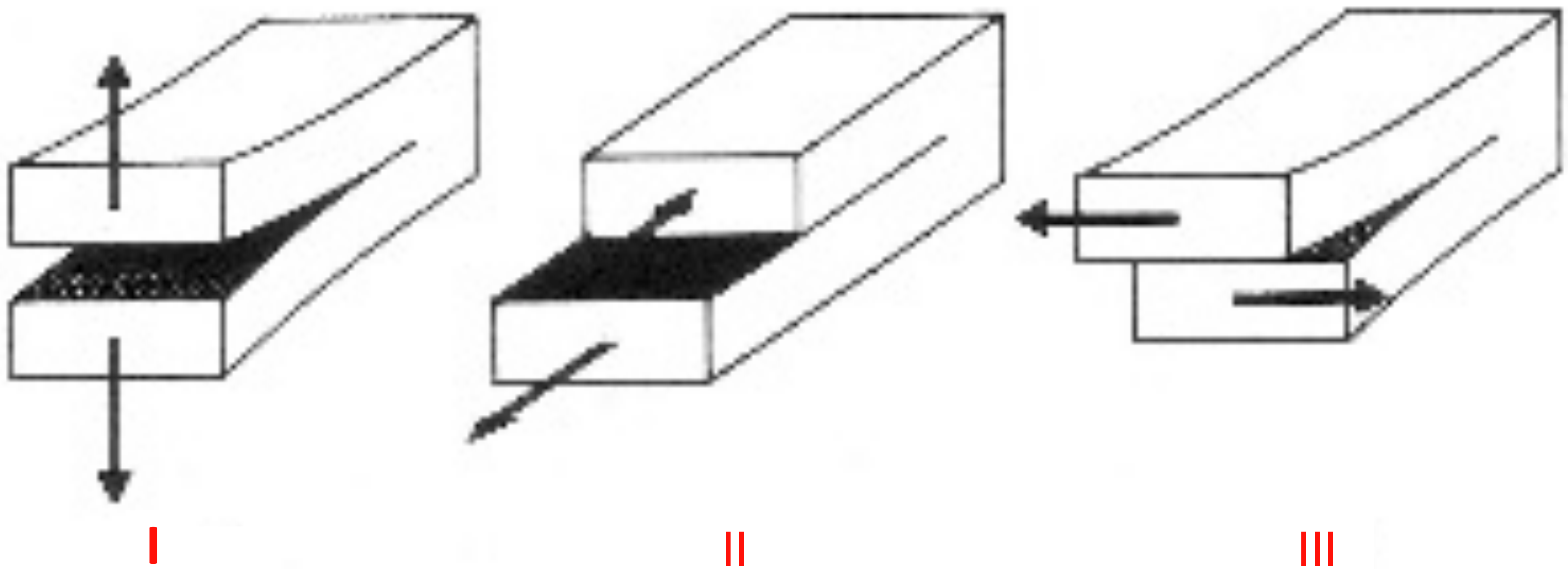

Mode I= Tensile or opening mode: displacement is normal to the crack walls

Mode II= Longitudinal shear mode: displacement is in the plane of the crack and normal to the crack edge (~ edge dislocation)

Mode III= Transverse shear mode: displacement is in the plane of the crack and parallel to the crack edge (~ screw dislocation)

Infinite Strike-Slip fault

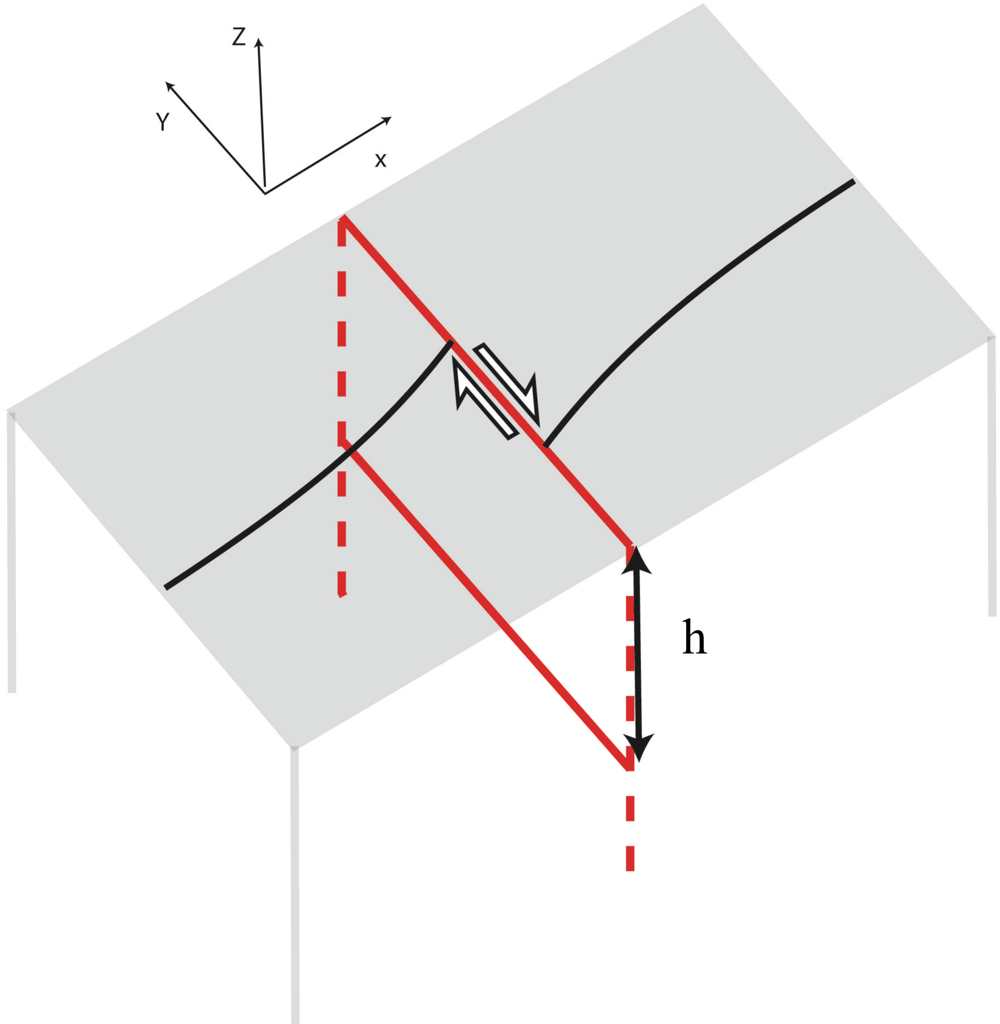

Let's consider a fault parallel to Oy, with infinite length, and surface deformation due to uniform slip, equal to S_y, extending from the surface to a depth h.
(Slip vector is $(0,S_y,0)$ // Oy)

(e.g., Segall, 2010)

Infinite Strike-Slip fault

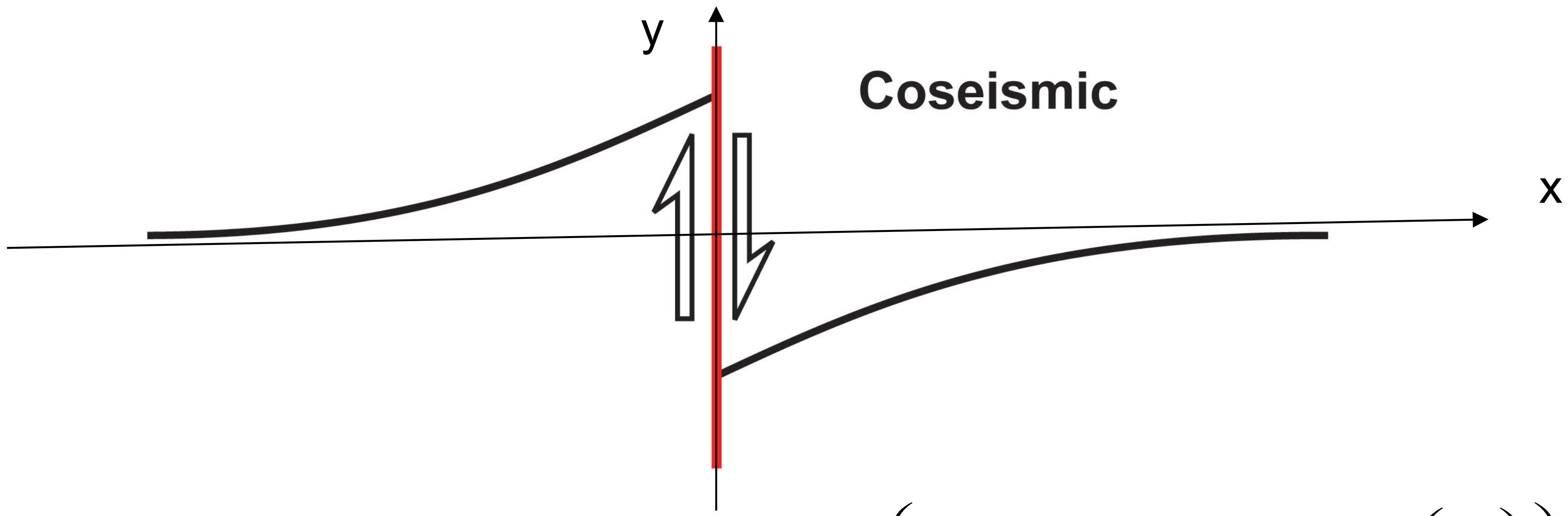

Co-seismic displacement parallel to Oy

$$\Delta y_{CO}(x) = S_y \left(sign(x)\frac{1}{2} - \frac{1}{\pi}\tan^{-1}\left(\frac{x}{h}\right)\right)$$

Co-seismic slip

S_y (>0 for a left-lateral fault)

Co-seismic strain

$$\varepsilon_{xy}(x) = \frac{1}{2}\frac{\partial \Delta y_{co}}{\partial x} = \frac{S_y}{2\pi h}\frac{1}{1+\left(\frac{x}{h}\right)^2}$$

(e.g., Segall, 2010)

Infinite Thrust fault

Surface displacements due to slip *S* on a fault dipping by *θ* of to depth *D*

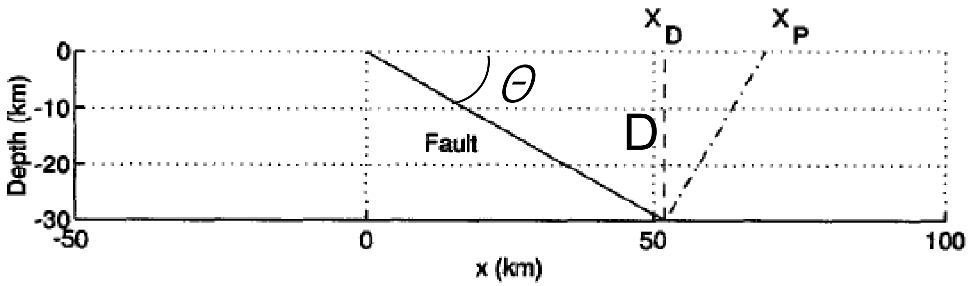

$$\Delta x(x) = \frac{S.\cos\theta}{\pi}\left[\tan^{-1}\left(\frac{x-x_D}{D}\right) + \frac{(x-x_P)\cdot D}{(x-x_D)^2+D^2} - sign(x)\frac{\pi}{2}\right]$$

$$\Delta z(x) = \frac{S.\sin\theta}{\pi}\left[\tan^{-1}\left(\frac{D}{x-x_D}\right) - \frac{x\cdot D}{(x-x_D)^2+D^2} - \frac{\pi(1-sign(x))}{2}\right]$$

where $\quad x_D = \frac{D}{\tan\theta}$

$$x_P = \frac{D}{\sin\theta.\cos\theta}$$

(*e.g.*, Manshina and Smylie, 1971; Cohen, 1996)

Infinite Thrust fault

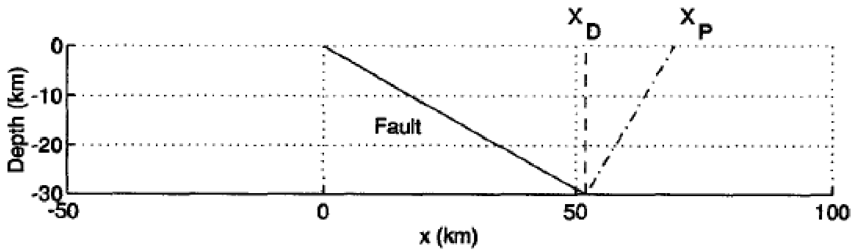

Surface displacements

$$\Delta x(x) = \frac{S.\cos\theta}{\pi}\left[\tan^{-1}\left(\frac{x - x_D}{D}\right) - \frac{(x - x_P)\cdot D}{(x - x_P)^2 + D^2} - sign(x)\frac{\pi}{2}\right]$$

$$\Delta z(x) = \frac{S.\sin\theta}{\pi}\left[\tan^{-1}\left(\frac{x - x_D}{D}\right) - \frac{x\cdot D}{(x - x_D)^2 + D^2} - \frac{\pi(1 - sign(x))}{2}\right]$$

Horizontal strain

$$\varepsilon_{xx}(x) = \frac{\partial \Delta x}{\partial x} = \frac{S.\cos\theta}{\pi}\left[\frac{2D(x - x_P)(x - x_D)}{\{(x - x_P)^2 + D^2\}^2}\right]$$

Infinite Thrust fault

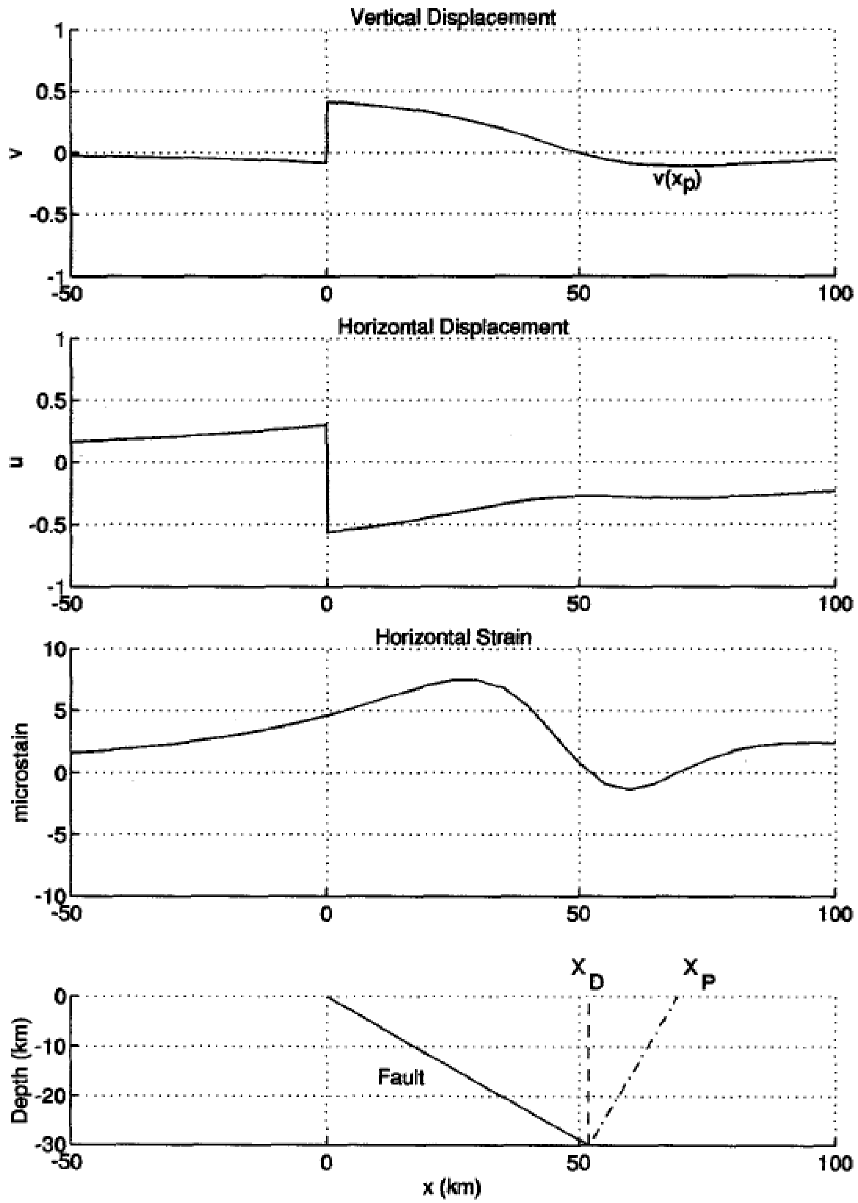

Note that x_D coincides with the 'hinge line' (zero uplift)

(see Cohen, 1996)

Dislocation Elements in 3-D

- Slip is assumed uniform on some idealized planar fault patch
- Half-space with isotropic homogeneous elastic properties (2 parameters: shear modulus, Poisson coefficient)
- Rectangular elements: Okada (1985, 1992)

e.g.: https://depts.washington.edu/clawpack/users-4.6/okada.html

- Triangular Elements: Meade (2007)

https://summit.fas.harvard.edu/software/triangular-dislocations

Okada (1985, 1992)

Function [ux,uy,uz] =
calc_okada(U,x,y,nu,delta,d,len,W,fault_type,strike)

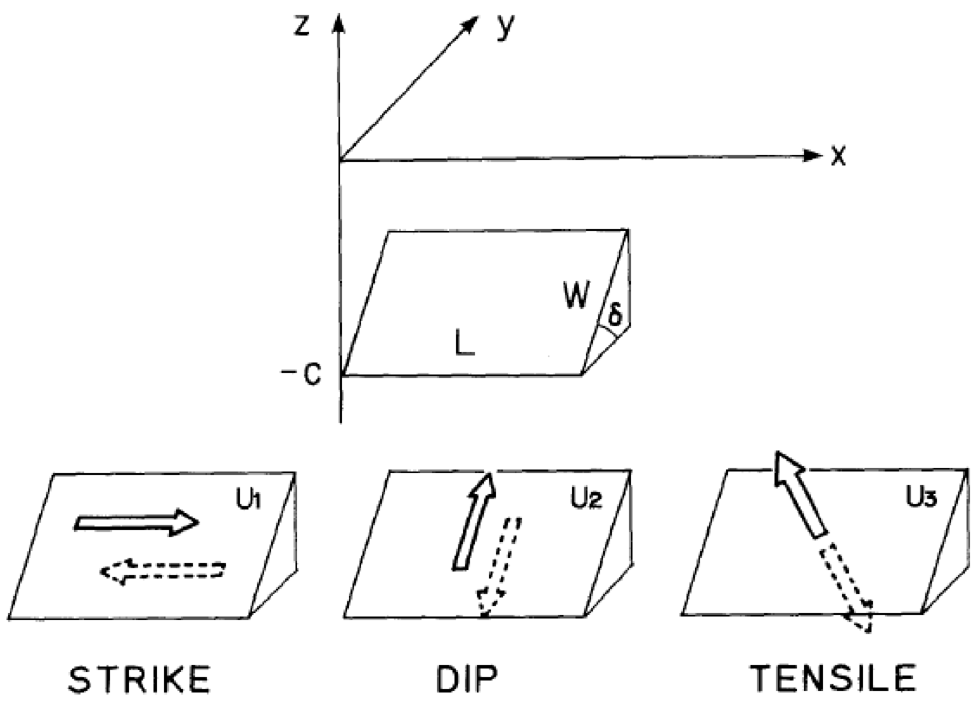

This function computes the displacement field [ux,uy,uz] on the grid [x,y] assuming uniform slip, on a rectangular fault with

U: slip on the fault

nu: Poisson Coefficient

delta: dip angle

d: depth of bottom edge

len=2L: fault length

W: fault width

fault_type: 1=strike,2=dip,3=tensile,4=inflation

NB:C is the middle point of bottom edge

The anti-plane crack model

A rectangular fault extending from the surface to a depth h, with uniform stress drop ('infinite Strike-Slip fault)

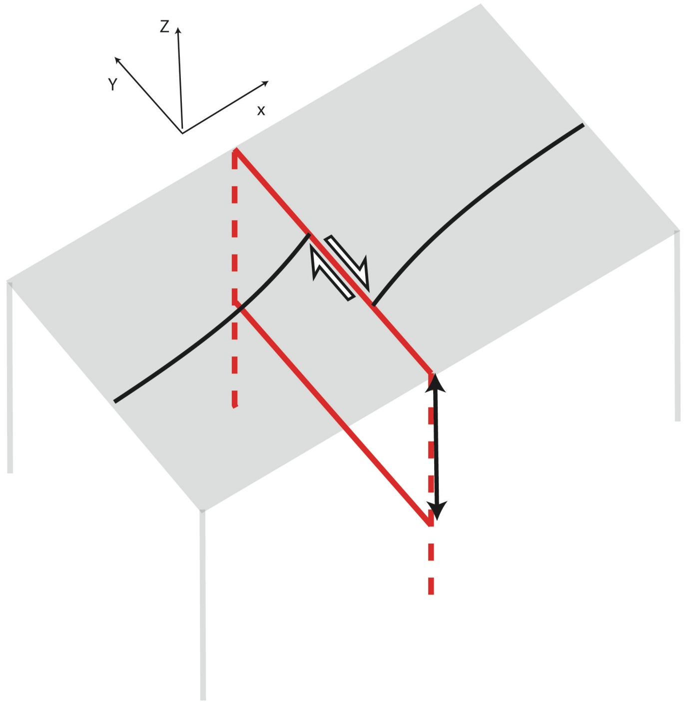

$$\boxed{\Delta u = \frac{2\Delta\sigma}{\mu}\sqrt{a^2 - z^2}}$$

i. The predicted slip distribution is <u>elliptical with depth</u>
ii. Maximum slip should occur at the surface

See Pollard et Segall, 1987 or Segall, 2010 for more details

The circular crack model

A planar circular crack of radius a with uniform stress drop, Δσ, in a perfectly elastic body (Eshelbee, 1957)

$$\boxed{\Delta u = \frac{4}{\pi}\frac{(1-\nu)}{(2-\nu)}\frac{\Delta\sigma}{\mu}\sqrt{a^2 - x^2}}$$

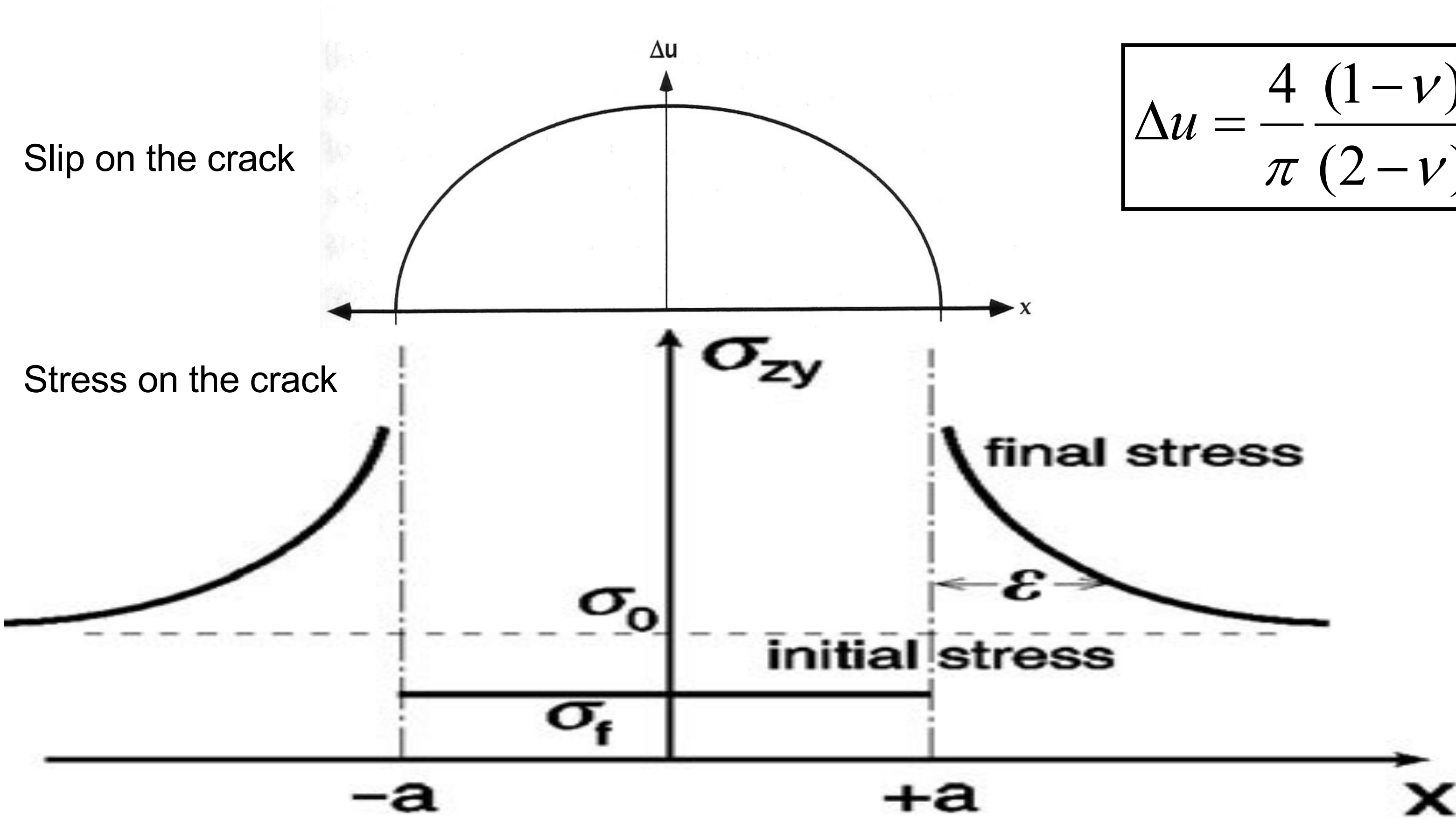

NB: This model produces infinite stress at crack tips, which is not realistic

See Pollard et Segall, 1987 or Scholz, 1990 for more details

The circular crack model

A planar circular crack of radius a with uniform stress drop, $\Delta\sigma$, in a perfectly elastic body (Eshelby, 1957)

i. The predicted slip distribution is elliptical
ii. D_{mean} and D_{max} increase linearly with fault length (if stress drop is constant).

$$\boxed{\Delta u = \frac{4}{\pi}\frac{(1-\nu)}{(2-\nu)}\frac{\Delta\sigma}{\mu}\sqrt{a^2 - x^2}}$$

$$D_{\max} = \Delta u_{\max} = \frac{4}{\pi}\frac{(1-\nu)}{(2-\nu)}\frac{\Delta\sigma}{\mu}a$$

$$D_{mean} = \overline{\Delta u} = \frac{8}{3\pi}\frac{(1-\nu)}{(2-\nu)}\frac{\Delta\sigma}{\mu}a$$

Slip on the crack

Stress on the crack

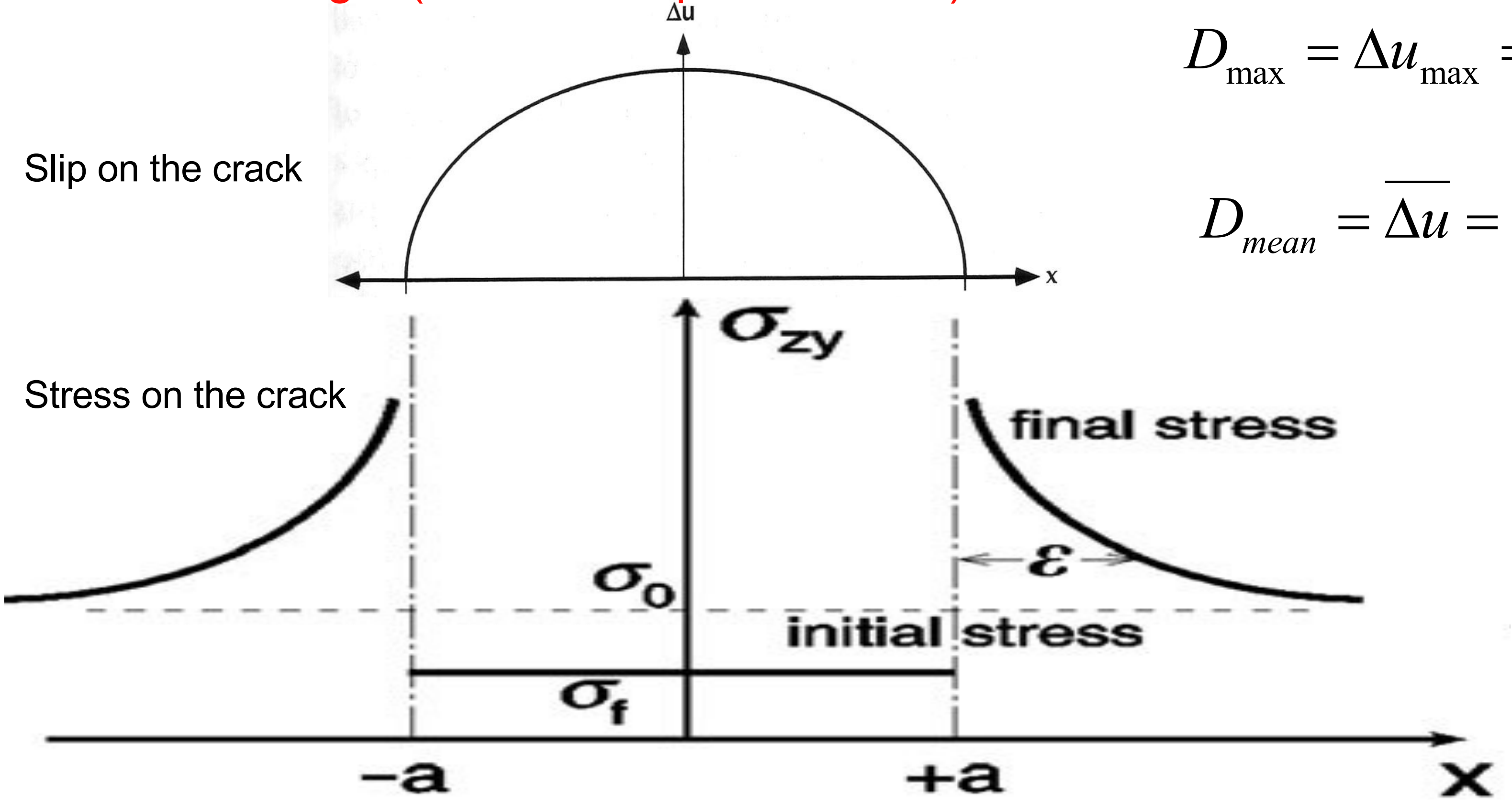

NB: This model produces infinite stress at crack tips, which is not realistic

See Pollard et Segall, 1987 or Scholz, 1990 for more details

Here the measured SAR interferogram is compared with a theoretical interferogram computed based on the field measurements of co-seismic slip using the elastic dislocation theory

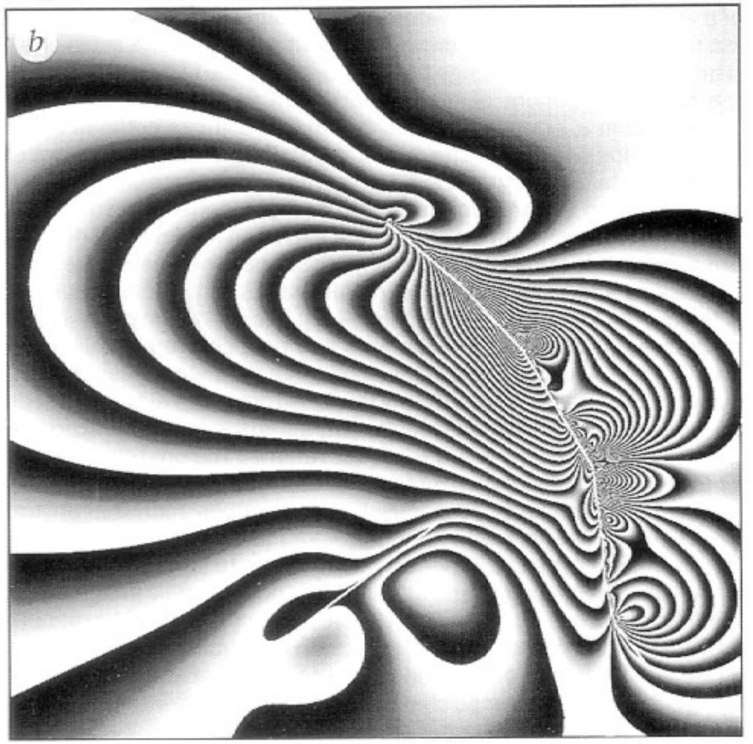

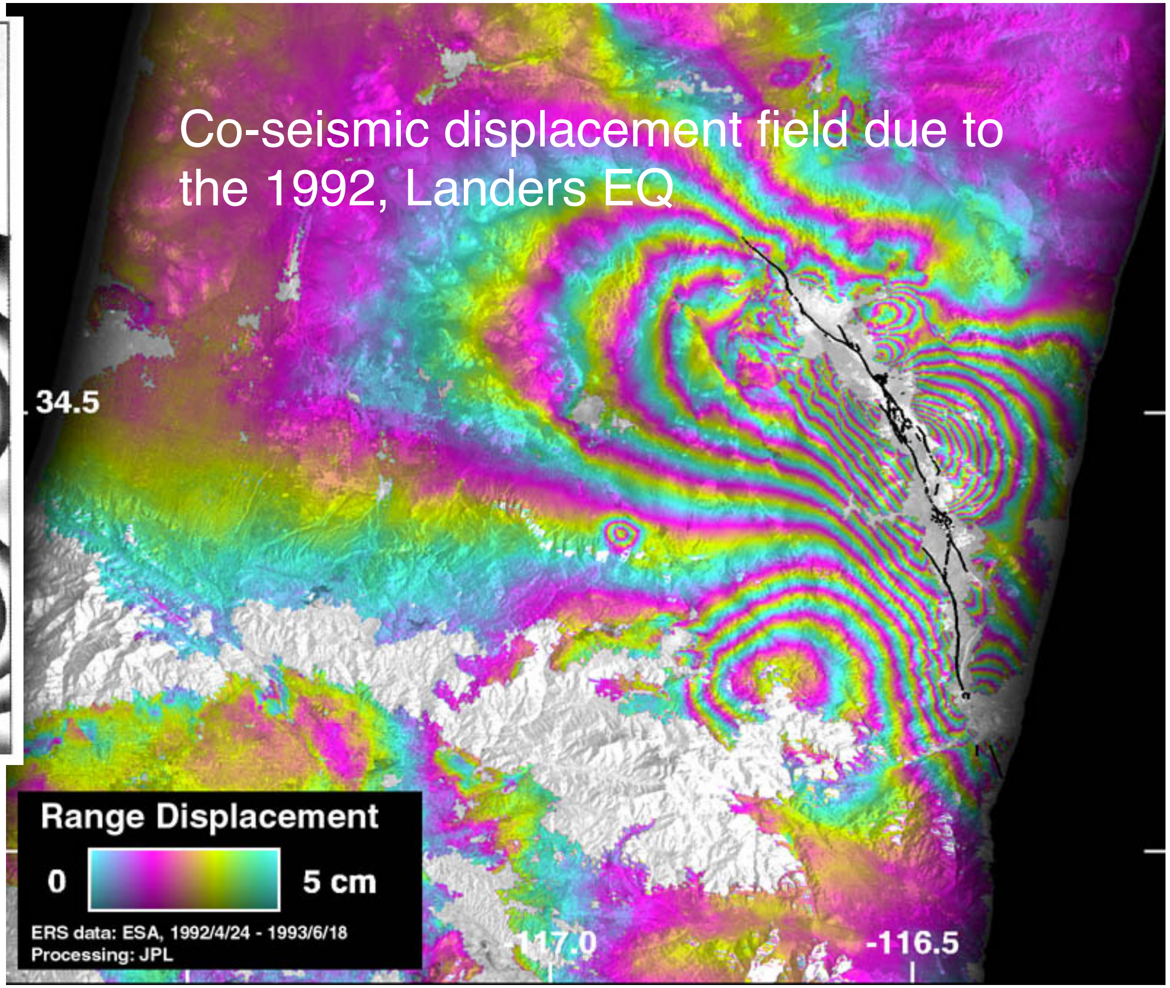

This is a validation that coseismic deformation can be predicted acurately based on the elastic dislocation theory

(based on Massonnet et al, Nature, 1993)

The theory of elastic dislocations can be used to model surface deformation predicted for any slip distribution at depth,

Inverting for slip distribution

- Build a mesh describing the faults geometry (with rectangular, or triangular fault patches),
- Represent fault slip with a matrix listing strike-slip and dip-slip components

  → $\underline{m}$
- Assemble your data (measurements with associated uncertainties). You might need resampling the data.

  → $\underline{d}, \underline{\underline{C}}_d$
- Calculate the Green functions relating unit slip along strike, or along dip for each slip patch at each data point.

  → $\underline{\underline{G}}$
- Solve:

$$\boxed{\underline{d} = \underline{\underline{G}}\,\underline{m}}$$

Over-determined problem (n>m)

- Least-squares inversion with account for data uncertainties → $\underline{d} = \underline{\underline{G}}\,\underline{m}$ $\quad \underline{\underline{C}}_d^{-1}(\underline{d} - \underline{\underline{G}}\,\underline{m}) = 0$
- Chi-squares minimisation:

$$\chi^2 = (\underline{d} - \underline{\underline{G}}\,\underline{m})^T \underline{\underline{C}}_d^{-1} (\underline{d} - \underline{\underline{G}}\,\underline{m}) = (\underline{d} - \underline{\underline{G}}\,\underline{m})^T \underline{\underline{C}}_d^{-1} (\underline{d} - \underline{\underline{G}}\,\underline{m})$$

if data are uncorrelated --> $\boxed{\chi^2 = \sum_i \left(\frac{d_i^{obs} - d_i^{pred}}{\sigma_i} \right)^2}$

- Solution:

$$\underline{\underline{G}}^T \underline{\underline{C}}_d^{-1} \underline{d} = \underline{\underline{G}}^T \underline{\underline{C}}_d^{-1} \underline{\underline{G}}\,\underline{m}$$

$$\boxed{\underline{m} = \left(\underline{\underline{G}}^T \underline{\underline{C}}_d^{+} \underline{\underline{G}} \right)^{+} \underline{\underline{G}}^T \underline{\underline{C}}_d^{+} \underline{d}}$$

→ $\boxed{\underline{m} = \left(\underline{\underline{G}}^T \underline{\underline{C}}_d^{-1} \underline{\underline{G}} \right)^{-1} \underline{\underline{G}}^T \underline{\underline{C}}_d^{-1} \underline{d}}$

Pseudo-inverse

$$A = USV^T$$
$$A^+ = A = VS^+U^T$$
$$S = diag(s_1, s_2, \ldots, s_n, 0, .., 0)$$
$$S^+ = diag(1/s_1, 1/s_2, \ldots, 1/s_n, 0, .., 0)$$

Resolution Matrix $\quad \underline{\underline{R}} = \left(\underline{\underline{G}}^T \underline{\underline{C}}_d^{-1} \underline{\underline{G}} \right)^{-1} \underline{\underline{G}}^T \underline{\underline{C}}_d^{-1} \underline{\underline{G}}$

Under-determined problem (m>n)

- The pb is ill-posed (more variables to solve for than data available)
- Additional ‘regularization’ constraints are generally added (linear operator)
- Tikhonov Regularisation constraints: $\underline{\underline{\Lambda}}\,\underline{m} = \underline{c}$
  - Moment, slip potency. $\underline{\underline{\Lambda}} = \underline{\underline{1}}$
  - Gradient $\underline{\underline{\Lambda}} = \underline{\underline{\nabla}}$
  - Laplacian (smoothness) $\underline{\underline{\Lambda}} = \underline{\underline{\Delta}} = \underline{\underline{\nabla}}^2$

--> Minimize: $$\left\|\underline{d} - \underline{\underline{G}}\,\underline{m}\right\|_2^2 + \sum_i \lambda_i \left\|\underline{\underline{\Lambda}}_i\,\underline{m} - \underline{c}_i\right\|_2^2$$

- This is equivalent to solving a new set of linear equations now (over-determied):

$$\underline{d} = \underline{\underline{G}}\,\underline{m}$$

$$\underline{\underline{\Lambda}}_i \underline{m} = \underline{c}_i$$

$$\rightarrow \quad \boxed{\underline{m} = \left(\underline{\underline{G}}^T \underline{\underline{C}}_d^{-1} \underline{\underline{G}} + \sum_i \lambda_i^2 \underline{\underline{\Lambda}}_i^T \underline{\underline{\Lambda}}_i \right)^{-1} \underline{\underline{G}}^T \underline{\underline{C}}_d^{-1} \underline{d}}$$

- How to choose the weight (λ_i) on the regularization criteria?
  - L-curve corner (Hansen, 1992)
  - Reduced Chi- squares~1

References-Elastic dislocation&Crack models

Segall, P, Earthquake and Volcano Deformation, Princeton University Press, 2010.

Cohen, S. C., Convenient formulas for determining dip-slip fault parameters from geophysical observables., *Bulletin of seismological society of America*, *86*, 1642-1644, 1996.

Cohen, S. C., Numerical models of crustal deformation in seismic zones, *Adv. Geophys.*, *41*, 134-231, 1999.

Geertsma, J. (1973), Land subsidence above compacting oil and gas reservoirs, *Journal of Petroleum Technology*, *25*(JUN), 734-744.

Okada, Y., Surface deformation to shear and tensile faults in a half space, *Bull. Seism. Soc. Am.*, *75*, 1135-1154, 1985.

Okada, Y., Internal Deformation Due To Shear And Tensile Faults In A Half-Space, *Bulletin Of The Seismological Society Of America*, *82*, 1018-1040, 1992.

Madariaga, R. (1976), Dynamics of an expanding circular fault, *Bulletin of the Seismological Society of America*, *66*(3), 639-666.

Massonnet, D., K. Feigl, M. Rossi, and F. Adragna (1994), Radar interferometry mapping of the deformation in the year after the Landers earthquake, *Nature*, *369*, 227-230.

Meade, B. J. (2007), Algorithms for the calculation of exact displacements, strains, and stresses for triangular dislocation elements in a uniform elastic half space, *Computers & Geosciences*, *33*(8), 1064-1075.

Savage, J., A dislocation model of strain accumulation and release at a subduction zone, *Journal of Geophysical Research*, *88*, 4984-4996, 1983.

Singh, S. J., and S. Rani (1993), Crustal deformation associated with two-dimensional thrust faulting., *Journal of Physics of the Earth.*, *41*, 87-101

Sun, W., Okubo, S., Fu, G. & Araya, A., 2009. General formulations of global coseismic deformations caused by an arbitrary dislocation in a spherically symmetric earth model: applicable to deformed earth surface and space-fixed point, Geophys. J. Int., 177, 817–833

Vergne, J., R. Cattin, and J.-P. Avouac, On the use of dislocations to model interseismic strain and stress build-up at intracontinental thrust faults., *Geophysical Journal International*, *147*, 155-162, 2001.